UNIVERSITY OF TRENTO - Italy
Department CIBIO

International PhD Program in Biomolecular Sciences

Department of Cellular, Computational and Integrative Biology – CIBIO

XXXII Cycle

microRNAs as biomarkers: case study and technology development

Tutor

professor Michela Alessandra Denti

Università degli Studi di Trento, Department CIBIO

Ph.D. Thesis of

Simone Detassis

Università degli Studi di Trento, Department CIBIO

Academic Year 2018-2019

INDEX

ACKNOWLEDGMENTS

Alla mia famiglia, supporto costante in questi anni. Dall'inizio dell'università (e da sempre) fino a questo traguardo, sarebbe stato impossibile continuare senza mai fermarsi, se non avessi avuto il vostro aiuto. Il più importante grazie va a voi.

Alla mia ragazza Mery, per aver affrontato insieme a me questi anni standomi vicino nei momenti belli e brutti. Supportandomi, sostenendomi e facendomi evadere dalla vita di laboratorio. La colonna portante della mia vita.

A tutti i miei amici, in particolare Mattia, Mic e Coa, perché le risate e il tempo passato insieme anche dopo tanti anni sono più importanti di qualsiasi traguardo professionale.

Al laboratorio di RNA Biology and Biotechnology. Grazie a Michela per il supporto, la pazienza, la costante e instancabile passione per la scienza e il metodo rigoroso che mi ha insegnato e che mi guiderà da qui in poi.

A Margherita e Valerio, per avermi fatto integrare nel laboratorio e avermi aiutato. Moltissimo di quello che so fare è grazie a voi. Un grazie grande perché non mi avete fatto mancare il supporto anche quando, non più membri del laboratorio, poteva non essere più di vostro interesse. E grazie per la vostra amicizia, il tempo passato a parlare, ridere e scherzare.

Un grandissimo grazie anche alla famiglia di Optoi, che ha creduto in me fin dall'inizio. Una scommessa che avete colto dal tirocinio magistrale fino ad ora. Grazie perché con onestà e trasparenza mi avete introdotto in un mondo molto diverso da quello che

conoscevo fino a quel momento. Guidato e consigliato in ogni momento. Un grazie particolare a Cristina: sempre presente e disponibile.

A mi familia en España. Ja que puedo escribir en español (más o menos) es una prueba de lo que habéis hecho para mi. Y eso es lo mínimo. Gracias por haberme aceptado, ayudado y guiado. Además de las experiencias profesionales, siempre voy a tener en mi corazón España, Granada y sobre todo vosotros. De todos que conocí un agradecimiento especial a Salvo, Rossella, Juanjo, Antonio Marín, Antonio Fara, Quique, Bárbara, Mavys y Pepo.

To Hugh and Margaret, citizens of the world. For their support throughout this whole period, for always being kind, professional and friends to me.

Aos meus amigos brasileiros. Eu passei quatro meses incríveis no Brasil, pessoal e profissionalmente. Quero agradecer, em particular, à professora Tania Pasa por me permitir ficar em seu laboratório e pelo apoio prestado. Julia e Moriel por ajudarem na vida cotidiana, as caminhadas e o incrível amanhecer às 5 da manhã. Outro agradecimento especial a Leonardo e Chiara, pois quando eu mais precisava, eles sempre estavam lá. Muito obrigado meus amigos do Brasil.

ORIGINAL AUTHORSHIP DECLARATION

I, Simone Detassis, confirm that this is my own work and the use of all material from other sources has been properly and fully acknowledged.

ABSTRACT

MicroRNAs are a class of small non-coding RNAs involved in post-transcriptional regulation. Their role in almost all processes of the cell, make microRNAs ubiquitary players of cell development, growth, differentiation, cell to cell communication and cell death. Thus, cells' physiological or pathological conditions are reflected by variations in the levels of expression of microRNAs, enabling them to be used as biomarkers of such states. In the past decade, there has been an exponential increase of studies using microRNAs as potential biomarkers for cancer, neurodegenerative diseases, inflammation and cardiac diseases, from tissues and liquid biopsies. However, none of them has reached the clinics yet, due to inconsistency of results through the literature and lack of assay standardization and reproducibility. Technological limitations of microRNAs detection have been, to date, the biggest challenge for using these molecules in clinical settings. In fact, although microarrays, RT-qPCR and RNA-seq are well-established technologies, they all require complex procedures and trained personnel, for performing RNA extraction, labelling of the target and PCR amplification. All these steps introduce variability and, in addition, since no universally standardized protocol – from sample extraction to analyte detection - has been produced yet, methodological procedures are difficult to reproduce. For this reason, we developed a new platform for the rapid detection of microRNAs in biofluids composed of an innovative silicon-photomultiplier (SiPM) based detector and a new chemistry for nucleic acid testing (Chem-NAT). Chem-NAT exploits a dynamic labelling chemistry which allows the sensitive detection of nucleic acids till single base level. On the other hand, SiPM-based device, compared to normal vacuum photomultipliers, grants miniaturization and higher capacity of fitting in a bench-top solution for clinical settings, among other advantages.

The new platform – ODG – has been validated for the direct detection – neither RNA extraction nor PCR amplification needed - of microRNA-21 in plasma of lung cancer patients.

In this work, we also explored the use of microRNAs as biomarkers in metastatic castration resistant prostate cancer (mCRPC). We collected plasma samples from mCRPC patients before and after abiraterone acetate treatment – androgen deprivation type of drug – and performed a miRnome analysis for discovering microRNAs predicting the efficacy of the drug. We chose miR-103a-3p and miR-378a-5p and we validated them via TaqMan RT-qPCR. We discovered that the ratio between the two microRNAs is able to predict the efficacy of abiraterone acetate and follow the responsiveness in time.

In liquid biopsies, extracellular vesicles are getting increasing importance for diagnostic and prognostic purposes. Therefore, in this work we also explored the expression of some microRNAs in extracellular vesicles from plasma, isolated via nickel-based method. We discovered that microRNA-21 and microRNA-223 are not enriched in vesicles from healthy individuals.

INTRODUCTION

[The basis for part of this section is founded on a literature review redacted during my PhD. **Detassis, S.**, Grasso, M., Del Vescovo, V., and Denti, M.A. (2017). microRNAs Make the Call in Cancer Personalized Medicine. Front. Cell Dev. Biol. 5, 86. doi:10.3389/fcell.2017.00086]

1. microRNAs biology

microRNAs (miRNAs) are small non-coding RNAs described for the first time in 1993 (Lee et al., 1993). They are found in plants (Jones-Rhoades et al., 2006), animals and viruses (Grundhoff and Sullivan, 2011). They function as post-transcriptional regulators of gene expression, having also a role in pathological processes including cancer and neurodegenerative diseases (Reddy et al., 2016) (Molasy et al., 2016) (Mohammadi et al., 2016) (da Silva Oliveira et al., 2016). miRNAs may be present as independent transcriptional units and both in introns or exons of other genes (Godnic et al., 2013). They are mainly transcribed by RNA Polymerase II, capped and polyadenylated forming primary miRNAs (pri-miRNA). A small group is generated by RNA Polymerase III. The pri-miRNA is processed in the nucleus with a mechanism of recognition distinguishing true pri-miRNA from other hairpin RNAs. The major determinants are a) ~35bp stem harboring a GHG (H = A, C or T) motif, b) a basal UG motif, c) an apical UGUG motif and d) a CNNC motif. These elements interact with positive or negative regulators of pri-miRNA processing such as hnRNPA1 and SRSF3 or HUR/MSI2 and ADAR respectively (Auyeung et al., 2013) (Fang and Bartel, 2015). The regulators facilitate or abrogate the interaction of Drosha and two DGCR8 molecules with the pri-miRNA generating a precursor miRNA (pre-miRNA) - about 70 nt - (Lee et al., 2003) (Nguyen et al., 2015).

Subsequently, the pre-miRNA is transported out of the nucleus via exportin-GTPase RAN system, where is further processed by Dicer producing the double-stranded miRNA of 19-22nt (Wilson et al., 2015). Dicer, together with Hsp90 chaperone (Miyoshi et al., 2010) serves as a ruler measuring the cleavage site from the basal end to the apical loop which is liberated (MacRae et al., 2006). Of note, Dicer mechanism is not always the same, generating different duplex miRNAs from the same pre-miRNA. A complex made of AGO proteins binds the duplex and forms the RISC complex in an ATP-dependant manner (Iwasaki et al., 2010). AGO2 unwinds the duplex liberating the passenger strand and maintaining only one strand: the guide strand (Kobayashi and Tomari, 2016). The RISC complex has an important post-transcriptional role in gene expression, regulating stability and turnover of mRNAs. The loaded miRNA can target mRNAs, exploiting its sequence complementarity. If the match is perfect the system leads to mRNA degradation (Yekta et al., 2004), otherwise it impedes its translation (Ipsaro and Joshua-Tor, 2015) (Figure 1). Because of their short length, miRNAs, which usually bind the 3'UTR of target mRNAs, are able to target several distinct mRNAs and, on the other hand, any given mRNA may present many binding sites for different miRNAs (Bartel, 2009). Several instances of miRNAs targeting also 5'UTR and coding sequence (CDS) have been found (Broughton et al., 2016).

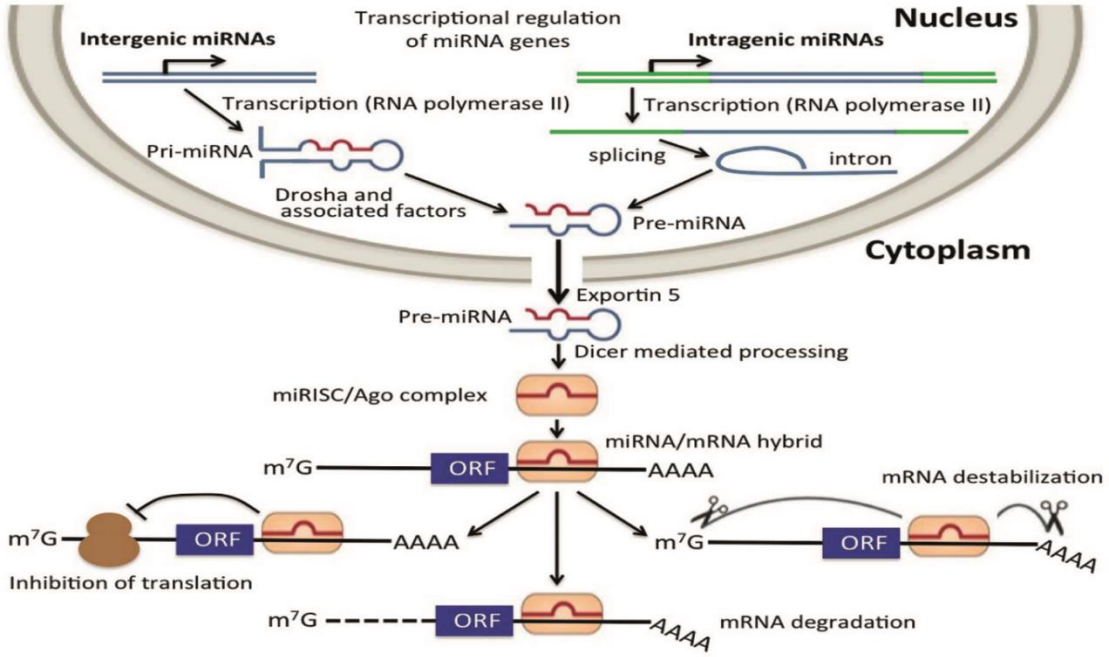

Figure 1. [Adapted from (Piva et al., 2013)] miRNA biogenesis and function on target mRNAs.

2. Circulating microRNAs

The discovery that miRNAs are released from the cells and have a role in cell to cell communication and microenvironment shaping, suggests the involvement of miRNAs not only in the proximal region of origin but also in distant sites (Fusco et al., 2015). For example, miRNAs secreted from adipose tissue are able to reverse variation in hepatic gene expression after a transplant with normal adipose tissue in fat-specific DICER knockout mice (Thomou et al., 2017). miRNAs enriched in extracellular vesicles (EVs) derived from bone marrow mesenchymal stem cells can be absorbed by tubular epithelial cells resulting in the inhibition of expression of the known targets (Collino et al., 2010). Over the last two decades, it has been demonstrated that a substantial number of miRNAs are present in blood and other body fluids, the so-called “circulating miRNAs” (c-miRNAs). C-miRNAs have been reported to be very stable under harsh conditions such as high temperatures, extreme pH, and RNase activity. The reason for this high resistance

is their association with EVs and mostly with RNA-binding proteins (Ago2, HDL, etc) (Makarova et al., 2016) (Figure 2).

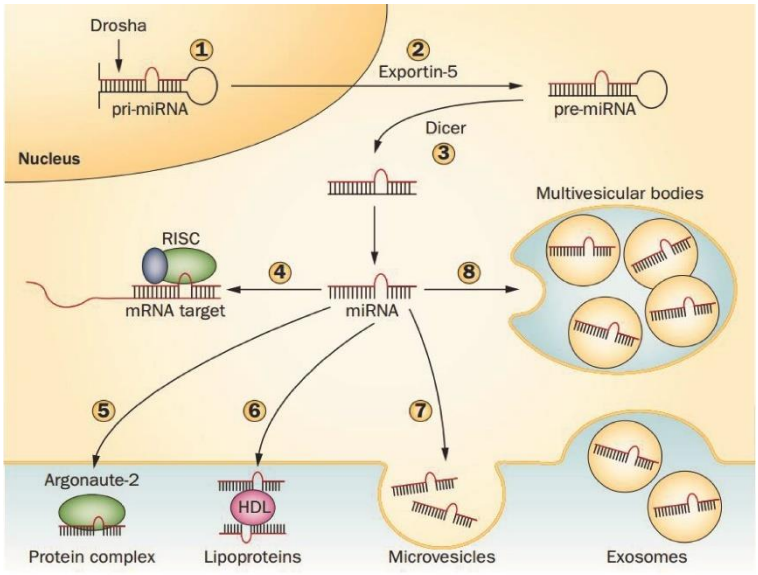

Figure 2. [Adapted from (Guay and Regazzi, 2013)] Circulating miRNAs associated with protein complexes, lipoproteins, microvesicles and exosomes.

In a study by Tuschl and colleagues, RNA-seq on 12 healthy individuals gave a comprehensive view of the RNA status and categorization in serum and plasma, taking into account fluctuations in time (12 samples per patient over a 2-month period), gender, female menstrual cycle and food intake. In blood of healthy individuals, miRNAs are the most represented RNA category, accounting for 53% and 80% of total RNA in serum and plasma respectively, while mRNA about 4-5%. rRNA, tRNA and scRNA, together with mRNAs, are more represented in serum (32%) than in plasma (12%) while both presented about 10-15% of nonannotated reads (Figure 3). The concentration of miRNAs in both plasma and serum was calculated about 5-10pM with no significant gender differences, which is instead manifested for specific miRNAs such those related to epithelial cell-type-enriched, muscle-specific and neuroendocrine-specific pathways (Max et al., 2018).

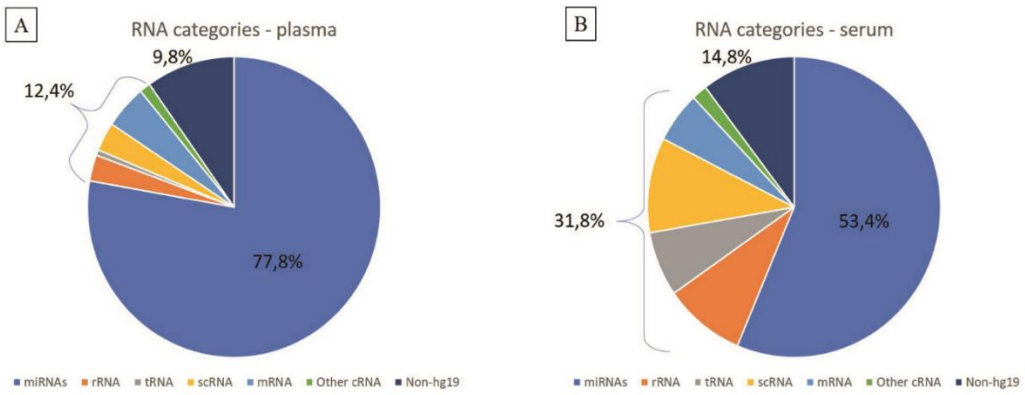

Figure 3. [Data from (Max et al., 2018)]. Abundancy of RNA categories in plasma (A) and serum (B)

In urine, miRNAs have been found in both cellular and EVs fraction. miRNAs abundance in urine of healthy volunteers is different among urine fractions and gender, while their profiling is similar in cellular versus EVs extracts (Ben-Dov et al., 2016). c-miRNAs are also detected in saliva (Rapado-González et al., 2018), seminal fluid (Zhang et al., 2019) and cerebrospinal fluid (CSF) (Kopkova et al., 2018). It is still debated whether the amount of miRNAs in circulation is enough to drive expression changes in recipient cells in vivo. Some works show that the average amount of miRNAs in exosomes is about 1 unit per exosome (Chevillet et al., 2014) (Guzman et al., 2015) raising some skepticism around the role of c-miRNAs in cell to cell communication. However, it has also been demonstrated that some EVs associated miRNAs are a small percentage of the total pool of c-miRNAs (5% - miR-16) (Arroyo et al., 2011), while others may be more represented in EVs fraction (40-70% - let7a), revealing the need of a miRNA-dependent reasoning. Moreover, the semi-quantitative approach does not take into account the accumulation of miRNAs in recipient cells and the content heterogeneity of EVs.

2.1 Extracellular vesicles

The EVs are represented by various populations of membranous particles with different origins and sizes. They have been observed in several body fluids such as blood (Caby et al., 2005), urine (Gonzales et al., 2010), saliva (Palanisamy et al., 2010), breast milk (Admyre et al., 2007), seminal fluid (Machtinger et al., 2016) and CSF (Izadpanah et al., 2018). Historically they were observed for the first time in the 1950s (Sager and Palade, 1957) and then continuously described in several biological kingdoms (Sotelo and Porter, 1959) (De, 1959) (Jensen, 1965) always considered non-functional remnants of cells. 1996 was a turning point when Raposo and colleagues described a possible biological meaning for EVs (Raposo et al., 1996). Generally EVs may be divided into three classes: microvesicles, exosomes and apoptotic bodies. They can be discriminated by size, composition and origin. Exosomes are about 50-150nm, microvesicles 150-1000nm and apoptotic bodies 1000-5000nm (Woith et al., 2019). Microvesicles generate by the outward budding of the plasma membrane while apoptotic bodies are the result of the programmed cell death. Exosomes biogenesis consists mainly of three different stages: 1) formation of endocytic vesicles by invagination of plasma membranes, 2) formation of multivesicular bodies (MVBs) from the inward budding of the endosome and 3) fusion of the MVBs with the plasma membrane and release of the exosomal content. The exosomes formation is a tightly regulated process generally divided into endosomal sorting complex required for transport (ESCRT)-dependent and ESCRT-independent mechanisms. ESCRT is composed of four proteins (ESCRT0-I-II-III) associated with AAA ATPase Vps4 complex (Henne et al., 2013) (Stuffers et al., 2009). However, other molecules, such as lipids, are implicated in exosome biogenesis playing a crucial role. Lipids' composition is central in exosomes formation, structure, shape and ultimately

function (McMahon and Boucrot, 2015). For instance, it was shown that low production of ceramide from sphingomyelin by sphingomyelinase 2, leads to decrease in exosomes biogenesis (Trajkovic et al., 2008). Other proteins such as tetraspanins, heat shock proteins, lactadherin and platelet-derived growth factor receptors are involved in exosomes formation (Conde-Vancells et al., 2008) (Subra et al., 2010) (Figure 4).

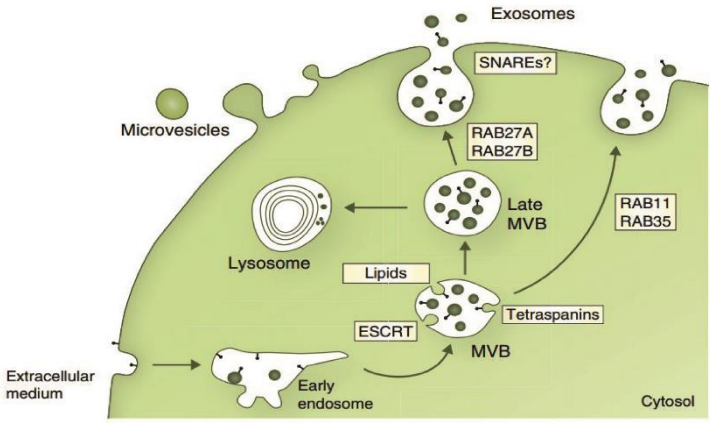

Figure 4. [Adapted from (Kowal et al., 2014)] Exosome biogenesis and secretion. The origin and release of exosomes from intraluminal vesicles, to early endosomes and multivesicular bodies involves several molecules, among which the ESCRT machinery. The intracellular transport of the multivesicular bodies is primarily regulated by RAB proteins.

Considering the multitude of cell types, it is reasonable to think of different characteristics of EVs depending on the cell origin, creating subclasses which may have different biological functions. However, there are no officially and universally recognized EVs subtypes. On the contrary, some general analytical markers both localized in the membrane and in the vesicular lumen are well described. Exosome main markers are phosphatidylserine, tetraspanins CD9, CD63, CD81, LAMP1 and TSG10 (György et al., 2011). Microvesicles are generally characterized by phosphatidylserine (Connor et al., 2010) - while apoptotic bodies by phosphatidylserine and fragmented DNA (György et al., 2011). The content of EVs spans from DNA, RNA and proteins (Van Niel et al., 2018). Exchange of RNAs between glioblastoma and endothelial cells, oncogenic DNA

sequences and retrotransposon elements from medulloblastoma to endothelial cells, and proteins between glioma cells, were reported (Skog et al., 2008) (Balaj et al., 2011) (Al-Nedawi et al., 2008). Toxic components such as prion PrPsc (Vella et al., 2007) or CCR5 for transmission and propagation of HIV-1 (Mack et al., 2000), have also been shown to be delivered by EVs. The uptake of EVs and cargo delivery is not completely unveiled. Several reports show a scenario in which the biological function of EVs is cell-type and physiological- and pathological-condition dependent. For instance, EVs from oligodendrocytes are preferentially uptaken by microglia compared to neurons (Fitzner et al., 2011). Similar behavior was observed for primary neurons whose EVs are internalized only by other neurons, while EVs from neuroblastoma cells bind equally well to astrocytes (Chivet et al., 2014). Conversely to this specific internalization process, HeLa cells seem to take several types of EVs from different cell lines (Costa Verdera et al., 2017) (Svensson et al., 2013). Even EVs size may have a role in the mechanism of uptake (Mulcahy et al., 2014). In general, the mechanism of uptake may be divided in endocytosis and fusion. Endocytosis comprehends clathrin-dependent and clathrin-independent pathways mediated by caveolin, macropinocytosis, micropinocytosis, lipid raft-mediated endocytosis and phagocytosis (Mulcahy et al., 2014). The second mechanism is based on the direct fusion of the EV membrane with the cell plasma membrane. Interestingly, acidic pH conditions enhanced EVs release and uptake in melanoma cells (Parolini et al., 2009). Strictly connected to the way of internalization is how the content of the EVs is released inside the acceptor cells. The main pathways involved would lead to either lysosomal degradation, or recycling of the EVs, or functional target release inside the acceptor cell (Mathieu et al., 2019) (Momen-Heravi et al., 2014) (Kanada et al., 2015). Moreover, EVs may exert their function without internalizing in the acceptor cell, such as EVs transporting histocompatibility complex-

peptide complexes that can activate T cell receptors on T lymphocytes (Raposo et al., 1996) (Tkach et al., 2017). However, our knowledge of how EVs operate from biogenesis to uptake and release in the acceptor cell, remains limited, leaving space for comprehensive studies including molecular, cellular and functional characterization of EVs and their subtypes. The need of a better understanding of EVs biology is also reflected in the area of RNA therapeutics, where, because of the urgency of developing delivering systems for therapeutic oligonucleotides, there is an effort in studying the possibility of using EVs as cargoes (Momen-Heravi et al., 2014) (Ohno et al., 2013).

2.2 Extracellular vesicles and microRNAs

The presence of miRNAs enriched in EVs was first described in a study where among all the RNA species detected, some miRNAs were expressed more in exosomes compared to mast cells (Valadi et al., 2007). The mechanism by which miRNAs are loaded into EVs is not fully understood yet, however it is generally recognized that both passive and active mechanisms are involved. Pigati and colleagues found a strong correlation between miRNAs in MCF-7 cells and in the supernatant, proposing that the passive release of the miRNAs can occur. However, the same group showed that a considerable part of the miRNAs detected did not follow this pattern, opening to an active mechanism of EVs loading (Pigati et al., 2010). There are several reported guided mechanisms for the loading of miRNAs in EVs: a) the affinity between the RNA and raft-like membrane regions of the MVBs (Janas et al., 2015), b) changes in expression of the miRNAs targets inside the donor cell for which low expression of an mRNA would lead to an increased loading of the miRNAs targeting it into EVs (Squadrito et al., 2014) and c) neutral sphingomyelinase 2-dependent pathway involved in EVs biogenesis and in miRNA upload (Kosaka et al.,

2010). Interestingly, KRAS status was reported to have a role in miRNAs sorting in EVs (Cha et al., 2015). In 2013, Sànchez-Madrid group showed discordance between intracellular and extracellular miRNAs and mRNA pool composition via microarrays analyses in the miRNAs and mRNA profiles among T-lymphoblasts and their EVs. They also reported a short sequence motif (GGAG) enriched in EVs associated miRNAs and that among the many heterogeneous nuclear ribonucleoproteins (hnRNPs) precipitating with intracellular and EVs associated miRNAs, only hnRNPA1 and hnRNP2B1 seemed to bind exclusively the latter (Villarroya-Beltri et al., 2013). Vps4A, a key regulator of exosomes biogenesis, has been discovered to regulate the loading of oncogenic and oncosuppressor miRNAs in exosomes, favoring the inclusion of the first ones (Wei et al., 2015). Post-transcriptional modifications may also have a role in the sorting of miRNAs into EVs. In B cells, 3'end adenylated miRNAs appear to be enriched in cells compared to 3′end uridylated isoforms which are more present in exosomes (Koppers-Lalic et al., 2014). If it is known that the sorting into EVs may be passive or active, it is unclear if the secretion of these particles follows the same dual fate. Turchinovich and colleagues found a positive correlation between the content of c-miRNAs in culture media and the increase of cell death (Turchinovich et al., 2011), and Cayota group described individual miRNAs expression in intracellular fractions of MCF-7 cells correlated directly with extracellular miRNAs (Tosar et al., 2015), both supporting a passive secretion behavior of extracellular-associated miRNAs. If for the EVs uptake the mechanism is still to be elucidated – as mentioned above – the function of the miRNAs after their release in the acceptor cell has been more described and it may occur in two ways: 1) post-transcriptional regulation or 2) act as ligands. EVs associated miR-105 released from MCF10A and MDA-MB-231 cells targets ZO-1 in endothelial cells promoting lung and

brain metastasis (Zhou et al., 2014). Alternatively, miR-21 and miR-29a have been shown to be bound by toll-like receptors activating the immune system (Fabbri et al., 2012).

3. microRNAs and cancer

miRNAs are involved in many aspects related to the hallmarks of cancer (Hanahan and Weinberg, 2011). Here some examples (Figure 5).

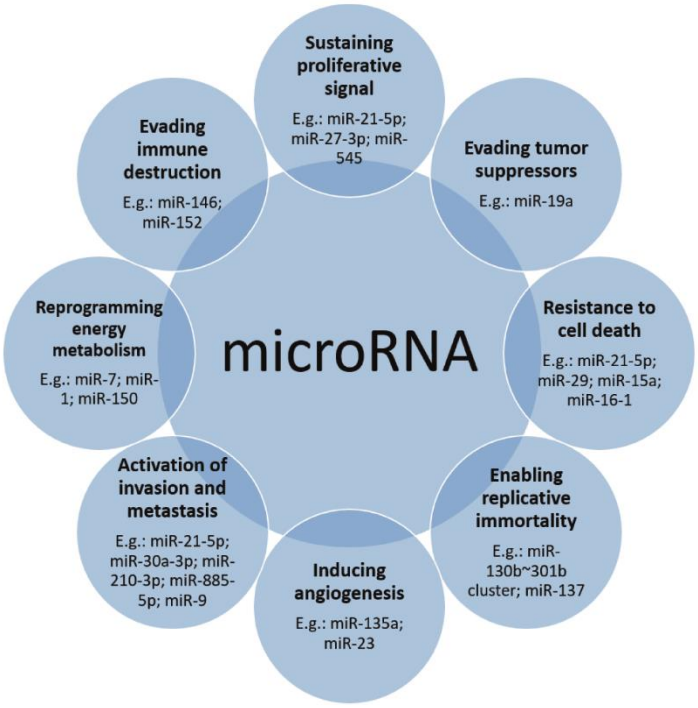

Figure 5. [Adapted from (Detassis et al., 2017)] miRNAs are involved in all hallmarks of cancer making them ubiquitary players of the disease.

1. *Sustaining the proliferative signal and evading tumor suppressors*. miRNAs have a role in carcinogenesis via cancer cell proliferation and control of dormancy in cancer cells. Dysregulation in the epigenetic players of the quiescent state, such as miRNAs, may trigger high proliferative rate and high metabolic activity of cancer cells. For instance,

patterns of differentially expressed miRNAs in dormant and non-dormant cancer cells were found in osteosarcoma, glioblastoma (Almog et al., 2013), breast cancer (Gao et al., 2014) and liposarcoma *in vivo* models (Almog et al., 2012), demonstrating the role of miRNAs in regulating quiescent and proliferative states. Indeed, miRNAs may target several positive and negative proliferative regulators. miR-27a-3p was shown to be increased in nasopharyngeal cancer compared to healthy tissues, promoting *in vitro* 5–8 F cell proliferation, migration and invasion targeting MAPK10 (Li and Luo, 2017). On the contrary, miR-545, through EGFR down-regulation, dampens proliferation and colony formation capacity *in vitro* in colorectal cancer cell lines (Huang and Lu, 2017). Tumor suppressor activity is also targeted by miRNAs in cancer dysregulation. PTEN, a well-known tumor suppressor, was shown to be regulated by the miR-17-92 cluster in lymphomas; up-regulation of c-myc induces over-expression of the miR-17-92 cluster dampening the expression of PTEN (Xiao et al., 2008) (O'Donnell et al., 2005). TIA1, involved in stress granuli formation and in the apoptotic pathway, is targeted by miR-19a promoting cell proliferation and migration in colorectal cancer cells (CRC), boosting also tumor growth in xenograft mice (Liu et al., 2017).

2. *Resistance to cell death*. Cell death may occur in several ways, mainly apoptosis, necrosis and autophagy. Cancer cells modify the normal pathways of cell death in order to continue the proliferation. It has been reported that miRNAs may have a role in this process. Intrinsic apoptotic pathway factors such as BCL2 and MCL1 are targets of miRNAs whose dysregulation may lead to cancer progression and treatment resistance (Singh and Saini, 2012) (Ji et al., 2013) (Sacconi et al., 2012) (Taniai et al., 2004). For instance, miR-29 is an endogenous regulator of MCL-1 protein expression, and it has been found down-regulated in cholangiocarcinoma cell lines (Mott et al., 2007). Similarly, miR-15a and miR-16-1, found deleted or down-regulated in the majority of

chronic lymphocytic leukemias (CLLs), can directly negatively regulate BCL-2 in CLL. Their expression was described as inversely correlated to BCL2 expression in CLL and their over-expression may induce apoptosis in a leukemic cell line model through BCL2 repression (Cimmino et al., 2005). miRNAs may also impact on extrinsic apoptotic pathways regulating TRAIL family members (Felli et al., 2005) (Galardi et al., 2007), and p53, directly (Feng et al., 2011) or indirectly (Hermeking, 2012). The endoplasmatic reticulum (ER) stress-induced apoptosis may also be affected by dysregulation in miRNAs expression. For instance, the miR-23a-27a-24-2 cluster stimulates the expression of components involved in ER, such as CHOP, TRIB3, ATF3 and ATF4 inducing apoptosis in HEK293T cells (Chhabra et al., 2011). Avoidance of necrosis may also take place via the dysregulation of miRNAs. It has been demonstrated in malignant pleural mesothelioma that the expression of miR-193a-3p, an important tumor suppressor in this cancer, is lower than in normal pleural cells and that 193a-3p is associated with the induction of necrosis (Williams et al., 2015). Cancerous cell behavior includes also aberrant autophagy. miR-26 inhibits cell autophagy of non-small cell lung cancer (NSCLC), through inhibiting TGF-β expression in a JNK-dependent manner (Guo et al., 2019). Same for miR-384 which down-regulates Collagen α-1(X) chain inhibiting cell proliferation and promoting cell autophagy in NSCLC cells (Song et al., 2017).

3. *Enabling replicative immortality.* Aberrant senescence mechanism may induce cancer progression and malignant phenotype. miR-130b~301b cluster, a regulator of senescence mechanism, is hypermethylated in prostate cancer cells (Ramalho-Carvalho et al., 2017) (Chen et al., 2015). Similarly, miR-137 levels are significantly reduced in human pancreatic cancer leading to a defective senescence response via the KDM4A pathway (Neault et al., 2016). Cancer stemness, a not yet fully understood behavior of malignant cells, which involves maintenance, reprogramming, pluripotency and

differentiation, is also partially regulated by abnormal changes in miRNAs expression (Khan et al., 2019a). For instance, miR-203, miR-375, miR-100, miR-221, miR-222 and miR-125b were found deregulated in breast cancer stem cells (Hao et al., 2014).

4. *Inducing angiogenesis*. The formation of new vessels from a pre-existing vascular network plays a central role in tumor progression, invasion and metastasis. The major players involved are regulators of growth factors or modulators of the proliferation of endothelial cells, like HIF1-alpha, VEGF, FGF and LPA (Chung et al., 2010) (Bergers and Benjamin, 2003). miRNAs normally regulate the expression of those factors for development, tissue maintenance and survival, however, aberrant miRNAs expression may impact on deviant angiogenesis supporting cancer growth. miR-135a is generally decreased in gastric cancer tissues compared to normal samples. Through the inhibition of FAK, an important regulator and effector of VEGF in tumor angiogenesis, miR-135a controls angiogenesis and thus normal cell growth. It has been described that upon miR-135a over-expression in gastric cancer cell lines, reduced levels of FAK dampen tumor growth, migration, invasion and angiogenesis (Cheng et al., 2017). Conversely, miR-23 under hypoxic conditions is up-regulated and directly targets prolyl hydroxylase 1 and 2 in lung cancer cells, enhancing the accumulation of the HIF1-alpha, ultimately increasing angiogenesis. In addition, secreted miR-23a also inhibits tight junction protein ZO-1, thereby increasing vascular permeability and cancer trans-endothelial migration (Hsu et al., 2017).

5. *Activation of invasion and metastasis*. Tumor detachment from the primary site and migration to distant sites is a crucial step in the malignancy progression, often leading to poor prognosis for the patients. miRNAs may regulate the expression of several pro-metastatic genes or metastatic suppressors. Down-regulation of miR-30a-3p and up-

regulation of miR-210-3p were significantly associated with the presence of distant metastases in RNA-seq analysis of formalin-fixed paraffin-embedded (FFPE) lung adenocarcinomas from patients with and without detectable metastasis disease (Daugaard et al., 2017) (Kumarswamy et al., 2012). miR-182, through targeting FOXO3 and MITF, metastatic suppressors, enhances the invasive and metastatic capacity of melanoma cells (Segura et al., 2009). Cancer cell adhesion plays a fundamental role in metastatic behavior. miRNAs, such as miR-200c, can target adhesion-related molecules changing invasive capabilities of cancer cells (Hurteau et al., 2007). Epithelial to mesenchymal transition (EMT) may also be aberrantly controlled by miRNAs acting on the disassembly of cellular junctions, reorganization of cytoskeleton, loss of epithelial polarity and disequilibrium in epithelial versus mesenchymal marker expression. Members of the miR-200 family have been shown to impact on the expression of ZEB transcription factor proteins, downstream molecules in the epidermal growth factor receptor (EGFR) pathway, inducing E-cadherin expression (Davalos et al., 2012). miR-885-5p targets directly the 3'UTR of CPEB2 which negatively regulates TWIST1, a well-known player in EMT (Siu-Chi Lam et al., 2017). Microarray analysis and quantitative PCR by the Law laboratory identified and validated up-regulated miR-885-5p in liver metastases when compared to primary CRCs. Furthermore, over-expression of miR-885-5p *in vitro* led to cell migration, invasion and *in vivo* development of liver and lung metastases. Alike, miR-9 may promote ovarian cancer metastasis targeting E-cadherin and upregulating N-cadherin and Vimentin, mesenchymal markers (Zhou et al., 2017). In this context of reorganization of the tumoral mass, the microenvironment is a key player and the communication between cells becomes crucial. Indeed, even if the field is still in its infancy, we know that miRNAs are used as signals between cancer cells, being released

in protein complexes or protected by microvesicles, exosomes or apoptotic bodies (Su et al., 2014). For these reasons, they are also found in biofluids (Arroyo et al., 2011).

6. *Reprogramming energy metabolism.* Fine regulation of metabolism in cells is essential for balanced cell behavior, and if not controlled, it may lead to cancer. In this regard, reactive oxygen species (ROS) are required to carry out physiological cellular functions and generally are found increased in cancer cells, mainly due to high metabolic rate in mitochondria, ER and cell membranes. In fact, high levels of ROS may oxidize DNA, leading to lesions in the genome which may contribute to the cancerous progression (Van Houten et al., 2018). The same may occur to RNA, impacting on post-transcriptional and translational regulation (Fimognari, 2015). miRNAs expression may also be affected by ROS unbalance in cells, such as miR-199a and miR-125b in ovarian cancer cells, inhibited by an increase of ROS levels (He et al., 2012). Conversely, miRNAs can alter ROS homeostasis by regulating ROS producers and antioxidants synthesis. For instance, overexpression of miR-34a is found in glioma cells to induce apoptosis through NOX2 mediated ROS production (Li et al., 2014b). Interestingly, the interplay between miRNAs and ROS might be even more complicated with a feedback regulation. For example, ROS can regulate the expression of miR-21 and miR-146a, which through targeting NFkB can regulate ROS production (Ling et al., 2012) (Zhang et al., 2012). Many other pathways of cell metabolism are hit by miRNAs. Glucose, fatty acid, amino acid and pentose phosphate pathways are regulated directly or indirectly by miRNAs (Subramaniam et al., 2019). Glucose transporter GLUT1 suppressor miR-132 has been reported to be downregulated in several cancers enhancing glucose uptake (Qu et al., 2016). miR-26a regulates pyruvate dehydrogenase protein X component decreasing its expression in CRC and thus inhibiting the conversion of pyruvate to acetyl-CoA (Chen et al., 2014). Even the fatty acid pathway is regulated by miRNAs, such as miR-125b which targets SCD-1

dampening the conversion of monosaturated fatty acids from saturated fatty acids (Cheng et al., 2016). miR-7 via LKB1-AMPK-mTOR signaling has been demonstrated to decrease the usually up-regulated metabolic autophagy in pancreatic cancer cells (Gu et al., 2017). Another tumor suppressor, miR-1, has been described to be down-regulated in CRC cell lines compared to normal colon epithelial cells. miR-1 decreases cancer cell proliferation dampening aerobic glycolysis, lactate production and glucose uptake *in vitro* targeting HIF-1α and impacting SMAD3 pathway (Xu et al., 2017).

7. *Evading immune destruction.* Bidirectional communication between cancer cells and the tumor microenvironment is a key factor in cancer development. Among all cells in the microenvironment, immune cells play a central role in cancer destruction or even progression. In fact, tumor cells may regulate the tumor microenvironment making it favorable for progression, invasion and ultimately metastasis formation. As discussed previously, miRNAs released in the tumor microenvironment may regulate its behavior transforming it in a tumorigenic site. Macrophages are crucial effectors in wound healing, immune response homeostasis and cancer. Their differentiation from lymphoid-myeloid progenitors to granulocyte-macrophage progenitors, monocytes and then mature macrophages, is, together with polarization states, one of the factors most involved in the equilibrium between pro- and anti-tumorigenic cells. miRNAs are involved in hematopoietic stem cell differentiation and therefore they can regulate macrophage development. Knockdown of miR-128a upregulates Lin28a expression reverting myeloid differentiation blockage in acute myeloid leukemia (De Luca et al., 2017), while miR-223 has been shown to promote granulocyte differentiation (Fazi et al., 2005). Polarization and activation of macrophages are also partially regulated by miRNAs (Li et al., 2018), as demonstrated by the differential expression of miRNAs in M1 to M2 macrophage transition in murine models (Lu et al., 2016). Natural killer (NK) cells,

involved in the early immune response against pathogens and tumor surveillance (Vivier et al., 2011), are regulated by miRNAs during their development and differentiation process. miR-155 targets phosphatase SHIP-1 and inhibits T-bet/Tim-3, regulating IFN-γ production in human and mouse NK cells. It may also decrease the activation of several signaling pathways such as those involving PI3K, NF-κB, and calcineurin (Sullivan et al., 2013). The same miRNA has been found downregulated after Hepatitis C virus infection leading to the release of T-bet/Tim-3, which suppresses IFN-γ production thereby helping the virus to evade immune clearance (Cheng et al., 2015). miR-183 abrogates the tumor cell killing function of NK cells by targeting DAP12 (Donatelli et al., 2014). Other types of T-cells are affected by miRNAs dysregulation. Khorrami and colleagues showed that over-expression of miR-146 in a CRC cell line co-cultured with peripheral blood mononuclear cells extracted from healthy donors, increased T_{reg} frequencies and anti-inflammatory cytokines like TGF-β and IL-10, leading to an overall immune suppression in the tumor microenvironment (Khorrami et al., 2017) (Rusca and Monticelli, 2011). On the other hand, miR-152 was shown to be decreased in gastric cancer cell lines as well as in human gastric cancer tissues. Restoration of its expression leads to enhanced T cells proliferation and effector cytokines production through the inhibition of the B7-H1/PD-1 pathway (Wang et al., 2017).

The network between cancer and miRNAs is complicated and far from being completely understood. Another level of intricacy is the likelihood of a miRNA to be involved in multiple roles in different type of cancers. For instance miR-21 has been found to a) be an anti-apoptotic factor in breast cancer (Si et al., 2007), b) increase pro-proliferative signal targeting PTEN in cholangiocarcinoma (Wang et al., 2015) (He et al., 2013a) and c) sustain EMT signaling and IL-6 levels affecting the tumor immune microenvironment (De Mattos-Arruda et al., 2015). This is mainly due to the promiscuity of miRNAs for

their target. miR-21 can target AKT and mTOR pathway (Meng et al., 2007), but also PTEN (Wang et al., 2015), FOXO1in large B-cell lymphoma (Go et al., 2015) and TPM1 which normally is considered a tumor suppressor gene, regulating microfilament formation and anchorage-independent growth in a breast cancer cell line (Zhu et al., 2007). Some miRNAs may also have a dual role, pro- and anti-tumorigenic effect, in different cancer types. miR-181a when overexpressed, was described in human glioma cells to induce apoptosis and dampen cell invasion (Shi et al., 2008) and migration in NSCLC (Cao et al., 2017), while in human gastric cancer cells, it has been reported to be an onco-miR, promoting cell proliferation, wound healing invasion and EMT targeting RASSF6 (Mi et al., 2017).

4. microRNAs as biomarkers in cancer

The post-transcriptional regulation exerted by miRNAs adds an enormous layer of complexity to cell, tissues and organs homeostasis. Their promiscuous binding affinity to mRNA targets creates a redundant network that allows finely tuned gene regulation. Being a dynamic system, any change to the canonical condition, is reflected in a change of cell behavior and vice versa. Thus, variations in miRNAs expression may give insights on the molecular events running into the tissues or organs, either physiological or pathological, making them good biomarkers (Figure 6). The definition of biomarker evolved with time and is not unique, but it could be summarized as “a characteristic that is objectively measured and evaluated as an indicator of normal biological processes, pathogenic processes, or pharmacologic responses to a therapeutic intervention” (Strimbu and Tavel, 2010). In this regard, miRNAs possess most of the characteristics of the ideal biomarker, considering analytical criteria and clinical utility. They present some

advantages over other types of molecules used as biomarkers, such as mRNAs, proteins and ctDNA and also over circulating tumor cells. miRNAs, being nucleic acids, allow the use of gold-standard RT-qPCR procedures or high-throughput RNA-seq, compared to proteins that need lengthy mass spectrometry analysis, ELISA methods or western blots. Moreover, miRNAs are usually more abundant in biofluids than other nucleic acids categories – as mentioned above – making them better targets for liquid biopsies analysis. First discoveries that expression patterns of miRNAs can discriminate groups of patients, came in the first decade of 2000, in the general attempt to classify normal and tumor tissues. Lu and colleagues implemented a bead-based profiling method in order to assess miRNAs expression in normal and tumor tissues. Specific expression fingerprints of some miRNAs could, not only distinguish tumor origin, but also the degree of differentiation and classify poorly undifferentiated tumor tissues (Lu et al., 2005). Similarly, differential miRNAs expression was also seen between adenocarcinoma (AD) and squamous cell carcinoma (SCC) tissues and between distinct prognosis (Yanaihara et al., 2006b). A wider analysis on 22 different types of tumor tissue, revealed a signature of 48 microRNAs able to reach a classification accuracy greater than 90% (Rosenfeld et al., 2008). Because of the above-mentioned complex network in which miRNAs are involved, their deregulation may be either part of a direct mechanism resulting from the aberrant behavior of tumor cells, or the indirect consequence of the tumor development, microenvironment modifications, immune system response and ongoing inflammation. As for the use of such fingerprints, researchers focused on the clinical questions arising from normal clinical settings. Thus, biomarkers in cancer may be used to 1) diagnose cancer early, 2) classify cancer origin and its molecular background, 3) predict short- and long-term prognosis, 4) predict treatment efficacy, follow-up patients after treatment and discover relapses.

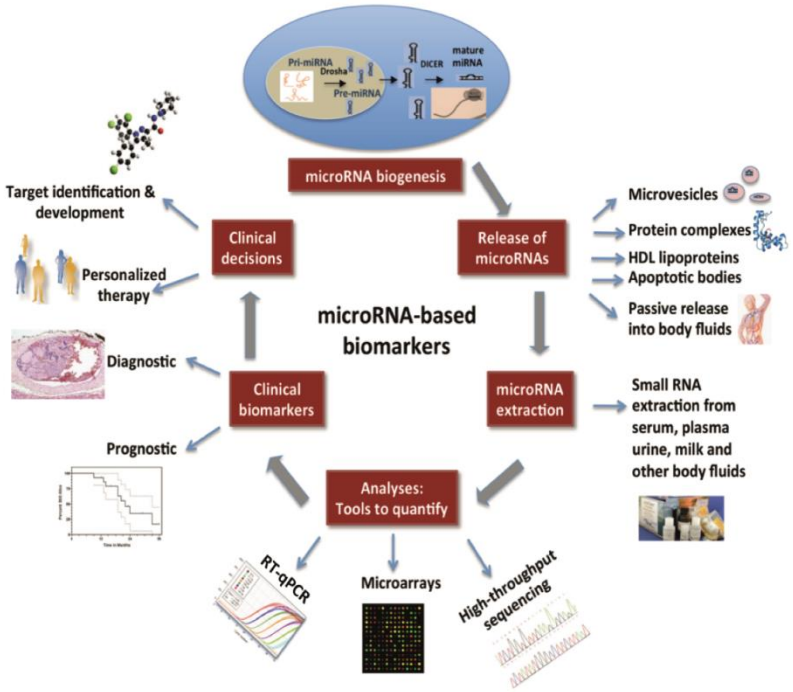

Figure 6. [Adapted from (Sundarbose et al., 2013)]. miRNAs, being involved in all cellular processes, are potentially optimal biomarkers. They can be extracted from tissues or liquid biopsies and then processed via gold-standard techniques such as RT-qPCR, microarrays and sequencing. miRNAs differential expression may have a diagnostic or prognostic value, leading clinical decisions and helping moving towards the so-called personalized medicine

1. Early diagnosis. The first study analyzing miRNAs for cancer diagnosis was published in 2002, classifying leukemia via miR-15a and miR-16-1 (Calin et al., 2008). Since then, considering their ease of use, miRNAs have been studied for several tumor classifications. miR-17/92 cluster was shown to diagnose B-cell lymphomas (Calin and Croce, 2006) and colorectal adenomas (Diosdado et al., 2009), while miR-21 is over-expressed in many cancer types (Iorio et al., 2005) (Volinia et al., 2006) (Iorio et al., 2007) (Markou et al., 2008) (Hezova et al., 2015) (Parafioriti et al., 2016) (Kapodistrias et al., 2016) (Cui et al., 2017) (Nakka et al., 2017a) (Calatayud et al., 2017) (Chen et al., 2017). Several studies pointing out the same miRNAs for different cancers raised an issue of the absence of specificity. For this reason, researchers started to investigate signatures of a pattern of miRNAs rather than single molecules to deliver a specific diagnosis. A nine miRNAs signature was able to discriminate between breast cancer tissues and normal

cancer tissues collected from TCGA, with a high accuracy value and AUC of 0.995 (Xiong et al., 2017). Another example comes from the He group which found five miRNAs (miR-424, miR-326, miR-511, miR-125b-2 and miR-451) able to provide high diagnostic accuracy of hepatocellular carcinoma starting from miRNAs expression profiles of 377 hepatocellular carcinoma patients (Lu et al., 2017). A summary is shown in Table 1.

2. Classification of tumor origin. As finding the pathological condition is relevant, the step forward is to understand what is the origin of the tumor to better address the therapy. It is well-known that each cancer type is composed of several subtypes coming from different cellular origins and each of them has to be treated accordingly. A study on muscle-invasive bladder cancer in 2016 revealed a signature of 63 miRNAs able to discriminate between basal and luminal tumors and a 15 miRNAs based signature able to show basal and luminal tumors with apparent fibroblast infiltration (Ochoa et al., 2016). Similarly, Blenkiron and colleagues performed a model-based discriminant analysis for basal-like and luminal A breast tumors finding a set of miRNAs able to discriminate between those groups (Blenkiron et al., 2007). Another approach by the Jang lab exploited the expression of 1733 miRNAs to build an unsupervised clustering in order to distinguish subtypes of pancreatic tumors. As result, they found 3 subtypes which could be associated with patient prognosis (Namkung et al., 2016). In lung cancer, in the data of the Volante lab, 10 miRNAs were able to distinguish between lung neuroendocrine (NE) tumors histotypes, 9 of which also discriminated between carcinoids and high-grade NE carcinomas (Rapa et al., 2015). In addition, the combination of miR-21 and miR-205 was found to be able to distinguish lung AD from SCC (Lebanony et al., 2009) and this can be further improved with the analysis of miR-375 (Patnaik et al., 2015). As a matter of fact, our lab demonstrated the non-perfect reliability of miR-205 in discriminating AD

versus SCC lung cancer histotypes (Del Vescovo et al., 2011). A summary is present in Table 2.

3. *Predict short- and long-term prognosis*. Understanding the aggressiveness and progression of cancer via the prognosis of the patient is of enormous relevance in clinical practice. miRNAs have been reported to evince patient prognosis in several types of cancer. A cohort of 143 lung cancer tissues was analyzed for the expression of let7 which resulted significantly down-regulated compared to normal tissues. Moreover, reduced let7 associates with higher disease stages and poor post-surgery survival and prognosis. Taking into account only the AD samples, these distinctions are maintained (Takamizawa et al., 2004). A wider analysis led to discover a 5 miRNAs signature (miR-221 and let7a protective, while miR-137, miR-372 and miR-182-3p risky) able to discriminate between NSCLC patients with higher or lower median overall survival (OS) independently from stage or histology. Moreover, this signature is also able to predict patient survival within histological type AD or SCC (Yu et al., 2008). With a similar strategy, a pattern of unique 15 miRNAs was able to discriminate between lung SCC and normal tissues, while a signature of 20 miRNAs was able to predict the OS (Raponi et al., 2009). Some of these miRNAs were more significant, like miR-146b which had the highest prediction score within 3 years, and some had already been linked to lung cancer in other studies like let-7 and miR-155 (Yanaihara et al., 2006a). Interestingly, in all these studies, the different isoforms of let-7 found, were down-regulated in patients with poor prognosis. More recent data show that low expression of miR-448 associates with lung SCC progression and poor patients' overall survival (Shan et al., 2017). Reduced expression of miR-383 was found in NSCLC tumor tissues compared to adjacent non-tumorous samples and moreover, low miR-383 expression associated with poor post-operative prognosis (Shang et al., 2016). miR-448 and miR-383 are down-regulated, acting like tumor-suppressors,

also in ovarian cancer (Lv et al., 2015), hepatocellular carcinoma (Zhu et al., 2015) (Chen et al., 2016a), colorectal cancer (Li et al., 2016), breast cancer (Li et al., 2011), Hodgkin lymphoma (Paydas et al., 2016), glioma (He et al., 2013b) (Xu et al., 2014) testicular carcinoma (Huang et al., 2014) (Lian et al., 2010) and medulloblastoma (Li et al., 2013). Another study revealed that miR-187 expression was significantly increased in NSCLC tissue samples compared to adjacent non-lung tumor tissues and that this condition associated with TNM classification and shorter OS (Peng et al., 2016). A summary is present in Table 3.

4. *Predict treatment efficacy, follow-up patients after treatment and discover relapses.* As a consequence of the intricacy of underlying driving mechanisms of cancer, the therapeutic efficacy of a single treatment can change depending on the patient and its type of cancer. miRNAs have been associated with, and also predictive of, therapeutic outcome. miR-21 seems to be a general signal for chemotherapy resistance. In 2008, Schetter and colleagues found that miR-21 expression, in typical colon AD from patients treated with fluorouracil based adjuvant chemotherapy, is higher in patients with a poor therapy outcome (Schetter et al., 2008) (Schetter et al., 2009). Similar results were obtained for pancreatic cancer (Hwang et al., 2010). Even in lung cancer, high-expression of miR-21 was associated with chemotherapy resistance in tissues of patients who had undergone platinum-based chemotherapy treatment (Gao et al., 2012). It was shown that A549/DDP lung AD cell line has lower expression of eIF3a compared to its parental cell line, and it displays chemoresistance to cisplatin. Other miRNAs are also involved. miR-488 targets the 3'UTR of eIF3a transcript enhancing sensitivity to the treatment and inhibiting cell proliferation, migration and invasion (Fang et al., 2017) (Fang et al., 2016). Another study reported increased sensitivity of A549/DDP cells to cisplatin after up-regulation of miR-138. Increased levels of miR-138 correlated with the down-regulation

of ERCC1 in A549/DDP cells (Wang et al., 2011). In another study on pancreatic ductal AD, patients with resectable or locally advanced disease showed relative low miR-10b expression associated with highly predictive response to gemtabicine based multimodality neoadjuvant chemoradiotherapy. Moreover, by logistic regression, low miR-10b expression was able to predict surgery efficacy (Preis et al., 2011). In CRC, miR-148 expression had the potential for predicting therapeutic efficacy of 5-fluorouracil and oxaliplatin in stage IV patients, as low levels of this miRNA associated with a bad therapeutic response (Takahashi et al., 2012). Besides chemotherapy, targeted therapy is an important standard of care for several tumors. Even in this field, miRNAs may be helpful. In a cohort of metastatic CRC patients wild type for KRAS and BRAF, a miR-31-3p up-regulation and miR-592 down-regulation were found associated with poor response to anti-EGFRmAb (Mosakhani et al., 2012). An Italian study reported a signature of three miRNAs (miR-let7c, miR-99a and miR-125b) able to predict EGFR monoclonal antibody therapy outcome in colorectal cancer patients. Indeed, high-level of the signature expression showed a good discrimination capacity for patients which were more responsive to cetuximab or panitumumab compared to low responsive patients (Cappuzzo et al., 2014). In two independent studies, miR-31 was found to be associated with PFS after the administration of anti-EGFRmAb in metastatic colorectal cancer patients. Mlchocova and colleagues found both miR-31-5p and -3p, while Shinomura group only miR-31-5p, to be higher in patients with lower PFS compared to those with low levels of the miRNA (Mlcochova et al., 2015) (Igarashi et al., 2015). miRNAs have been discovered to be predictive also of kinase inhibitors efficacy in hepatocellular carcinoma, renal cell carcinoma and NSCLC (Li et al., 2014a) (Garcìa-Donas et al., 2016) (Nishida et al., 2017). An emerging field in cancer treatment is immunotherapy. Some studies describe miRNAs as biomarkers of immunotherapy efficacy. In a report on 82

renal cancer patients and 19 healthy individuals, miR-183 has been found up-regulated in sera associated to less efficacious cancer cytotoxicity by natural killer cells, which are the effectors of the IL-2 immunotherapy (Zhang et al., 2015b). Nagano group described that miR-6826 and miR-6875 can be good predictor of vaccine treatment efficacy in metastatic CRC, where high expression in plasma of the two miRNAs was associated with poorer prognosis (Kijima et al., 2016). A summary is present at Table 4.

In diagnostics, liquid biopsies possess the high potential to make a difference in clinical settings (Lianidou and Pantel, 2019). Minimally invasive approaches are desirable such as plasma or urine samplings (Maxim et al., 2014). Because of their stability in body fluids c-miRNAs as biomarkers have some advantages increasing the feasibility of their use in clinical applications (Mitchell et al., 2008). C-miRNAs from liquid biopsies have been reported to be biomarkers for cancer screening, diagnosis, prognosis and to drive treatment decisions (Chen et al., 2008) (Giannopoulou et al., 2019). For instance, miR-15a, miR-15b and miR-27b were identified in serum as potential diagnostic markers of NSCLC patients (Hennessey et al., 2012). In plasma a signature of 12 miRNAs discriminates NSCLC patients from healthy subjects, and three of them can also distinguish between computed tomography (CT)-identified NSCLC and benign pulmonary nodules (Shen et al., 2011).

The redundancy of miRNAs found in the literature with different discriminatory capacity for the same cancer type or same miRNAs having contradictory roles in different tumors, made evident that the complexity of post-transcriptional regulation exerted by the miRNAs is a double-edged sword for biomarker purposes. The limitations come from both a biological and a technological side. Biologically speaking, more accurate sources from where miRNAs are analyzed, might be a partial answer. Even if plasma and serum

are the most used liquid biopsies in c-miRNAs studies, because of their well-radicated uses in clinical settings, an effort to exploit more biologically meaningful biofluids in a disease-dependent manner has increased. Urine, has been recently used for prostate (Lewis et al., 2014) and renal illnesses. Urinary miR-328-3p shows putative discriminatory capacity in renal cell carcinomas against small renal masses (Di Meo et al., 2020). Seminal fluid is also studied for similar purposes in prostate cancer detection (Selth et al., 2014). Alike, saliva, produced by the salivary glands, has been proposed as a source of biomarkers for oral cancers (Ghizoni et al., 2019). For instance salivary miR-21 and miR-184 were found upregulated in oral squamous cell carcinomas compared to healthy individuals (Zahran et al., 2015). For neuro-oncology CSF is likely the most relevant biofluid since it passes through the central nervous system collecting a plethora of possible tumor-related markers (Sindeeva et al., 2019). miRNAs expression in CSF was found to correlate with the miRNAs expression in glioblastoma tumors and a nine miRNAs signature discriminated cancer patients from healthy subjects (Akers et al., 2017). Following the same reasoning, EVs have been recently used more frequently since they may be specific of a cell type and reflect this difference for miRNAs expression (Ingenito et al., 2019). A four exosomal miRNAs signature was reported to early diagnose NSCLC patients (Jin et al., 2017) and miR-182 was found in exosomes from sera of prostate cancer patients (Mihelich et al., 2016). Interestingly, CSF EVs showed some specific miRNAs not found in the serum of the same healthy donors (Yagi et al., 2017). However, even for EVs fraction some miRNAs, such as miR-21, are found similarly deregulated in several cancer types (Hannafon et al., 2016) (Shi et al., 2015) (Mousavi et al., 2019) (Tanaka et al., 2013) (Au Yeung et al., 2016). Another helping factor may reside on exploiting the specific and unique origin of some miRNAs, such as the hepatic miR-122 (Thakral and Ghoshal, 2015) (Dear, 2018) (Rivoli et al., 2017).

Table 1. Summary of analyzed studies for miRNAs as biomarkers in “Early diagnosis”. When -3p or -5p is not specified, it was not clearly reported. “Not specified” refers to incomplete information on tissue type.

miRNA	Patients	Cancer	Tissue type	Reference
22-miRNAs signature	Pancreatic ductal adenocarcinoma (n=165), ampullary cancer (n=59), duodenal cancer (n=6), distal common bile duct cancer (n=21), and gastric cancer (n=20); chronic pancreatitis (n=39); and normal pancreas (n=35)	Pancreatic cancer	FFPE	Catalayud et al. 2017
miR-486-3p, -486-5p, -21-5p, 139-5p, -204-3p, -489-3p, -223-3p, -196b-5p, -31-5p, -422a, -328-3p, -146b-5p	Toung squamous cell carcinoma and matched controls (n=25)	Toung squamous cell carcinoma	FFPE	Chen et al.2017
miR-21-5p	Wilms' tumor and paired homolateral adjacent non-tumorous renal tissue (n=41)	Wilms' tumor	Flash-frozen	Cui et al. 2017
miR-17-92 cluster	Colorectal tumors (n=55) and controls (n=10)	Colorectal cancer	Fresh tissue	Diosdado et al. 2009
miR-21-5p, -203-3p	Esophageal adenocarcinoma (n=23), esophageal squamous cell carcinomas (n=22), adjacent esophageal mucosa (n=17)	Esophageal cancer	Not specified	Hezova et al.2015
miR-21-5p, -155-5p, -10b-5p, -125b, -145-5p	Breast tumor (n=76), six pools of five normal breast tissue each and four additional single breast tissue	Breast cancer	Not specified	Iorio et al. 2005
miR-200a-3p, -141-3p, - 200c-3p, -200b-3p, -199a, -140-3p, -145-5p, -125b-1-5p	Serous ovarian cancer (n=31), endometrioid (n=8), clear cell (n=4), poorly differentiated (n=9), mucinous carcinoma (n=1), normal ovary (n=15)	Epithelial ovarian cancer	Flash-frozen	Iorio et al. 2007
miR-155-5p, -21-5p, -145-5p, -143-3p, -451	Liposarcoma (n=62), lipoma (n=21)	Liposarcoma	FFPE	Kapodistrias et al. 2017
33-miRNAs signature	Hepatocellular carcinoma (n=377), normal control (n=37), tumor and matched non-tumor (n=37)	Hepatocellular carcinoma	TCGA plus tissues	Lu et al. 2017
miR-21-5p, -205-5p	Non small cell lung cancer and matched controls (n=48)	Non small cell lung cancer	Flash-frozen	Markou et al. 2008
miR-21-5p, -221-3p, -106a-5p	Osteosarcoma (n=61), healthy (n=25)	Osteosarcoma	Plasma	Nakka et al. 2017
miR-181b, -1915-5p, -1275-5p	Ewing's sarcoma (n=20), normal donor (n=4)	Ewing's sarcoma	FFPE	Parafioriti et al. 2016
Multiple-miRNAs signature	Lung cancer (n=123), breast cancer (n=79), colon cancer (n=46), gastric cancer (n=20), endocrine pancreatic cancer (n=39), prostate cancer (n=56), healthy (n=177)	Multiple cancer	Not specified	Volinia et al. 2006
miR-21-5p, -96-5p, -183-5p, -182-5p, -141-3p, -200a-3p, -429 -3p, -139-5p, -145-5p	Breast cancer (n=1110), healthy (n=104)	Breast cancer	TCGA database	Xiong et al. 2017

Table 2. Summary of analyzed studies for miRNAs as biomarkers in “Classification of tumor origin”. When -3p or -5p is not specified, it was not clearly reported. “Not specified” refers to incomplete information on tissue type

miRNA	Patients	Cancer	Tissue type	Reference
137-miRNAs signature	Breast cancer (n=99), normal tissue (n=5)	Breast cancer	Flash-frozen	Blenkiron et al. 2007
miR-205-5p, -21-5p	Adenocarcinoma (n=25), Squamos cell carcinoma (n=24), adenonosquamous carcinoma (n=1)	Non small cell lung cancer	FFPE	Del Vescovo et al. 2011
miR-205-5p, -21-5p	Adenocarcinoma (n=60+8+15), squamous cell carcinomas (n=62+8+12+27), large cell lung carcinoma (n=4), nonsquamous (n=52)	Non small cell lung cancer	FFPE	Lebanony et al. 2009
19-miRNAs signature	Pancreatic cancer (n=104)	Pancreatic cancer	Flash-frozen	Namkung et al. 2015
63-miRNAs signature	Basal bladder cancer (n=28), luminal bladder cancer (n=34)	Bladder cancer	Flash-frozen	Ochoa et al. 2016
miR-205-5p, -375-3p	Adenocarcinomas (n=57), squamous cell carcinoma (n=45)	Non small cell lung cancer	FFPE	Patnaik et al. 2015
miR-129-5p, -409-3p, -409-5p, -431-5p, -185-5p, -22-3p, -497-5p, -129-3p, -15a-5p, -141-3p	Typical carcinoid (n=28), atypical carcinoid (n=21), neuroendocrine carcinoma (n=19)	Non small cell lung cancer	Flash-frozen	Rapa et al. 2015

Table 3. Summary of analyzed studies for miRNAs as biomarkers in “Predict short- and long-term prognosis”. When -3p or -5p is not specified, it was not clearly reported. “Not specified” refers to incomplete information on tissue type.

miRNA	Patients	Cancer	Tissue type	Reference
miR-383	Hepatocellular carcinoma and matched normal tissue (n=64)	Hepatocellular carcinoma	Flash-frozen	Chen et al. 2015
miR-448	Colorectal cancer and matched normal tissue (n=28)	Colorectal cancer	Flash-frozen	Li et al. 2016
15-miRNAs signature	Squamous cell lung carcinoma (n=61), normal tissue (n=10)	Non small cell lung cancer	Flash-frozen	Raponi et al. 2009
miR-187	Non small cell lung cancer and adjacent non-tumor (n=74)	Non small cell lung cancer	Flash-frozen	Peng et al. 2016
miR-448-5p	Squamous cell lung carcinoma (n=140), normal tissue (n=20)	Non small cell lung cancer	Flash-frozen	Shan et al. 2017
miR-383-5p	Non small cell lung cancer tissues and adjacent non-tumor tissue (n=139)	Non small cell lung cancer	Flash-frozen	Shang et al. 2016
let-7	Adenocarcinomas (n=105), squamous cell carcinomas (n=25), large cell carcinomas (n=9) and adenosquamous cell carcinoma (n=4)	Non small cell lung cancer	Flash-frozen	Takamizawa et al. 2004
miR-221-3p, -let-a, -137-3p, -372-3p, -182-3p	Non small cell lung cancer (n=174)	Non small cell lung cancer	Flash-frozen	Yu et al. 2008
miR-155-5p, -let7-a-2-5p	Non small cell lung cancer tissues and adjacent non-tumor tissue (n=136)	Non small cell lung cancer	Not specified	Yanaihara et al. 2006
miR-448-5p	Hepatocellular carcinoma tissues and adjacent non-tumor tissue (n=117)	Hepatocellular carcinoma	Not specified	Zhu et al. 2015
miR-383-5p	Glioma (n=16), normal brain (n=8), glioma and matched controls (n=6)	Glioma	Not specified	Zhou et al. 2014

Table 4. Summary of analyzed studies for miRNAs as biomarkers in “Predict treatment efficacy, follow-up patients after treatment and discover relapses”. When -3p or -5p is not specified, it was not clearly reported. “Not specified” refers to incomplete information on tissue type.

miRNA	Patients	Cancer	Treatment	Tissue type	Reference
miR-let7-c-5p, -99a-5p, -125b	Colorectal cancer (n=183)	Colorectal cancer	Anti-EGFR	FFPE	Cappuzzo et al. 2014
SNP of miR-5197, -605-5p, -146a-5p, -27a-3p	Non smal cell lung cancer (n=408)	Non small cell lung cancer	Platinum-based chemotherapy	Whole blood	Fang et al. 2016
miR-21-5p	Non small cell lung cancer tissues (n=58) and matched plasma (n=32)	Non small cell lung cancer	Platinum-based chemotherapy	Flash frozen and plasma	Gao et al. 2012
miR-1307-3p, -221-3p, -155-5p	Renal cell carcinoma (n=138)	Renal cell carcinoma	Tyrosine kinase inhibitor	FFPE	Garcia-Donas et al. 2016
miR-21-5p	Treated pancreatic cancer (n=52), non-treated pancreatic cancer (n=27)	Pancreatic cancer	Adjuvant chemotherapy, combined chemoradiotherapy or both	FFPE	Hwang et al. 2010
miR-31-5p	Colorectal cancer (n=102)	Colorectal cancer	Anti-EGFR	FFPE	Igarashi et al. 2015
miR-200c-3p	Non small cell lung cancer (n=150)	Non small cell lung cancer	Tyrosine kinase inhibitor	FFPE	Li et al. 2014b
miR-31-5p, -31-3p	Colorectal cancer (n=93)	Colorectal cancer	Cetuximab	FFPE	Mlchocova et al. 2015
miR-181a-5p, -339-5p	Hepatocellula carcinoma (n=69), healthy control (n=8)	Hepatocellular carcinoma	Sorafenib	Serum	Nishida et al. 2017
miR-6826-5p, -6875-3p	Colorectal cancer (n=93)	Colorectal cancer	Vaccine	Plasma	Kijima et al. 2016
miR-10b-5p	Pancreatic ductal adenocarcinoma (n=105), benign pancreatic ductal adenocarcinoma (n=14)	Pancreatic cancer	Neoadjuvant gemcitabine-based chemoradiotherapy	FFPE	Presi et al. 2011
miR-31-3p, 592-5p, -140-5p, -1224-5p, -let7 family	Colorectal cancer (n=33)	Colorectal cancer	Anti-EGFR	Not specified	Mosakhani et al. 2012
miR-21-5p	Colon adenorcinoma and adjacent non tumorous tissue (n=197)	Colon cancer	Fluorouracil based adjuvant chemotherapy	Flash frozen and plasma	Schetter et al. 2008
miR-148a-3p	Colorectal cancer (n=273) and normal colonic mucosa of healthy individuals (n=20)	Colorectal cancer	5-fluorouracil-based adjuvant chemotherapy and 5-fluorouracil and oxaliplatin-based chemotherapy	FFPE	Takahashi et al. 2012

5. Technical limitations of c-miRNAs as tools for personalized medicine

If biological complexity is difficult to fully comprehend and thus, difficult to exploit, the current technical limitations in c-miRNAs analysis make these tools impracticable for clinical settings. In fact, despite the growing interest of the scientific community, the enormous amount of articles published in recent years (entry "circulating microRNAs cancer biomarker" on PubMed; 2012 = 123; 2013 = 189; 2014 = 254; 2015 = 335; 2016 = 329; 2017 = 338; 2018 = 356; 2019 = 310) has been not translated in clinical assays yet. The limiting factors may be divided in three categories: 1) pre-analytical, 2) analytical and 3) post-analytical (Table 5) which lead to a lack of standardized procedures and eventually strong pitfalls in miRNAs quantification (Sourvinou et al., 2013).

1) Pre-analytical factors. As miRNAs reflect pathological and physiological changes, levels of expression may be varied by several factors which ultimately can influence the assay results. In fact, it has been suggested that in plasma, smoking status (Takahashi et al., 2013), diet (Witwer, 2012), active exercise (Baggish et al., 2011) and circadian rhythm - in sera of mice (Shende et al., 2011) - can affect the total levels of c-miRNAs. Moreover, it is reasonable to add that comorbidities may also be confounding factors (Neal et al., 2011). On the other hand, gender, menstrual cycle and food intake do not affect total c-miRNAs levels in plasma and serum (Max et al., 2018). In urine, time of voids does not seem a variable to consider, while gender and fractionation of the sample (EVs vs sediment cells) may be important (Ben-Dov et al., 2016). On top of that, inter-individual variability should be taken into account considering that the concentration of miRNAs in plasma can be counted as from 9000 to 130.000 copies per uL (Mitchell et al., 2008). Thus, patient's condition and habits are a factor of variability

which may be reduced by worldwide standardized clinical protocols for liquid biopsies sampling and more rigorous and transparent criteria for scientific publications, helping reproducibility. Sample collection techniques may be critical. Blood collection has been the most studied protocol for c-miRNAs expression variation. General factors are a) venipuncture which may cause haemolysis, b) time from sampling and processing, c) choice of plasma or serum and d) if plasma, the choice of the anti-coagulant. Tewari group showed that blood cells are the major contributor to c-miRNAs, therefore variations in blood cells counts and haemolysis can affect the interpretation of c-miRNAs signatures. They studied several oncological biomarkers reported in literature: many of them are highly expressed in blood cells. They demonstrated that this kind of c-microRNAs correlates with blood cell counts and that miR-122, which is not expressed in blood cells, doesn't follow this trend. Moreover, in haemolyzed plasma samples, red blood cell-associated miRNAs vary up to 30-fold compared to non-hemolyzed samples, further proving that c-miRNAs pool is affected by blood cells composition (Pritchard et al., 2012). Duttagupta and colleagues tried to discriminate between whole blood miRNAs derived from blood cells - "contaminant miRNAs" - and what they called "truly circulating microRNAs". Starting from whole blood samples and collecting different fractions from multiple centrifugation steps they found that from the first fraction (cloudy supernatant) to the second one, the content of the "contaminant microRNAs" dropped, while the true c-miRNAs content stays more or less unchanged. On top of that, they showed that the variability of expression of marker c-miRNAs among a cohort of males and females decreases after the removal of the cellular contaminants originated from cellular miRNAs signatures (Duttagupta et al., 2011). This points out how much the processing of the samples may affect the pool of c-miRNAs. Another study (Cheng et al., 2013) confirmed this variability, reporting that different plasma processing led, for the

majority of c-miRNAs, to a variation in their expression levels, mainly due to different platelets and microvesicles content. Moreover, the choice of the anti-coagulant for plasma separation may have an impact, inhibiting some steps downstream of the sample collection (Bottani et al., 2019) (Boeckel et al., 2013). Not only c-miRNAs are affected by sample preparation and storage. Tissue samples may be generally prepared and stored as FFPE or as flash-frozen. Formalin fixation may introduce some biases in the stability of miRNAs depending on their GC content (Kakimoto et al., 2016) and moreover, the concordance between the FFPE and flash-frozen samples is lost during time (years) creating discrepancies in analysis done with one type of preparation or the other (Meng et al., 2013) (Szafranska et al., 2008).

2) Analytical factors. The analysis of c-miRNAs has to pass through two main steps: a) the extraction of RNA (except for some new assays developed (Asaga et al., 2011) (Songia et al., 2018)) and b) the detection of the miRNAs. Different extraction kits have distinct efficiencies in small RNAs recovery (Monleau et al., 2014) and moreover, the guanidium thiocyanate plus phenol-chloroform RNA extraction suffer from several limitations. In this context, the use of an exogenous control such as cel-miR-39 may be helpful in standardizing sample-to-sample variation after sample collection (Sourvinou et al., 2013). However, Kim group in 2012 showed that miRNAs low in GC content are extracted via TRIZOL-based protocol in a total RNA concentration-dependent manner, posing the basis for a sequence-dependent RNA extraction efficiency. Starting from a lower number of cells some miRNAs were retained during RNA extraction misleading differential expression results (Kim et al., 2012). Regarding the detection methods, RT-qPCR, ddPCR, microarrays and NGS are the main technologies used. Despite the fact that they are universally accepted for nucleic acid analysis, several pitfalls dampen the reliability and the reproducibility of these techniques required for clinical settings. The

reverse transcription step has been shown to create high variability depending on the target (Ståhlberg et al., 2004). The main source of problems is the nature of amplification-based technologies, which rely on primer hybridization and enzymatic amplification. Primer design for miRNAs is complicated because of their short sequence. Accurate single sequence-dependent primer selection can increase the specificity of the amplification, whilst decreasing the throughputness of the assay. On the other hand, methods relying on universal primers may introduce amplification biases for sequences with optimal temperature of melting (Tm) and decrease specificity for very similar miRNAs. Moreover, discrimination between pri-, pre- and mature forms becomes difficult. Even in PCR-free techniques like microarrays the labelling of the target together with probe Tm may constitute a source of variability (Chugh and Dittmer, 2012).

3) Post-analytical factors. Except for ddPCR, the detection techniques rely on relative quantification, thus a normalization method is necessary. For miRNAs the choice of a good normalizer is tricky and, if incorrect, it may mislead differential expression results (Masè et al., 2017). The most used in literature are miR-16, snRNA U6 and spiked-in cel-miR-39, but there is no general consensus from the scientific community. For instance, among the several transcripts of U6, U6-1 was found to have high variability and U6-2 was not detectable, in a study on sera from Hepatitis B infected patients and matched controls (Zhu et al., 2012). In two different plasma studies on CRC, miR-16 was found to have quite high stability and little variability between control and case-patients (Huang et al., 2010) (Ng et al., 2009). In another case, it has been reported, in serum samples from lung cancer patients, miR-16 being inconsistent (Chen et al., 2008). Several authors have concluded that a universal endogenous control is unlikely to be discovered and a suitable reference should be assessed every time considering the different biological conditions of the samples. However, cost and sample requirements needed for the choice

of several reference RNAs are not always possible, especially in a clinical or diagnostic setting. Other strategies involve the use of a set of normalizers instead of a single one or normalizations based on mathematics such as quantile normalization, geometric mean normalization, cycle loess , rank-invariant normalization and weighted normalization (Rao et al., 2008) (Bolstad et al., 2003) (Qureshi and Sacan, 2013). Softwares have been implemented for the selection of the best normalizer from a set of genes, such as Normfinder, geNorm and BestKeeper, all having similar performances (De Spiegelaere et al., 2015).

Table 5. miRNAs analysis presents several challenges. Pre-analytical, analytical and post-analytical factors may have a fundamental impact on the variability and decrease reproducibility

Step of analysis	Challenges	
Pre-analysis	Subject status (e.g.: gender, smoking status) and physiological condition before sampling (e.g.: food intake, menstrual cycle, time of urine void, circadian rhythm)	All the limitations lead to a lack of standardized procedures and eventually strong pitfalls in miRNAs quantification
	Type of sample (e.g.: plasma, serum, saliva, FFPE, flash-frozen tissues)	
	Sample collection (e.g.: haemolysis, time from sampling to processing)	
	Sample processing (e.g: centrifugation steps)	
Analysis	RNA extraction: different commercial kits	
	Primer design: difficult with miRNAs	
	Retrotranscription: specific primers or universal primers	
	Melting temperature of probes for microarrays	
	Loss of sensitivity at single-base level	
Post-analysis	Choice of the normalizer	

6. DestiNA Genomics Chem-NAT

In the panorama of emerging technologies for nucleic acid detection DestiNA Genomics patented an innovative chemical method (Chem-NAT) (Bowler et al., 2010a). In the first demonstration they showed, using synthetic DNA resembling cystic fibrosis mutations, the ability to discriminate different targets with a single-base resolution. The chemistry is based on peptidic nucleic acid (PNA) probes complementary to the target of interest and aldehyde-modified nucleobases (SMART-NB). The PNA probes present an abasic site that exposes a free secondary amine. The aldehyde of the SMART-NB reacts with the secondary amine of the PNA molecule creating an iminium intermediate which can be further reduced. For Chem-NAT to happen two main events must occur (Figure 7): 1) the hybridization of the target to the PNA probe and 2) selective incorporation of the right SMART-NB. The incorporation of the SMART-NB, following the standard Watson-Crick base pairing rules, is a dynamic event for which potentially all the four possible SMART-NB can enter. However, only the right one is favored and eventually sufficiently stable to enter the abasic site and be covalently bound by the reduction. This reaction serves for 1) allowing the specific recognition of a target with a single-base resolution and 2) labeling the PNA probe when the right target hybridizes to it. Once the PNA probe is labeled by the SMART-NB, the detection may be done with any methodology, depending on the type of second modification the SMART-NB bears (e.g.: biotin, AP).

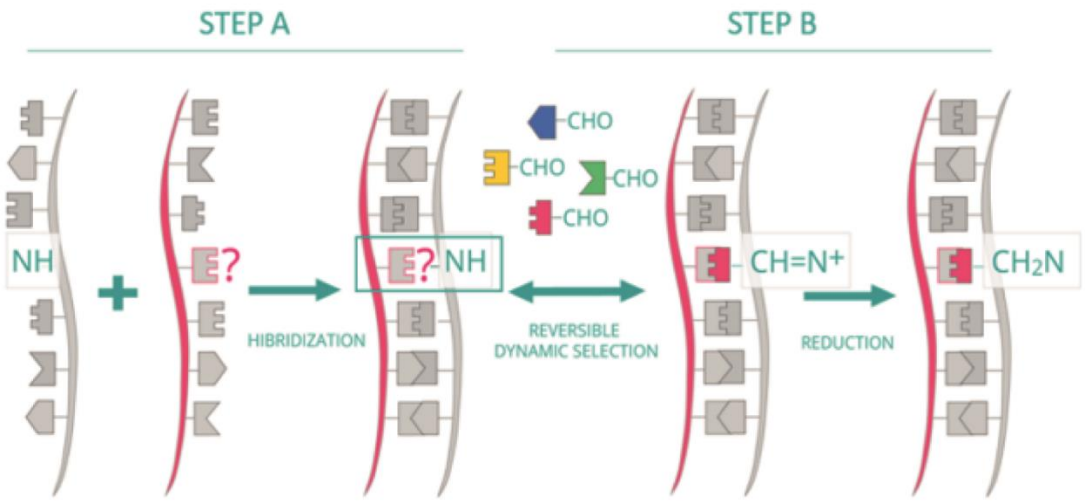

Figure 7. Chem-NAT enables the detection of a nucleic acid target (red helix) via a modified PNA probe (grey helix) with an abasic position (-NH). Two steps are required: STEP A) capturing of complementary nucleic acid, forming a chemical pocket (indicated by the rectangle); STEP B) selective incorporation of the correct SMART-NB. A reduction reaction locks the SMART-NB covalently within the abasic PNA probe (Detassis et al., 2019).

The technology has been validated in several contexts and it followed a development during the time this work has been performed. Chem-NAT started detecting a 155 base pair segment of the 28S ribosomal RNA gene, within a conserved homology region of Trypanosomatidae species (Angélica Luque-González et al., 2018). In this case, after PCR amplification of the region of interest, Chem-NAT was applied to distinguish among different Trypanosoma species and the SMART-NB was detected via MALDI-ToF. Subsequently, Chem-NAT evolved in the need of avoiding nucleic acid extraction and PCR amplification for reducing assay steps and possible sources of variability. Following this reasoning, miR-21 has been analyzed via Chem-NAT in lung and breast cancer cell lines via FACS (Delgado-Gonzalez et al., 2019). Since clinical diagnostics is moving towards the use of liquid biopsies, the technology has been tested – starting from this work – for the direct detection of miRNAs – no RNA extraction nor PCR amplification - in biofluids. Apart from the data produced in this work (Detassis et al., 2019) with miR-21, miR-122 was directly detected in serum of drug-induced liver injury patients without

PCR-amplification (Rissin et al., 2017) and also without RNA extraction (López-Longarela et al., 2020), as well as miR-451 in whole blood of healthy volunteers (Marín-Romero et al., 2018).

6.1 PNA chemistry

Nucleic acid biosensors use, as probes, DNA, RNA or synthetic analogs, generally exploiting base-pair hybridization. They are mostly adopted for genotyping and gene expression studies. Many of the current applications take advantage of synthetic polymers analog which carries several specific characteristics, overcoming limits of natural nucleic acid nature and enabling high specificity and sensitivity in biosensing systems. In particular, PNA and locked nucleic acid (LNA) have been used frequently because of their peculiar features. PNA, has a peptide backbone, which is the result of the polymerization of N-(2-aminoethyl) glycine units: each base is connected through a methylencarbonyl linkage. The PNA backbone is devoid of electrical charges and thus this molecule has a high affinity for its complementary DNA or RNA. Crystal structure of PNA binding DNA or RNA has been resolved. The heteroduplex formed by PNA/DNA creates double helices in A and B form (Menchise et al., 2003) while the heteroduplex PNA/RNA leads to an A double helix (Brown et al., 1994). PNA oligomers have higher affinity for their complementary DNA molecules compared to the equivalent ssDNA (Kuhn et al., 2002). The thermal stability of a nucleic acid duplex is: DNA/DNA < PNA/DNA < PNA/RNA < PNA/PNA (Ratilainen et al., 2000) both in antiparallel orientation (N-terminus of PNA corresponding to the 3'end of DNA or RNA) and in parallel orientation. This interaction is highly specific and, virtually, for every mismatch the loss in terms of thermal stability is higher in PNA/DNA-RNA compared to the

corresponding homoduplex. For a 9-12mer PNA molecule, a single mismatch with the complementary DNA leads to a drop of the melting curve to 15-20°C (Ratilainen et al., 2000). PNA is also insensitive to nuclease, peptidase and changes in pH or ionic strength, making it a very good candidate for biosensoristic applications (Briones and Moreno, 2012). In the last two decades, PNA molecules have been used in several different platforms for nucleic acid detection. In 1996, Wang and colleagues used a 15-mer PNA probe to detect DNA targets via a carbon-paste electrode transducer and redox indicators. In their work, there is one of the first attempts to recognize the value of PNA specificity in biosensors and single-mismatched DNA oligomers were detected with 3% of the signal generated by full complementary targets (Wang et al., 1996). Since then, improvements have been made in generating electrochemical systems with PNA-based methodologies (Raoof et al., 2011) (Hejazi et al., 2010). PNA molecules have also been used for blocking DNA polymerases in PCR reactions. In fact, exploiting the high specificity of such molecules, the discriminations between two SNPs with PCR was delivered by "hiding" one isoform with the PNA probe which would not allow the priming for DNA polymerase, resulting in the amplification of only the desired target (Kerman et al., 2006). Even microarrays systems took advantage of the PNA unique hybridization properties. In an attempt to avoid the labeling of the target, the peptidomimic nature of PNA molecules has been used for creating physicochemical signatures of phosphate and/or sugars upon DNA or RNA target hybridization (Brandt and Hoheisel, 2004). Detection of proteins was possible indirectly with PNA probes. ssDNA aptamers binding to the protein of interest were released from the protein by heating and measured via PNA probes (Le Floch et al., 2006). Other PNA-based sensors have been reported for the detection of miRNAs, the main focus of this work. For instance, Wu and colleagues reported the analysis of miRNAs in a highly sensitive and label-free method via PNA-functionalized

silicon nanowires, reaching a limit of detection of femtomoles (Zhang, 2011). Similarly, another group studied the detection of miRNAs without PCR amplification or ligations steps achieving a limit of detection of 10pM (Gao and Peng, 2011).

7. Optoi Microelectronics SiPM-based reader

Chem-NAT is an agnostic technology, meaning that it may be analyzed with different reading platforms. The choice of the reader has clearly an enormous impact on the application of the whole technology. Since our goal was to develop a bench-top solution for c-miRNAs analysis, the reader had to be, sensitive, small, compact and cost-effective. Optoi Microelectronics (Optoi) has developed an eight micro-wells silicon photomultiplier (SiPM)-based reader (Figure 8).

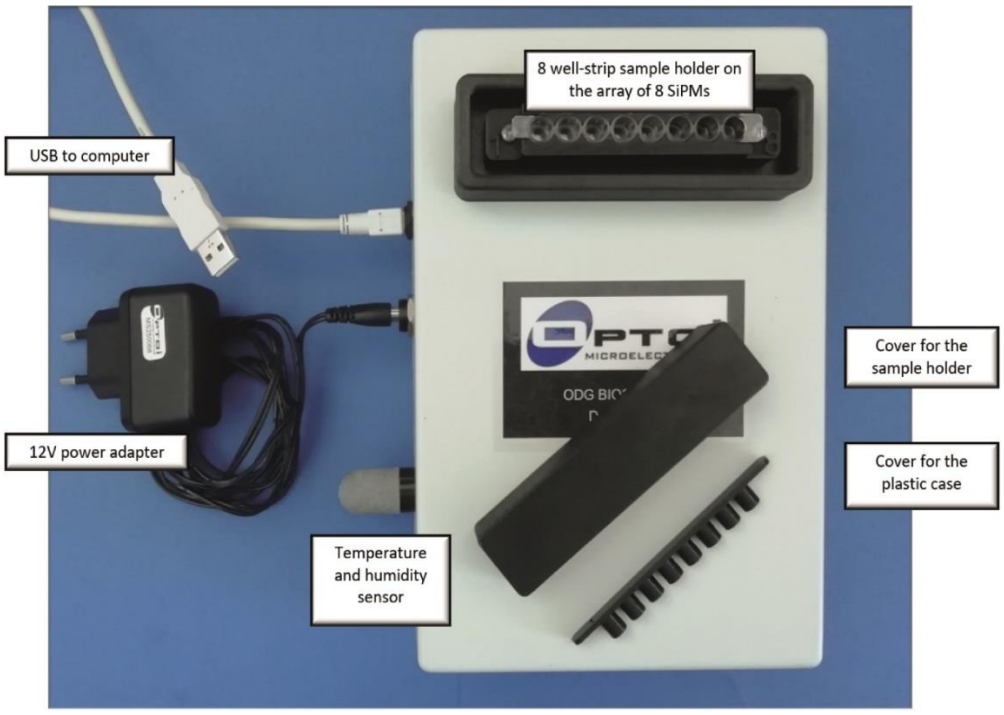

Figure 8. Optoi developed a 8-micro-wells strip SiPM-based reader. The signal coming from the SiPMs is registered by a software on a laptop connected to the device via a USB connector. Black covers ensure that no external light interferes with the detection of the photons generated by the sample.

A SiPM is a matrix of avalanche photodiodes operating in the so-called Geiger mode (reverse biased beyond the breakdown voltage). Each photodiode of the matrix acts as a binary device which is activated by the arrival of light. The single cell of the SiPM is a single photon avalanche diode (SPAD). SPAD technology works creating an avalanche event triggered by an incoming photon. The electric field generated inside the single cell accelerates the electrons hit by the photon triggering a self-sustaining avalanche. The SPAD technology, being a single photodiode, is not able to distinguish two concomitant incident photons, while the SiPM, which possess more photodiodes connected in parallel through a common silicon substrate, is able to discriminate multiple incoming photons returning a signal given by the sum of the outputs of all the fired cells proportional to the incident light flux. In the area of the low-light photodetectors the photomultiplier tubes (PMT) have been the standard technology so far. The SiPMs are becoming competitive to PMTs in the field of low-light level detection since, considering a comparable intrinsic gain, they are insensitive to magnetic fields, their working bias is rather low (25 - 75V), the time response is intrinsically very fast (less than 500ps) and the device itself is rugged and compact (few mm^2 size) (Dinu et al., 2007).

8. Prostate cancer

Prostate cancer (PCa) is one of the most common malignancy among men over 50 years. There are three main risk factors mostly recognized: age, ethnicity and family history. Age is an important risk factor for PCa. The incidence of PCa is 0.02% for men before 49 years; it becomes 0.4% after 50-59 years and 0.6% after 65 years (US data (USCS Data Visualizations - CDC)). Another important risk factor is the ethnicity: black men have the highest rate of getting PCa, while American Indian/Alaska Native and

Asian/Pacific Islander men the lowest (USCS Data Visualizations - CDC). PCa is also highly heritable and the risk linked to this factor has been estimated to be as high as 60% (Hjelmborg et al., 2014). It is thought that from 5 to 10% of the PCa cases are primarily due to inherited genetic factors or PCa susceptibility genes. There are other potential modifiers of PCa cancer risk like the endogenous hormones, both estrogens and androgens. For example, it was shown that eunuchs or people with very low levels of testosterone before puberty do not develop this type of malignancy (PDQ Cancer Genetics Editorial Board, 2002). In several studies, PCa was also associated with genes with potential clinical relevance, suggesting an elevated incidence of PCa in men with mutations in BRCA1, BRCA2 (Agalliu et al., 2007) and in some genes of the mismatch repair system (Soravia et al., 2003) (Haraldsdottir et al., 2014). The androgen receptor pathway is probably considered the most important genetic factor involved in prostate carcinogenesis. Several SNPs within this pathway have been linked to PCa (Chang et al., 2002) (Chang et al., 2003) (Sarma et al., 2008). Another important recognized factor in prostate cancer development is inflammation: proliferatory inflammatory atrophy is in 30% of the cases the precursor of prostate intraepithelial neoplasia (PIN) (De Marzo et al., 2007). PCa is considered a group of different malignant tumors: 95% are adenocarcinomas originating in the glands and duct of the prostate, while the rest are neuroendocrine tumors, generally of acinary type. PCa is often multifocal and more than 75% starts from the peripheral zone. Generally, PCa involves an accumulation of epithelial cells even if also non-epithelial cells play an important role. 25% of men below 50s and 90% below 80s develop a benign prostatic hyperplasia (BPH) but it is not considered a precursor of the carcinoma. On the other hand PIN (*in situ* carcinoma) is the precursor of invasive cancer and it begins usually in the peripheral zone of the prostate gland. As long as the basal layer of the prostate is not broken, the PCa remains *in situ*

(Knudsen and Vasioukhin, 2010). Several factors are involved in the initiation of PCa such as the decrease of Glutathione-S-Transferase P1 (GTSP1) (Lee et al., 1994), homeobox protein Nkx-3.1 (Swalwell et al., 2002) and increased lipid metabolism (Sung et al., 2007) as well as overexpression of ETS proteins (Tomlins et al., 2005) and serine protease inhibitor Kazal-type 1 (SPINK1) (Leinonen et al., 2010). When PCa involves high-grade lesions it generally invades the stroma and eventually it becomes a metastatic tumor (Knudsen and Vasioukhin, 2010). PTEN loss and c-MYC amplification are the most recognized players for high-grade PCa and progression to metastasis (Shen and Abate-Shen, 2007) (Jenkins et al., 1997). Depending on the stage of the malignancy, the treatment can vary. When patients have an organ localized cancer diagnosis, the curative approach can be attempted, and possible treatments are radical prostatectomy, external radiation therapy, brachytherapy, combined brachytherapy plus external radiation therapy and combined hormone treatment plus radiation therapy. Metastatic prostate cancer is generally treated with hormonal regimen, which takes advantage of the dependency of PCa to androgen. Hormone deprivation can be performed with surgical castration, luteinizing hormone-releasing hormone agonists and androgen antagonists. Chemotherapy is used after or in combination with hormonal therapy. Usually, after a first phase of response to the treatment, the cancer becomes castration resistant (Litwin and Tan, 2017). In this case, other treatments are available, which confer a median overall survival advantage of 4-5 months each: sipuleucel-T, enzalutamide, AA (Lorente et al., 2015). In particular, AA inhibits the enzyme CYP17A, dampening extra-gonadal testosterone production. Some metabolites of AA have been shown to target also the androgen receptor as agonist or antagonist (Caffo et al., 2018). In order to choose the right treatment, diagnostic tools are fundamental. For PCa, several are the standardly used tests: prostate specific antigen (PSA), digital rectum exploration, transrectal ultrasound,

ultrasound guided transperineal/transrectal prostate biopsies, skeletal scintigraphy, X-ray thorax and pelvic node staging (Litwin and Tan, 2017). Imaging techniques are mostly used for the staging of the disease: for example, considering that bones are a preferential site for the metastasis of prostate cancer, skeletal scintigraphy is often required. Even if new signatures of multiple genes are in development for diagnosis and prognosis of prostate cancer, and recently FDA-approved biomarkers (proPSA and PCA3) are entering the clinics, the most frequently used molecular diagnostic test is still PSA (Litwin and Tan, 2017) (Chistiakov et al., 2018). However, PSA can be found elevated for prostate benign neoplasia, prostatitis and prostate cancer. It is not a marker of PCa *per se*, but its increase is often associated with the presence of the malignancy (Pezaro et al., 2014). Regarding metastatic castration resistant prostate cancer (mCRPC) patients and AA treatment, the cost of the drug and the adverse effects call for biomarkers predicting its efficacy (Caffo et al., 2018). However, to our knowledge, apart from the work on AR-V7 (Antonarakis et al., 2014) and CTCs enumeration (Heller et al., 2018), little has been achieved on this side. Thus, there is still a need of biomarkers for a reliable diagnosis, prediction and prognosis, for making decisions of physicians less challenging.

In this context, as discussed in previous paragraphs, miRNAs may have an important role for PCa diagnosis, prognosis and prediction of treatment efficacy. The functional role of miRNAs in prostate cancer has already been extensively reviewed (Kanwal et al., 2017) (Khan et al., 2019b) (Aghdam et al., 2019) (Sharma and Baruah, 2019) and points towards the use of miRNAs as potentially good biomarkers in clinical settings. Chiorino group, recently showed that miR-103a-3p (also evaluated in this work) and let-7a-5p combined with PSA levels, could detect clinically significant tumors better than PSA alone (Mello-Grand et al., 2019). Interestingly, in their approach, they considered individuals with plasma levels of PSA higher than 16 ng/mL as patients. Individuals who showed PSA

less than 16 ng/mL, were analyzed for miR-103a-3p and let7-p building a score which was able to identify clinically equivocable samples as PCa or non-PCa with an AUC of 0,76. A similar approach has been developed for exosomes enriched cell-free urine samples, in which a logistic regression model made of five miRNAs and serum PSA indicated recurrence of PCa after radical prostatectomy (Fredsøe et al., 2019). miRNAs in urine samples have also been described for reclassification of patients enrolled in active surveillance (AS) programs, usually monitored via serological PSA, digital rectal exams and periodical invasive biopsies. A 3-marker panel based on miR-24, miR-30c and CRIP3 methylation in urine samples was able to predict correct reclassification of AS patients (Zhao et al., 2019). Therefore, miRNAs have been studied as auxiliary factors in PCa diagnosis, prognosis and prediction of treatments (Fredsøe et al., 2020) (Lyu et al., 2019). Perhaps, this approach may be the best option to partially overcome the high biological complexity of PCa which could present several confounding factors within a cohort of patients. Indeed, in the present study, the heterogeneity of the patients, together with the relatively low number of samples analyzed, has represented a limitation for driving strong conclusions.

RESULTS

1. Prediction and follow-up of abiraterone acetate efficacy in metastatic castration-resistant prostate cancer patients via plasma microRNAs

Prostate cancer is still one of the leading cause of cancer deaths. The urge for better understanding the efficacy of the treatments available calls for biomarkers aiding clinicians in choosing the best drug for each patient. Thus, predictive biomarkers may help in discriminating patients which will likely benefit from a drug, avoiding useless, painful and expensive treatments. In this context, we analyzed the expression of c-miRNAs in plasma of mCRPC patients before and after the administration of AA.

1.1 Patients' cohort

The patients cohort (see Materials and Methods section – "*Patients*" – paragraph 1.1) was composed of a consecutive series of 34 mCRPC patients who were treated with AA after docetaxel failure as part of regular clinical practice at Santa Chiara Hospital (Trento, Italy): 22 non-respondent (NR) and 12 respondent (R) patient. Daily oral AA (1000 mg) plus prednisone 5 mg was administered twice a day. The cohort showed no statistical difference in the median age between R and NR patients (All = 75 ± 8; NR = 76 ± 6.83; R = 73.5 ± 9.48). 6 out of 22 NR patients and 0 out of 12 R patients received enzalutamide prior AA; all patients received docetaxel; 9 out of 22 NR patients and 6 out of 11 R patients received cabazitaxel. The median PFS of NR patients was 3.85 months (± 1) and 13.15 (± 4.6) for R patients (Table 6).

Table 6. Patients' characteristics representing Gleason score, enzalutamide treatment (ENZ), docetaxel treatment (DCX), cabazitaxel treatment (CBX), abiraterone acetate treatment period (AA duration), objective response to AA treatment (OR), PSA levels changes after AA treatment (PSA), progression free survival after AA treatment (PFS). AA = abiraterone acetate; MR = mixed response; NE = not evaluable; PD = progression of disease; PR = partial response; S = PSA stabilization; SD = stable disease; UNK = unknown; <50% = PSA reduction less than 50% compared to baseline; >50% = PSA reduction more than 50% compared to baseline; Y=yes ; N=no.

	Patient code	Gleason score	ENZ	DCX	CBX	AA duration (months)	OR	PSA	PFS (months)
Non-respondent	P1	8	Y	Y	Y	3.93	PD	<50%	3.9
	P2	7	Y	Y	N	2.93	NE	<50%	2.7
	P3	8	N	Y	N	4.03	PD	<50%	3.7
	P4	9	N	Y	Y	6.8	MR	<50%	5.4
	P5	8	Y	Y	Y	3.77	PD	<50%	3.7
	P6	8	N	Y	N	3.73	PD	S	3.7
	P7	6	N	Y	Y	2.83	PD	S	2.8
	P8	UNK	N	Y	Y	3.87	PD	<50%	3.8
	P9	7	N	Y	N	1.93	NE	<50%	1.9
	P10	8	N	Y	N	3.97	PD	>50%	3.9
	P11	7	Y	Y	N	2.47	NE	<50%	2.4
	P12	9	N	Y	Y	4.8	PD	>50%	4.7
	P13	9	Y	Y	N	4.63	NE	<50%	4.2
	P14	7	N	Y	N	3.27	PD	<50%	3.7
	P15	8	N	Y	Y	5.57	MR	<50%	5.5
	P16	9	N	Y	Y	4.63	MR	>50%	4.6
	P17	9	N	Y	N	13.1	PD	>50%	1.8
	P18	8	N	Y	N	4.7	PD	<50%	4.6
	P19	10	N	Y	N	3.73	PD	>50%	3.7
	P20	6	N	Y	N	3.93	PD	<50%	3.9
	P21	9	Y	Y	N	2.67	PD	<50%	3.9
	P22	10	N	Y	Y	5.6	PD	>50%	5.5
Respondent	P23	9	N	Y	Y	12.17	PR	<50%	12
	P24	7	N	Y	N	4.67	PR	>50%	16.6
	P25	UNK	N	Y	Y	14.3	PR	>50%	13.1
	P26	7	N	Y	N	9.13	PR	<50%	9
	P27	7	N	Y	N	13.37	PR	<50%	13.2
	P28	9	N	Y	N	21.33	PR	>50%	21.7
	P29	6	N	Y	Y	15.1	SD/PR	>50%	14.9
	P30	9	N	Y	N	9.33	PR	>50%	8.7
	P31	9	N	Y	Y	7.5	MR	S	7.8
	P32	7	N	Y	Y	20.8	PR	>50%	20.8
	P33	7	N	Y	N	8.87	MR	>50%	8.7
	P34	9	N	Y	Y	4.43	PR	>50%	14.8

1.2 miRNome analysis reveals deregulation of c-miRNAs in different response to abiraterone acetate treatment

For the purpose of building a classifier to distinguish NR from R patients, we started analyzing 5mL of plasma samples (in EDTA tubes) from clinically unequivocable 9 R and 9 NR patients – sampled prior AA administration (preTRT) - assessing 752 miRNAs with Human Exiqon miRNome qPCR Panels. We took out from the analysis 319 miRNAs that were not detected in at least 20% of the samples. 198 miRNAs were present in all the samples; 2 miRNAs were not detected in any samples in the NR group; 332 miRNAs were present in at least 5 of the samples in the NR group, while 360 in at least 5 of the samples in the R group. The choice of the normalizer for the relative quantification is critical for an optimal analysis of the data. In this work, we based this choice on the Normfinder software (Andersen et al., 2004) feeding the algorithm with the miRnome panel data: miR-425-5p was the best normalizer. Afterward, we built the Volcano plot (Figure 9).

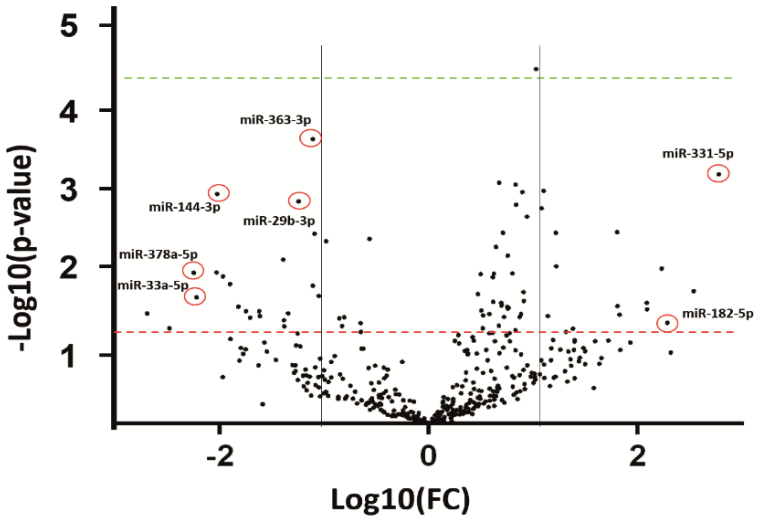

Figure 9. Volcano plot from Exiqon panels data. Normalized expression on miR-425-5p. Log(fold change) for NR versus R group (x axis) and negative of log(p-value) (y axis). Black lines show log(Fold Change) > 1 and <-1. -log(P-Value) legend: below red line p-value > 0.05, between red and green line 0.05 > p-value > 0.0001, above green line p-value < 0.0001. Red circles highlight the chosen miRNAs for further validation via the unbiased approach.

Exiqon miRnome panels do not have any technical replicates, thus a validation method is needed in choosing candidates for further analysis. We decided to select miRNAs for validation following two approaches: 1) target-wise and 2) unbiased.

1.3 miR-103a-3p is able to distinguish non-respondent vs respondent mCRPC patients

One of the main players in prostate cancer development is PTEN, which has also been found to be down-regulated in NR patients (Ferraldeschi et al., 2015). Therefore, for the target-wise approach we decided to select from the Exiqon panels, miRNAs which target PTEN. We retrieved from miRTARbase the miRNAs validated to target PTEN and to narrow the choice to a putative candidate we excluded miRNAs which 1) were expressed with a Cq value higher than 30 b) were down-regulated in NR patients in the miRNome analysis - following the reasoning of a down-regulation of PTEN in NR patients - and c) literature review (Mello-Grand et al., 2019) (Fu et al., 2016) (Xue et al., 2016) (Singh et al., 2014) (Yu et al., 2018) (Guo et al., 2015). From this analysis we chose miR-103a-3p for validation with TaqMan technology. We performed RT-qPCR for miR-103a-3p on plasma of the same 9 NR and 9 R patients preTRT. The results depicted in Figure 10, show that miR-103a-3p is able to discriminate between NR and R patients (p-value: 0.003).

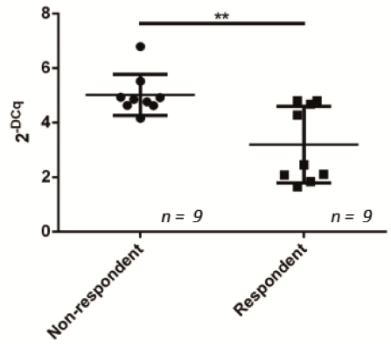

Figure 10. RT-qPCR for miR-103a-3p normalized with miR-425-5p. miR-103a-3p is able to distinguish non-respondent versus respondent patients treated with AA. ** = p-value = 0.003

1.4 The miRNome analysis identifies 67 microRNAs deregulated in non-respondent vs respondent mCRPC patients

In order to increase the robustness of the miR-classifier we also explored miRNAs in an unbiased approach from the miRNome data. We found 67 miRNAs significantly differentially expressed in NR versus R patients (Table 7). Among them we chose 7 candidates for further validation, taking into consideration a) fold change, b) p-value and c) literature review (Xue et al., 2016) (Zheng et al., 2018) (Singh et al., 2014) (Wang et al., 2018) (Song et al., 2018) (Fujii et al., 2016) (Epis et al., 2009) (Zhu et al., 2018) (Yang et al., 2015) (Guo et al., 2017) (Chen et al., 2016b) (Avgeris et al., 2014) (Chen et al., 2015) (Karatas et al., 2017) (Li et al., 2017): miR-182-5p, miR-331-5p (up-regulated in NR vs R), miR-144-3p, miR-29b-3p, miR-33a-5p, miR-363-3p and miR-378a-5p (down-regulated in NR vs R). We analyzed the 7 candidates on the same 9 NR and 9 R samples preTRT with TaqMan RT-qPCR technology (Figure 11).

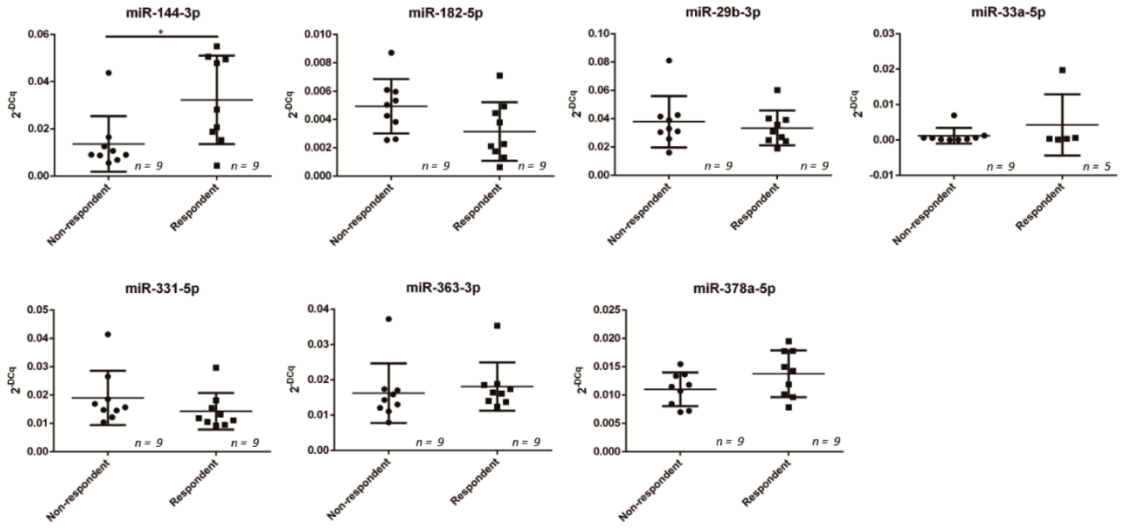

Figure 11. Validation analysis with TaqMan RT-qPCR. Expression values (2-DCq) of miRNAs candidates normalized with miR-425-5p. * = p-value < 0.05. miR-33a-5p did not show signal for four samples in the respondent group.

MiR-144-3p, miR-182-5p, miR-331-5p and miR-378a-5p expression showed a trend concordant with the miRnome analysis, however only for miR-144-3p the difference between the two groups was statistically significant. miR-33a-5p was discarded from further analysis because its expression levels were barely detectable (Cq values > 37). The expression levels of the miRNAs concordant with the miRnome analysis were coupled with miR-103a-3p analysis to explore a new signature with a higher capacity of discrimination. We calculated the ratio of 2^{-Cq} signals of the miRNAs and among all the combinations, we identified the miRNA score (miRS) of miR-103a-3p/miR-378a-5p as the best performer. miRS was able to discriminate between the groups of NR and R patients (p-value = 0.0001) as described in Figure 12A. To confirm this result, we increased our data set with 16 patients (13 NR and 3R) for a total of 21 NR and 12 R (1 NR sample from the discovery phase could not be further processed because of the scarcity of starting material). As depicted in Figure 12B, miRS is able to sharply discriminate between the two groups (p-value: 0.008). Therefore, miRS is a promising

biomarker for AA response in mCRPC patients and being a ratio of the expression values of two miRNAs it avoids the use of a normalizer.

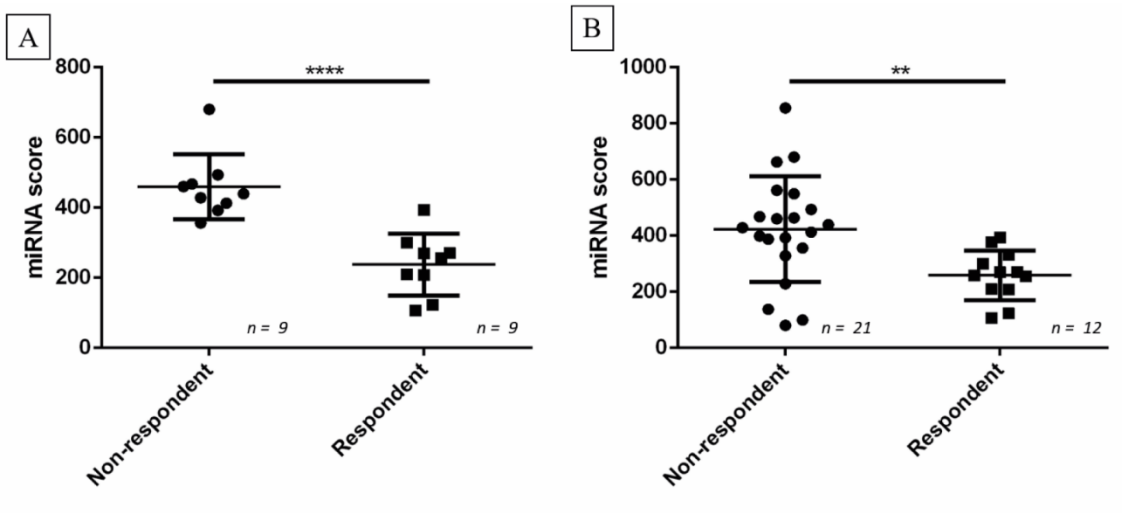

Figure 12. The ratio of 2^{-Cq} signal of miR-103a-3p and miR-378a-5p creates a score able to significantly distinguish non-respondent versus respondent patients (A) also in the expanded cohort (B). *** = p-value < 0.001. ** = p-value < 0.01

Table 7. List of deregulated genes from the miRNome analysis. The genes were filtered for statistically significant differential expression (p-value < 0.05). In bold, candidate genes chosen for the validation with TaqMan RT-qPCR.

miRNA	Fold change (NR vs R)	P-Value	miRNA	Fold change (NR vs R)	P-Value	miRNA	Fold change (NR vs R)	P-Value	miRNA	Fold change (NR vs R)	P-Value
hsa-let-7a-5p	2.1	2E-03	**hsa-miR-144-3p**	-4.1	1E-03	**hsa-miR-29b-3p**	-2.2	2E-04	hsa-miR-502-3p	-2.2	2E-02
hsa-let-7b-5p	1.8	1E-03	hsa-miR-146a-5p	1.4	2E-02	hsa-miR-29c-3p	-1.8	4E-02	hsa-miR-548k	5.8	2E-02
hsa-let-7c-5p	1.7	7E-03	hsa-miR-149-5p	4.3	3E-02	hsa-miR-30c-5p	1.8	8E-04	hsa-miR-574-3p	2.3	3E-03
hsa-let-7d-3p	1.7	1E-02	hsa-miR-151a-5p	1.5	4E-02	hsa-miR-30e-3p	1.5	1E-02	hsa-miR-579-3p	-3.3	4E-02
hsa-let-7d-5p	1.6	8E-04	hsa-miR-153-3p	-3.9	1E-02	hsa-miR-320a	1.4	3E-02	hsa-miR-598-3p	1.7	3E-02
hsa-let-7e-5p	1.9	2E-02	hsa-miR-155-5p	1.9	3E-02	hsa-miR-32-5p	-3.7	2E-02	hsa-miR-610	3.6	4E-02
hsa-let-7f-5p	2.1	1E-03	hsa-miR-15b-5p	3.5	3E-03	**hsa-miR-331-5p**	6.9	6E-04	hsa-miR-624-5p	-3.5	3E-02
hsa-let-7i-3p	-6.5	4E-02	hsa-miR-181a-5p	1.5	3E-02	hsa-miR-335-3p	1.8	4E-02	hsa-miR-628-3p	2.3	9E-03
hsa-miR-101-5p	-3.1	4E-02	**hsa-miR-182-5p**	4.9	5E-02	**hsa-miR-33a-5p**	-4.7	2E-02	hsa-miR-660-5p	-2.0	4E-03
hsa-miR-106b-5p	-1.5	4E-03	hsa-miR-196b-3p	-3.1	4E-02	hsa-miR-342-3p	1.6	3E-02	hsa-miR-663a	3.5	3E-02
hsa-miR-10b-5p	-2.6	5E-02	hsa-miR-197-3p	1.6	3E-02	**hsa-miR-363-3p**	-2.4	1E-03	hsa-miR-664a-3p	1.8	4E-02
hsa-miR-125a-5p	1.7	3E-02	hsa-miR-199a-5p	-2.1	2E-02	**hsa-miR-378a-5p**	-4.7	1E-02	hsa-miR-766-3p	1.9	2E-03
hsa-miR-126-3p	1.5	1E-02	hsa-miR-223-3p	1.6	3E-02	hsa-miR-411-5p	2.2	4E-02	hsa-miR-769-5p	-2.5	4E-02
hsa-miR-126-5p	1.4	1E-02	hsa-miR-23a-3p	1.9	1E-03	hsa-miR-421	1.7	3E-02	hsa-miR-92a-1-5p	4.3	3E-02
hsa-miR-136-5p	-3.4	4E-02	hsa-miR-23b-3p	2.0	3E-05	hsa-miR-423-5p	1.6	5E-03	hsa-miR-96-5p	-4.1	1E-02
hsa-miR-140-3p	-1.7	4E-02	hsa-miR-24-3p	1.7	4E-02	hsa-miR-450b-5p	4.7	1E-02	hsa-miR-98-5p	1.6	3E-03
hsa-miR-143-3p	-2.1	4E-03	hsa-miR-26a-5p	1.4	4E-02	hsa-miR-451a	-2.6	8E-03			

1.5 The miRS follows efficacy of abiraterone acetate in time

Since our miRS proved its ability in discriminating NR versus R patients, we tested it for its ability to follow-up the efficacy of the treatment. We could analyze - out of 12 R patients - the follow-up samples of 11 R at 3 months, 10 R at 6 months, 7 R at 9 months and – out of 21 NR patients – 14 NR at 3 months, 4 NR 6 at months and 0 NR at 9 months. The missing samples are due either to the death of the patients or the end of treatment. Our data indicate that the miRS is able to follow-up in time the responsiveness to AA (Figure 13A). We can speculate that the miRS of the R patients, becomes more and more similar to the miRS of the NR patients, reflecting the responsiveness of the patients who all become progressively resistant to AA. Importantly, to help proving this point we calculated the difference between the 3 months miRS and preTRT miRS (delta score) for each patient. Following our reasoning, we plotted the positive delta scores (9 samples out of 11) against PFS (Figure 13B). Interestingly, the delta score has a negative correlation trend with PFS. Thus, greater is the change in signal between the preTRT sample and the 3 months sample, lower is the PFS. PSA reduction, one of the standard parameter for clinical decisions, does not correlate with PFS, and fails in providing a more accurate scenario (Figure 13C). Considering the lack of good biomarkers to follow responsiveness to AA treatment, miRS may be of critical importance.

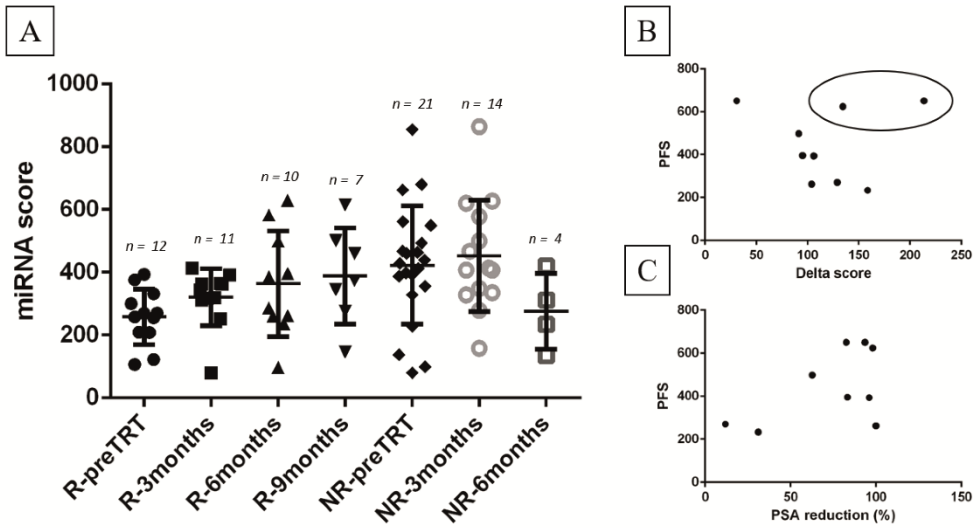

Figure 13. miRNA score analysis of follow-up samples at 3, 6 and 9 months after AA administration. (A) miRNA score follows the efficacy of AA for each patient in time. Average miRNA score for respondent patients becomes progressively similar to average miRNA score for non-respondent patients, reflecting the progressive acquisition of resistance to AA. (B) Delta score (preTRT miRS – 3months miRS) of R samples correlates negatively with PFS, except for two outliers (circle). (C) PSA reduction after three months from the first AA administration is not able to give an indication of the efficacy of AA in time.

1.6 Unsupervised clustering analysis confirms miRS ability to predict and follow abiraterone acetate efficacy in mCRPC patients

In order to increase the confidence in the miRS we analyzed our data with an unsupervised clustering model, feeding the algorithm with the miRS and without the post-treatment clinical evaluation. According to miRS, the clustering was able to classify the patients in two groups (p-value < 0.0001) which we named "1" and "2" (Figure 14A). The Kaplan-Meyer plot (Figure 14B) showed a statistically significant difference (p-value = 0.0003) between the median PFS of group 1 compared to the median PFS of group 2. We can consider group 1 as R patients and group 2 as NR patients. Compared to the clinicians' evaluation, 5 patients out of 15 of group 1 (R) were re-classified by our unsupervised model (clinicians' evaluation = NR); 2 out of 18 of group 2 (NR) was re-classified (clinicians' evaluation = R). The post-treatment samples showed the same trend observed in the previous analysis (Figure 14C-D). The negative correlation trend between the delta

score and the PFS is preserved (12 positive delta scores out of 15). Interestingly, the 5 re-classified patients in the R group had a PFS of 5.5, 5.5, 4.7, 4.6, 3.8 months, equal or higher than the average PFS of the NR group (3.8 months). Therefore, our miRS was able to classify them as respondent, however, we may subgroup them as "poor respondent". In fact, according to our hypothesis of miRS predicting a poor response in time, 3 of them also showed a high delta score during the first 3 months.

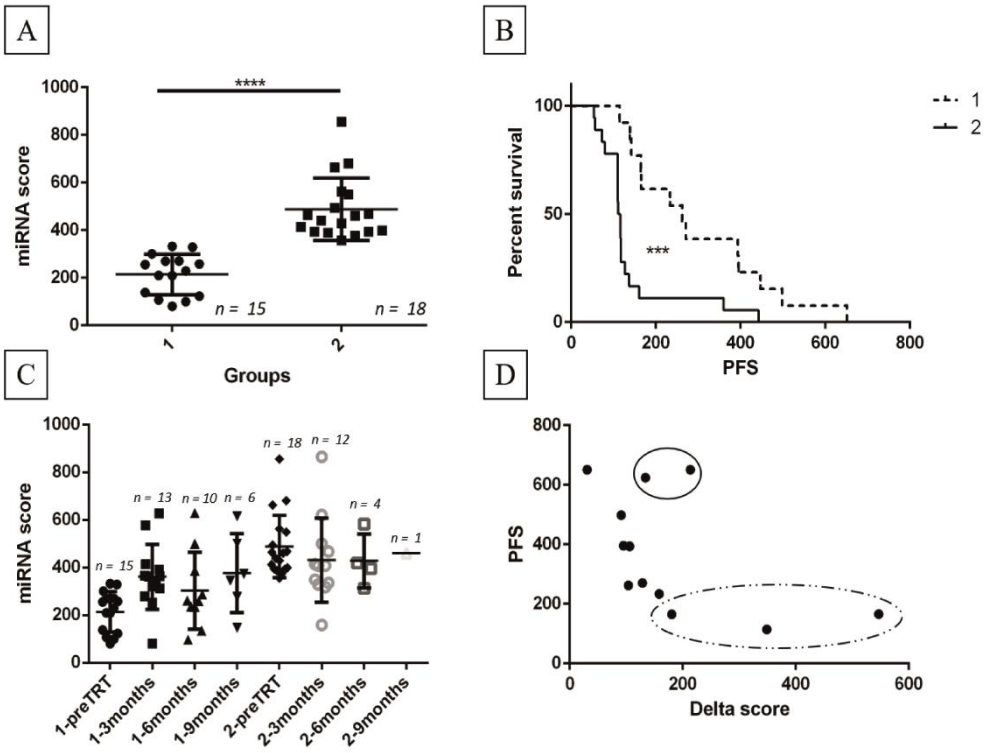

Figure 14. Unsupervised clustering for miRNA score data. (A) miRNA score is able to divide, by k-means clustering, the patients in two groups (1-2). (B) K-M plot based on the clustered groups by miRNA score shows a significant difference in PFS enabling the definition of the group 1 as respondent, while the group 2 as non-respondent. (C) The follow-up samples based on the clustered groups shows the same trend as the previous analysis with the pre-classified groups. (D) Delta score for the respondent group maintain the negative correlation with PFS (outliers in the solid-line circle). The dotted-line circle represents the re-classified patients which are considered as respondent, but with a low PFS after AA administration, as reflected by a high delta score. **** = p-value < 0.0001.

1.7 Bioinformatic analysis on miR-378a-5p and miR-103a-3p targets

miRNAs may be deregulated either as a direct or an indirect effect of the biological process under investigation. To have a better understanding of the possible roles of our

selected miRNAs, we analysed their predicted and validated targets (see Materials and Methods section - "*Bioinformatic analyses*" - paragraph 1.7). Among all, the most relevant genes linked to prostate cancer development, recurrence and resistance to therapies were: WNT2B, WNT7A (Ahmad and Sansom, 2018) (predicted) DICER1 (Bian et al., 2015), AGO (Bian et al., 2014), PTEN (Ferraldeschi et al., 2015) and SP1 (Hafner et al., 2010) (validated). Moreover, the promoters of miR-103a-3p and miR-378a-5p were searched for enriched consensus sequences of human transcription factors via GeneXplain software. We analysed four different Ensembl annotations: a) miR-103a1-3p b) miR-103a2-3p c) miR-378a-5p and d) PANK2. miR-103a is present twice in our genome (miR-103a1 and miR-103a2) with an identical mature miRNA sequence. Therefore, TaqMan RT-qPCR probes could not distinguish the two products, nor the target prediction is affected. However, being the two copies in two different genomic locations, the transcription factor analysis may yield different results. Since the transcription of an intronic miRNA may be regulated by either an internal promoter or by the promoter of the gene in which it is inserted, we chose to search for transcription factor binding sites in PANK2 promoter because miR-103a2 is in one of its introns. miR-378a-5p is also intronic but we could reach the promoter of the gene (PPARGC1B) with our analysis range (see Materials and Methods section - "*Bioinformatic analyses*" - paragraph 1.7); miR-103a1-3p is in the PANK3 gene but transcribed in antisense direction. The transcription factors, whose consensus binding sequence was enriched, were: ATF2, BRCA1, GMEB2, IRX2, LEF1, MAFA, SOX10, USF2, ZBTB33 and HOXB13 (Figure 15). HOXB13 is a transcription factor that belongs to the homeobox gene family and interestingly it has been already associated to early death after AA treatment (Miyamoto et al., 2018).

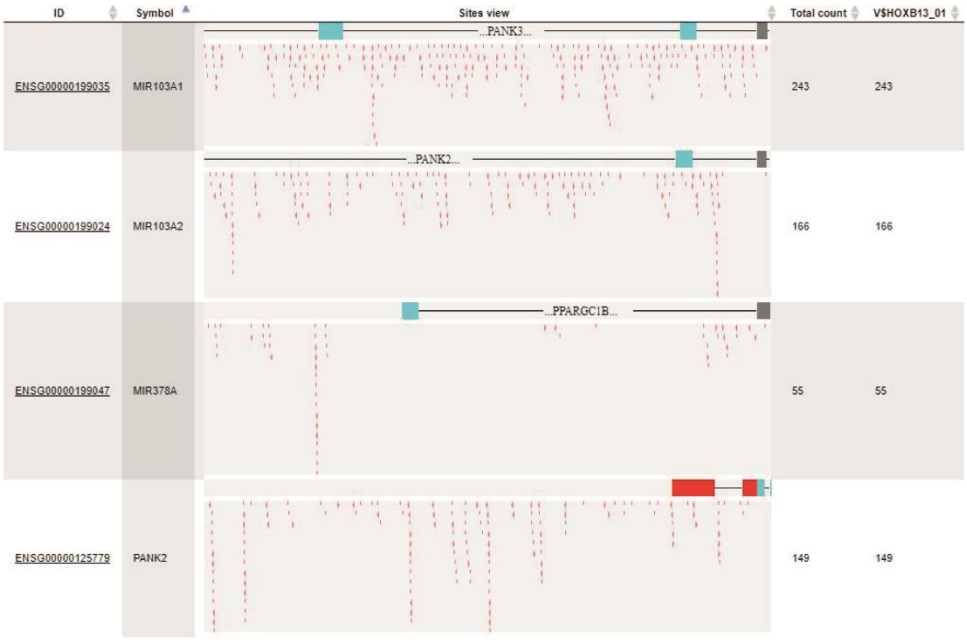

Figure 15. Capture from GeneXplain software of HOXB13 consensus sequence enrichment in the searched genome areas. Red arrows represent consensus sequence sense or antisense. HOXB13 is evidently enriched in promoters of miR-103a-3p and PANK2, in which intronic region resides miR-103a2.

1.8 Up-regulation of miR-103a-3p and inhibition of miR-378a-5p confer resistance to abiraterone acetate in LnCaP cell line

We explored in a cell line model whether miR-103a-3p and miR-378a-5p may have direct involvement in the induction of AA resistance in prostate cancer. We transfected LnCaP cell line (androgen-independent) with mimics for miR-103a-3p and inhibitors for miR-378a-5p alone and in combination: then we treated the cells with EC50 of AA - which we here previously experimentally determined (Figure 16). The up-regulation of miR-103a-3p and the down-regulation of miR-378a-5p reflected the expression levels of the two miRNAs in the plasma of a NR patient. In MTT assays (Figure 17) the transfection of mimics for miR-103a-3p alone but not of inhibitors for miR-378a-5p conferred resistance (resistance increment of 24% - ANOVA p-value = 0,01) to AA treatment. The same result was obtained when the synthetic oligos were transfected in combination at the same

concentration (resistance increment of 30% - ANOVA p-value: 0.03). Therefore, here we provide cell line data that shows the involvement of at least miR-103a-3p in the mechanism of resistance to AA in prostate cancer. It is important to highlight that LnCaP cell line is PTEN-null, therefore, these analyses are not meant to prove the axis miR-103a-3p/PTEN, but a general involvment of the two candidate miRNAs in the induction of AA resistance in prostate cancer.

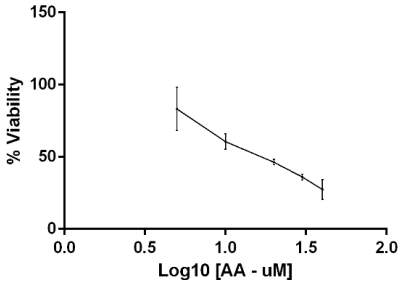

Figure 16. EC50 after 72h of AA treatment. LnCaP cells shows a EC50 of 18 uM. Each dot represents the mean of a biological triplicate

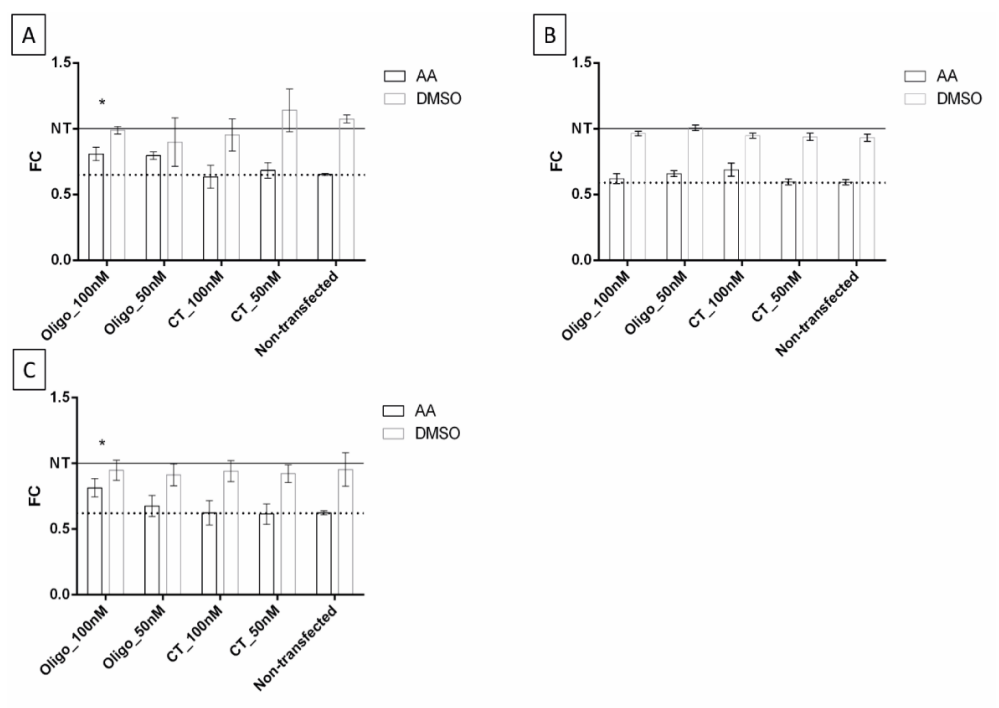

Figure 17. LnCaP resistance to AA after transfection with mimics of miR-103a-3p and inhibitors of miR-378a-5p. 100nM of mimics of miR-103a-3p alone (A) confer resistance to AA at 72h of treatment (24%) in LnCaP cells while 100nM of inhibitors of miR-378a-5p alone (B) do not. The transfection of 100nM of both mimics of miR-103-3p and inhibitors of miR-378a-5p in combination (C) confer resistance to AA at 72h of treatment (30%) in LnCaP cells. * = ANOVA p-value < 0.05. Solid line refers to non-treated and non-transfected cells used as control (NT); dotted line refers to the mean fold change of non-transfected cells treated with AA. CT = scramble oligo.

1.9 Abiraterone acetate stops LnCaP cells in G0/G1 phase

In order to better address the role of the miR-103a-3p and miR-378a-5p in the mechanism of resistance of prostate cancer to AA, we decided to explore the behavior of LnCaP cells after treatment with AA. We treated LnCaP cells with EC50 of AA and then we performed cell death and cell cycle analysis via FACS. Interestingly, after AA treatment, while the cell death analysis showed that only the number of necrotic cells increased – but it was not statistically significant – there was a statistically significant decrease of number of cells in S-phase with a block in G0/G1-phase (G0/G1 p-value = 0.006 – S p-value = 0.0002) (Figure 18). Thus, AA affects more the cell cycle behavior more than provoking cell death.

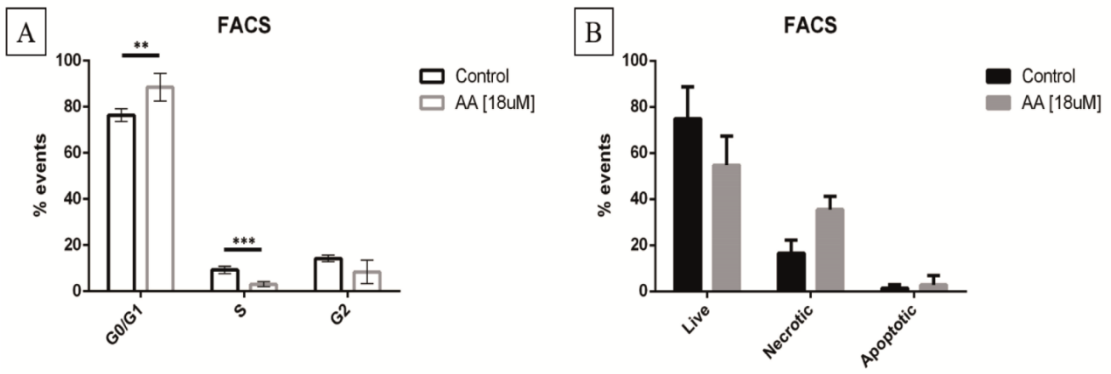

Figure 18. FACS analysis for cell cycle (A) and cell death (B) after 72h of AA treatment (at EC50 of 18 uM). LnCaP cells show a stop in G0/G1 after AA treatment while no statistically significant indication of increased necrotic or apoptotic cell death. Each bar represents the mean of a biological triplicate.

2. A new platform for the direct detection of microRNAs in biofluids

In the event of a full validation of the two c-miRNAs we discovered in the study on predictive biomarkers for AA treatment in mCRPC patients, a technology avoiding the limitations of the current techniques must be established. In this work, we present the ODG platform which comprises a novel SiPM-based reader in conjunction with Chem-NAT. Accurate miRNAs profiling without extraction, pre-amplification or pre-labeling of the target is now achievable.

2.1 Development of a new micro-wells strip SiPM-based reader

In this study, a new chemiluminescent micro-wells strip reader based on the SiPM technology was designed by integrating 8 SiPMs (provided by Advansid, FBK, Trento, Italy) into a 12cm x 20cm x 5cm support (Figure 19A). The single detector is 1mm X 1mm (active area, with single optical cells being a few microns) inserted into a Near Ultraviolet (NUV) SiPM capable of single photon resolution, with signal amplification (Figure 19B). It consists of an array of avalanche photodiodes reverse biased in Geiger mode. The arrival of a single photon generates an avalanche event due to impact

ionization, enabling good photon resolution in dark conditions by returning a strongly amplified signal. The SiPM brings the advantages of creating a high gain with low bias voltage (about 30 V against 1-2kV of a PMT), enabling the detection of low intensity light signals. The SiPM-based reader is able to analyze 8 samples simultaneously, using 8-wells strips in the platform. The read-out is reported live by software connected to the reader, via a USB connection. The analytical sensitivity of the reader was determined by creating a calibration curve using Horseradish Peroxidase (HRP) enzyme into HRP substrate (Figure 20) The curve was obtained by plotting the average of photocurrent generated versus different concentrations of HRP added into the device. The limit of detection (LOD) was calculated as 0.16 pmol/L in 35 uL of HRP substrate.

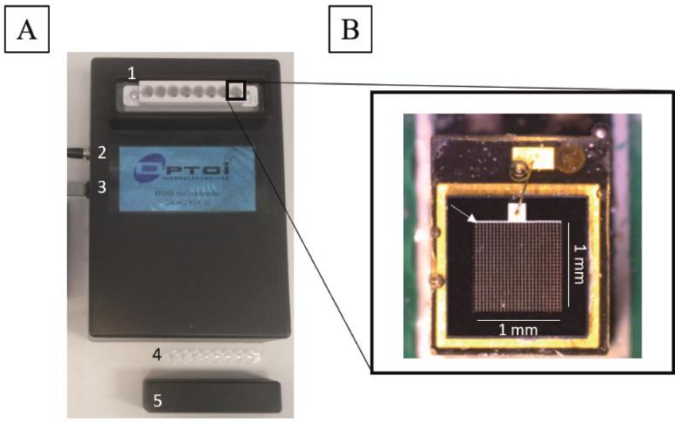

Figure 19. (A) The SiPM-based reader. A plastic support contains the electronic acquisition system with an array of 8 SiPM NUV (1). The reader is turned on via a power adapter (2). An USB connector (3) connects the reader to a laptop with a dedicated ODG software. The samples are loaded into the sample holder (4) and covered with a plastic case (5). (B) SiPM sensor: with the white arrow is indicated the 1mm X 1mm active area.

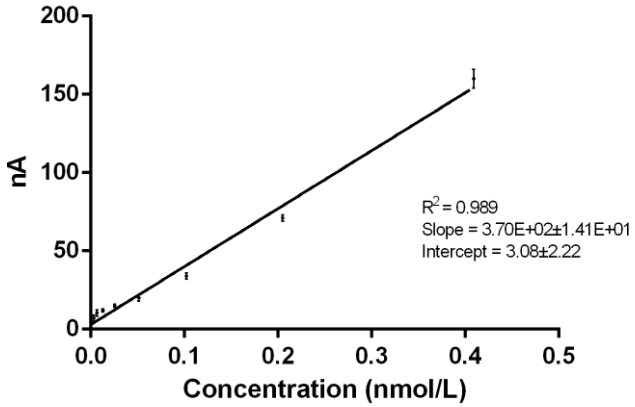

Figure 20. Calibration curve measuring the analytical sensitivity of the SiPM-based reader. The photocurrent signals generated by the reader (Y axis) correlate linearly with the concentrations of HRP added to substrates (X axis). Each dot represents the average signal of three independent measures (standard deviations in bars).

2.2 ODG platform

To achieve the merging of Chem-NAT and SiPM-based reader, an abasic PNA probe (aPP) complementary to hsa-miR-21-5p is covalently bound to magnetic beads (Figure 21, STEP 1). The complementary hsa-miR-21-5p is captured by the aPP, templating the incorporation into the duplex of a biotinylated aldehyde-modified adenine (SMART-A-Biotin) (Figure 21, STEP 2). Following this recognition, washing steps are performed to eliminate off-targets (Figure 21, STEP 3). Magnetic beads allow an effective phase-separation and an efficient washing process by using magnetic separation racks. The labelling is achieved via HRP-streptavidin (HRP-strep), which specifically recognizes the biotin in the duplex (Figure 21, STEP 4). A luminol-peroxidase substrate is added to generate a chemiluminescent signal. The oxidation of luminol by the peroxide is catalyzed by the HRP producing light. The read-out is performed by the SiPM-based reader (Figure 21, STEP 5).

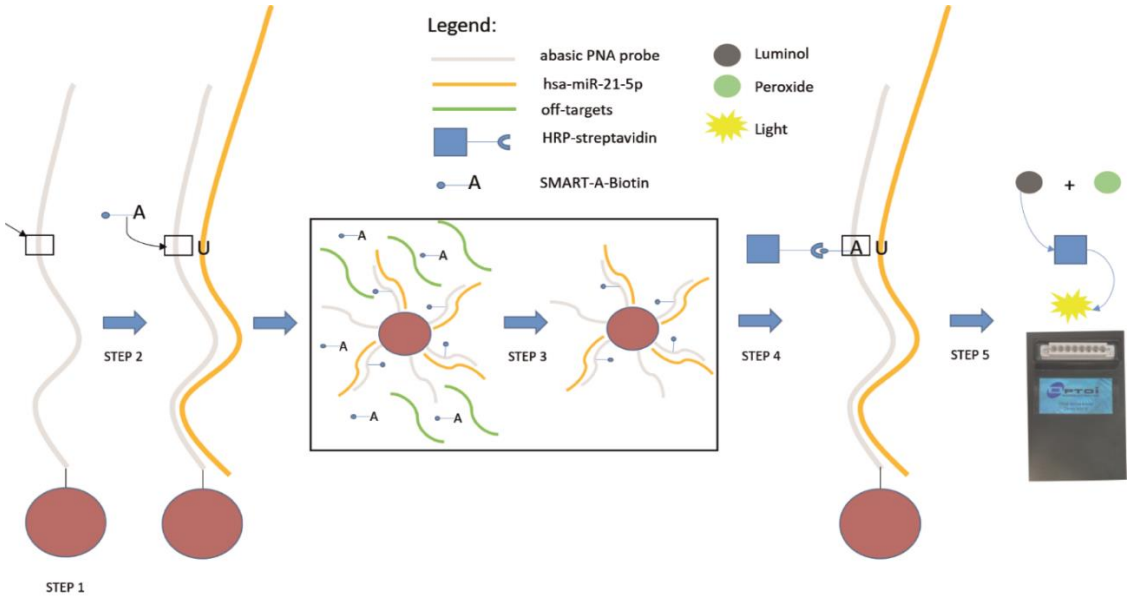

Figure 21. ODG platform workflow. aPP are bound to magnetic beads (STEP 1 – the arrow shows the abasic position). The target hybridizes to the probe and the SMART-nucleobase enters the pocket (STEP 2); off-targets are washed away (STEP 3); HRP-strep binds the biotin of the SMART-nucleobase (STEP 4). Chemiluminescent substrate is added and the signal generated by the oxidation of the luminol with peroxide via HRP catalysis is analyzed via the SiPM-based reader (STEP 5).

2.3 Abasic PNA probe optimization

aPPs were synthesized with amino-pegylated groups in order to be covalently bound onto magnetic beads (aPP-beads). As described by our group elsewhere (Venkateswaran et al., 2016), aPP under immobilization onto magnetic beads have been found to lack stability, and can exhibit a degree of undesirable deformation, affecting performance (e.g., specificity and/or sensitivity) of the aPP in this assay, and prevent proper miRNAs detection. To overcome risks of poor probe performance, four aPP (aPP1, aPP2, aPP3 and aPP4) were synthesized, containing a sequence of nucleobases to allow hybridization to the mature hsa-miR-21-5p strand. aPP1, aPP2, aPP3 used sequences of 17-mer, aPP4 of 19-mer. The aPP1 incorporated two PNA monomers containing propanoic acid modifications at gamma positions (Venkateswaran et al., 2016). The abasic site was positioned +8 from the C-terminal, so that post-hybridization, the mature hsa-miR-21-5p strands presented a guanidine at position +11 (from the 5'), thereby allowing

incorporation of a SMART-C-Biotin into the abasic pocket (Table 8). The other three aPPs (aPP2, aPP3 and aPP4) carried two PNA monomers containing propanoic acid modifications differently distributed (Table 8). The abasic monomer sites were positioned respectively at +9, +8 and +12 from the C-terminal, so that post-hybridization the mature hsa-miR-21-5p strands presented a uracil respectively at positions +14, +8 and +14 (from the 5'), thereby allowing incorporation of a SMART-A-Biotin into the abasic pocket (Table 8). Among the four sequences synthesized and tested, the aPP4 was selected, showing the best hybridization to the complementary hsa-miR-21-5p, as well as an improved SMART-A-Biotin incorporation (data not shown).

Table 8. Abasic PNA probe sequences and complementary targets. For abasic PNA probes: "*" chiral monomers; "__" abasic monomer. For targets: highlighted in red the regions of hsa-miR-21-5p that hybridize with the abasic PNA probes; highlighted in green the nucleobases interrogated by SMART nucleobases.

Code	**Abasic PNA probes (N-ter --> C-ter)**	**Targets hsa-miR-21-5p MIMAT0000076 (5' --> 3')**
aPP1	A A C A T C* A G T __ T G A T* A A G	UAG**CUUAUCAGACUGAUGUU**GA
aPP2	T C A A C A T* C __ G T* C T G A T A	UAGCU**UAUCAGACUGAUGUUGA**
aPP3	A T C A G T C T* G __ T A A G C* T A	**UAGCUUAUCAGACUGAU**GUUGA
aPP4	C A A C A T* C __* G T* C T G A T A A G C	UA**GCUUAUCAGACUGAUGUUG**A

2.4 Analytical sensitivity and limit of detection of the ODG platform

The analytical sensitivity of the ODG platform was determined by creating a calibration curve (performed in triplicate) using known concentrations of synthetic RNA-hsa-miR-21, respectively 0.029, 0.059, 0.117, 0.469 nmol/L (final concentration) in a total reaction volume of 50 uL (water was used as negative control). Chemiluminescent signals were detected by the SiPM-based reader. The average output signals show a linear correlation (Figure 22) according to the concentrations of RNA-hsa-miR-21.

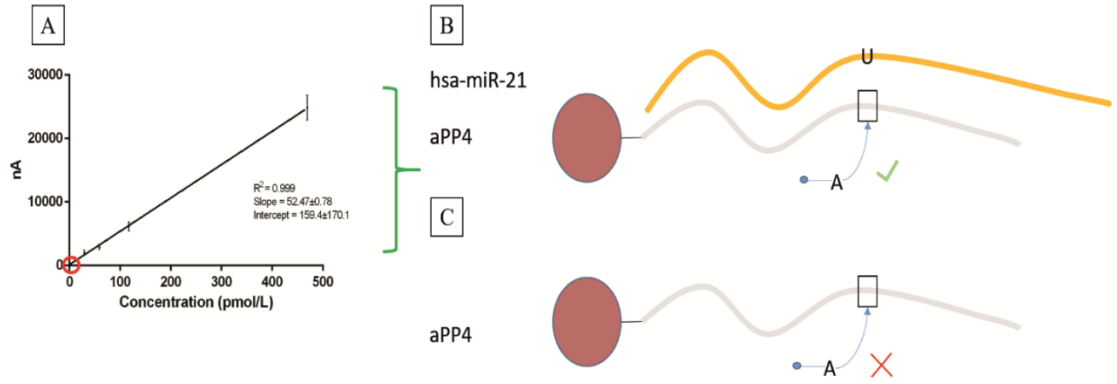

Figure 22. (A) The photocurrent signals generated (Y axis) correlate linearly with the concentration of RNA-hsa-miR-21-5p (X axis). Standard deviations of the technical triplicates in bars. Positive signals (green bracket) are given by the incorporation of the SMART-A-Biotin after hybridization of the target (B), while the negative control (red circle) signals are represented by incubation of aPP4 with water, such that no SMART-A-Biotin is able to enter into the pocket (C).

The LOD was calculated as 4.7 pmol/L (see Materials and Methods section – *Generation of calibration curves with ODG platform and RT-qPCR* – paragraph 2.5). In parallel, a comparative calibration curve was created using a conventional multi-mode microplate reader for the read-out with a LOD of 7.4 pmol/L (Figure 23).

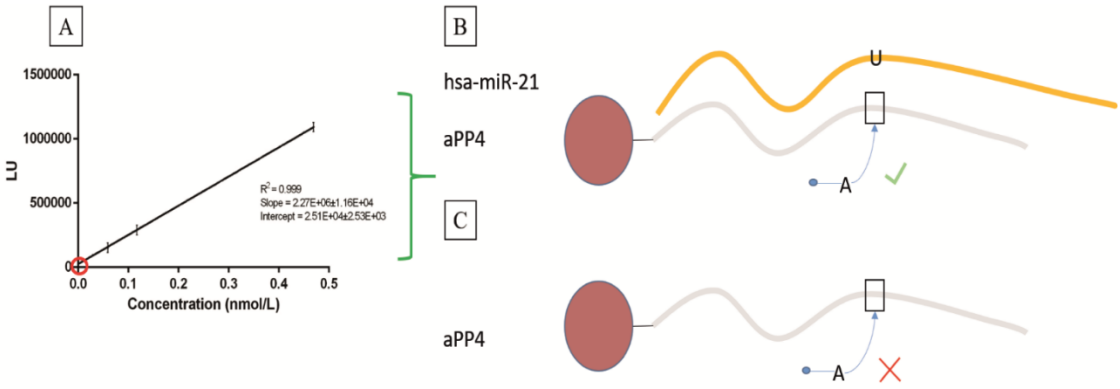

Figure 23. (A) The luminescent units generated (Y axis) correlate linearly with the concentration of RNA-hsa-miR-21 (X axis). Standard deviations of technical triplicates in bars. Positive signals are given by the incorporation of the SMART-A-Biotin after hybridization of the target (B), while the negative control signals are represented by incubation of aPP4 with water, such that no SMART-A-Biotin is able to enter into the pocket (C).

2.5 Hsa-miR-21-5p profiling using ODG platform for plasma of lung cancer patients

Following the generation of calibration curves and determination of LOD, the ODG platform was tested for the direct detection of hsa-miR-21-5p in plasma samples from eight NSCLC patients (performed in triplicate). 2.5 x 10E+05 aPP4-beads were dispersed directly into the plasma samples along with DestiNA's proprietary lysis buffer. The beads were incubated for one hour with the samples to allow the capture of free hsa-miR-21-5p by aPP4. The Chem-NAT reaction and protocol was performed as explained in Materials and Methods section (*Chem-NAT reaction for plasma samples analysis* – paragraph 2.7). The positive signal corresponds to the SMART-A-Biotin incorporation into the probe's abasic site upon hybridization with the hsa-miR-21-5p (Figure 24A), while the negative signal corresponds to an aliquot of the same sample incubated with a SMART-C-Biotin that cannot be incorporated (Figure 24B). As shown in Figure 4C, the ODG platform was able to directly detect hsa-miR-21-5p in plasma samples. Values of signal to background ratio (S/B) varied depending on the concentration of the target in the samples (Figure 24C).

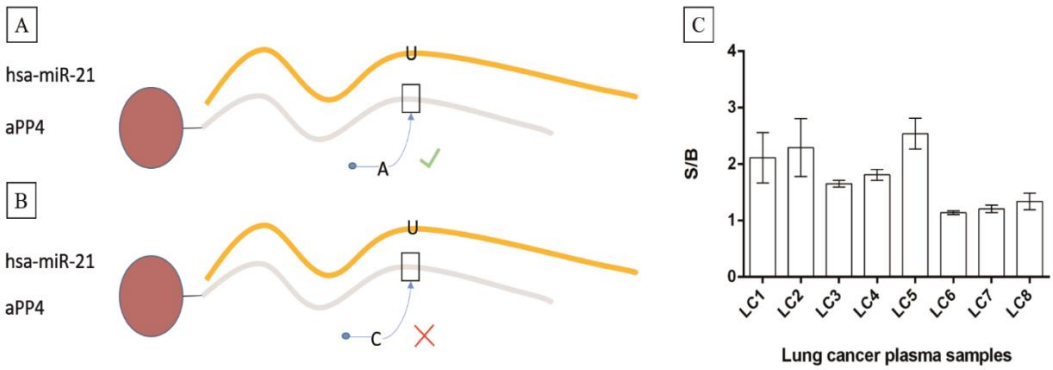

Figure 24. Direct detection of hsa-miR-21-5p in plasma of NSCLC patients. The positive signal (A) is given by the SMART-A-Biotin incorporated into the aPP4 after hybridization of hsa-miR-21-5p, while the SMART-C-Biotin which cannot pair with the nucleobase in front of the pocket (U) in aPP4 generates the background (B) of the platform. (C) Signal to background ratio generated by the ODG platform for each sample. Standard deviations of technical triplicates in bars.

Interpolating the S/B with the LOD curve generated previously with the ODG reader, we calculated an approximative range of concentration between 14 pmol/L and 45 pmol/L (Table 9), an expected value for highly expressed circulating miRNAs (Max et al., 2018). Hsa-miR-21-5p expression of the eight plasma samples was also assessed via RT-qPCR gold standard method for miRNA analysis (performed in triplicate). As shown by Figure 25, ODG platform showed a positive correlation with Cq values generated by RT-qPCR (R2=0.75, p=0.005), demonstrating that ODG platform can generate qualitative and quantitative data.

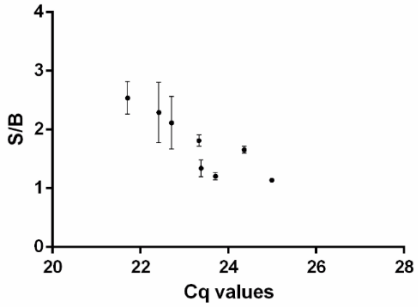

Figure 25. Signal to background ratios generated by the ODG platform correlate with TaqMan Cq values of the same plasma samples. Each dot represents the average of three independent measures (standard deviations in bars).

Table 9. Concentration of hsa-miR-21-5p in plasma of lung cancer samples calculated interpolating S/B values by the ODG reader with the LOD curve

Sample	S/B	Concentration (pmol/L)
LC1	2.32	33
LC2	2.10	29
LC3	1.88	25
LC5	1.76	23
LC6	3.06	46
LC7	1.35	15
LC8	2.07	28
LC9	1.31	15

2.6 Hsa-miR-21-5p quantitative evaluation in plasma of lung cancer patients via RT-qPCR

To translate the Cq values into number of moles, two calibration curves were generated (performed in triplicate) using cel-miR-39 spike-ins: 1) nine quantities of synthetic RNA-cel-miR-39 were reverse transcripted directly in 15 uL of aqueous solution and (2) nine quantities of synthetic RNA-cel-miR-39 were spiked into 200 uL of plasma, with extraction and reverse transcription (Figure 26A). Calibration curves for hsa-miR-21-5p were performed to confirm the equal efficiency of TaqMan probes of the two selected miRNAs (Figure 26B). Average RNA extraction efficiency was evaluated studying the difference between Cq values of the two curves. Error in slope and in intercept of the regression lines were taken into account, to provide approximate absolute concentrations (Table 10) spanning the pmol/L range (100 – 800 pmol/L). Importantly, the efficiency of RT-qPCR varies greatly from assay to assay, with an inverse proportional trend with the concentration of the miRNA under investigation. As a matter of fact, the smaller the amount of synthetic RNA spiked-in, the higher the loss in efficiency of RT-qPCR, either due to loss of RNA or presence of contaminants after the RNA extraction (Table 11-12). Therefore, the whole procedure for performing standard RT-qPCR fails partially in its inherent reproducibility and so the calculation of absolute amount of molecules with this technique has critical limitations. For this reason, the direct detection performed by the ODG platform is desirable.

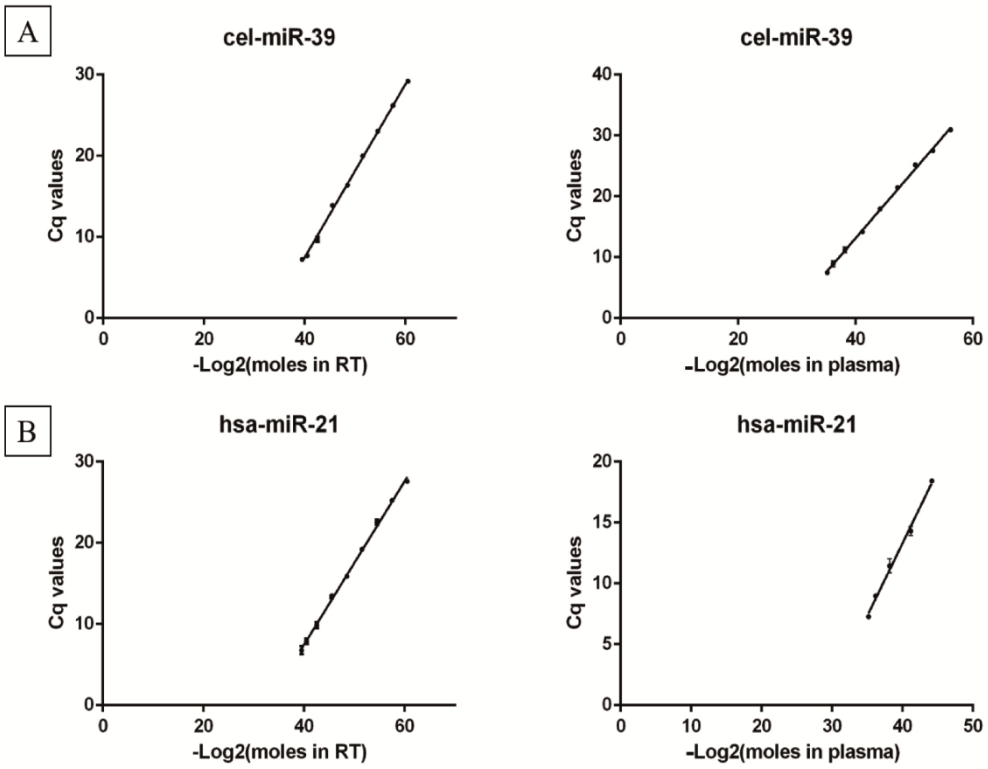

Figure 26. (A) RT-qPCR calibration curves for cel-miR-39 and (B) for hsa-miR-21-5p. Nine quantities of RNA-cel-miR-39 (or hsa-miR-21-5p) were directly reverse transcripted (left) and nine quantities of RNA-cel-miR-39 (or five quantities of hsa-miR-21-5p) were spiked in plasma before RNA extraction (right). Each dot represents the average of triplicate measures (standard deviations in bars).

Table 10. Cq values and range of concentration calculated for hsa-miR-21-5p in each of the plasma samples of lung cancer patients analyzed

Sample	Cq value	Range of concentration (mol/L)
LC1	22.71	3.94E-10 to 4.67E-10
LC2	22.42	4.72E-10 to 5.54E-10
LC3	24.36	1.36E-10 to 1.74E-10
LC4	23.33	2.63E-10 to 3.21E-10
LC5	21.71	7.47E-10 to 8.49E-10
LC6	24.99	9.09E-11 to 1.19E-10
LC7	23.72	2.05E-10 to 2.54E-10
LC8	23.38	2.55E-10 to 3.12E-10

Table 11. Cq values for calibration curves of cel-miR-39 and RNA extraction efficiencies. First column shows Cq values for the calibration curves generated by the spike ins directly reverse transcripted. Second column shows Cq values for the calibration curves generated by the spike-ins in plasma and extracted for RNA before reverse transcription. Each value represents the average of a technical triplicate.

Cq values – spike in RT	Cq values – spike in plasma	RNA extraction efficiency (%)
7.23	7.47	70.9
7.71	8.9	55.77
9.7	11.2	50.28
13.89	14.17	58.53
16.39	17.94	40.43
19.98	21.44	33.14
23.04	25.16	23.63
26.18	27.52	40.84
29.18	30.94	35.57

Table 12. Cq values for calibration curves of hsa-miR-21-5p and RNA extraction efficiencies. First column shows Cq values for the calibration curves generated by the spike ins directly reverse transcripted. Second column shows Cq values for the calibration curves generated by the spike-ins in plasma and extracted for RNA before reverse transcription. Each value represents the average of a technical triplicate.

Cq values – spike in RT	Cq values – spike in plasma	RNA extraction efficiency (%)
6.77	7.28	80.38
7.86	8.98	49.69
9.86	11.45	36.13
13.48	14.31	37.75
15.89	18.43	11.52

3. microRNAs analysis in extracellular vesicles fraction of plasma samples

As discussed, EVs may be the cargo of several molecules with important features of biomarkers, such as miRNAs. The advantage of using EVs in diagnostics is their selective and specific origin, decreasing background effects of molecules coming from different tissues than the one of interest. Moreover, from a technical point of view, EVs offer the possibility of enriching the intended target in a very small volume, facilitating the capturing and the detection. In this work, we explored the possibility of using EVs-enriched samples from plasma samples as a source of miRNAs for further application with the ODG platform.

3.1 Isolation and characterization of extracellular vesicles from healthy volunteers

We isolated EVs from 1 ml of plasma of 8 healthy volunteers with nickle-based isolation (NBI) technology (Notarangelo et al., 2019). We then measured the number of vesicles in suspension by Tunable Resistive Pulse Sensing (TRPS). As shown in Figure 27 the number of particles detected with two different nanopores (NP200 and NP400) indicates the presence of EV sub-populations. By comparing all the samples analyzed and the total particles recovered, the total number is approximately the same for all the samples (mean particles/mL = 3.5E+08). The mean particles diameter ranges from 162nm to 331nm for NP200 and 197nm to 400nm for NP400 measured samples.

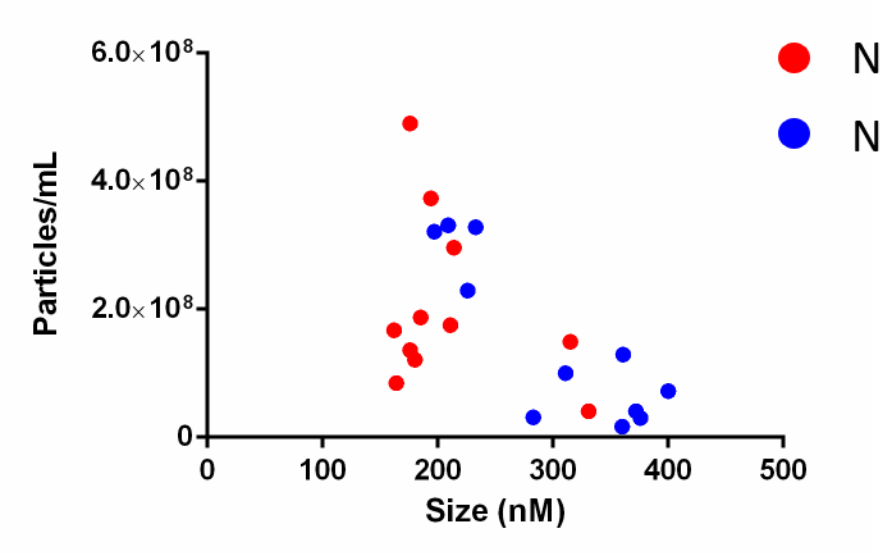

Figure 27. Size and mean number of particles per mL calculated with two different nanopores via TRPS: NP200 (red) and NP400 (blue)

3.2 microRNAs are detectable in NBI-isolated EVs by RT-qPCR

EVs have been demonstrated to carry several nucleic acids potentially investigated as biomarkers. miRNAs have been recently discovered and studied in EVs cargos bearing several functions in cellular communication. Plasma-circulating EVs can represent an important source of biologically meaningful information, such as miRNAs, thus becoming of potential clinical interest. We analyzed the expression levels of miR-223-3p and miR-21-5p in plasma samples, since the miRNAs were extensively described in literature as potential biomarkers for several diseases (Fassan et al., 2017) (Oksuz et al., 2015) (Guo et al., 2018) (Zhang et al., 2017) (Khalighfard et al., 2018) (Nakka et al., 2017b). To investigate the potential enrichment of these RNA species within EVs, we used TaqMan RT-qPCR to compare the EV-enriched sample, plus the corresponding depleted (dEVs) fraction of 8 healthy volunteers. In order to calculate an absolute value of molecules for each miRNA in the different fraction (Table 13), a calibration curve with synthetic cel-miR-39 (Figure 26A) was used as a reference. The ratio between the sum of

miR-molecules in EVs (miR_{EV}) plus dEVs fractions (miR_{dEV}) and miR-molecules in the total plasma fraction (miR_{tot}) should be one. Figure 28 shows that for all the miRNAs analyzed the ratio is approximately one, assuring a proper technical analysis for the subsequent calculations. The number of miR per sample in the different fractions is approximately 10^7 - 10^8 per mL. Figure 29 shows that generally the EV fraction is less populated by miRNAs compared to the depleted fractions: thus, there are more miR-223-3p and miR-21-5p out of the EVs associated to proteins or lipoproteic complexes.

Table 13. Number of miR-molecules in EVs (miR_{EV}), dEVs fractions (miR_{dEV}) and in the total plasma fraction (miR_{tot}) per mL of plasma for miR-223-3p and miR-21-5p

	miR-223			**miR-21**		
	miR_{tot} / mL	**miR_{EV} / mL**	**miR_{dEV} / mL**	**miR_{tot} / mL**	**miR_{EV} / mL**	**miR_{dEV} / mL**
S1	1.00E+08	1.10E+07	1.31E+08	1.99E+07	3.81E+06	4.28E+07
S2	5.66E+07	4.17E+06	2.82E+08	1.47E+07	1.64E+06	1.67E+07
S3	8.22E+07	8.46E+06	7.86E+07	2.89E+07	3.43E+06	3.19E+07
S4	2.65E+08	1.52E+07	2.15E+08	4.51E+07	1.94E+07	3.99E+07
S5	1.99E+08	1.48E+08	1.49E+08	2.79E+07	2.44E+07	3.48E+07
S6	4.37E+08	3.46E+07	3.26E+08	6.18E+07	8.70E+06	5.29E+07
S7	1.91E+08	5.86E+07	1.53E+08	4.20E+07	1.45E+07	3.04E+07
S8	1.07E+09	2.88E+07	1.05E+09	1.39E+08	1.01E+07	1.31E+08

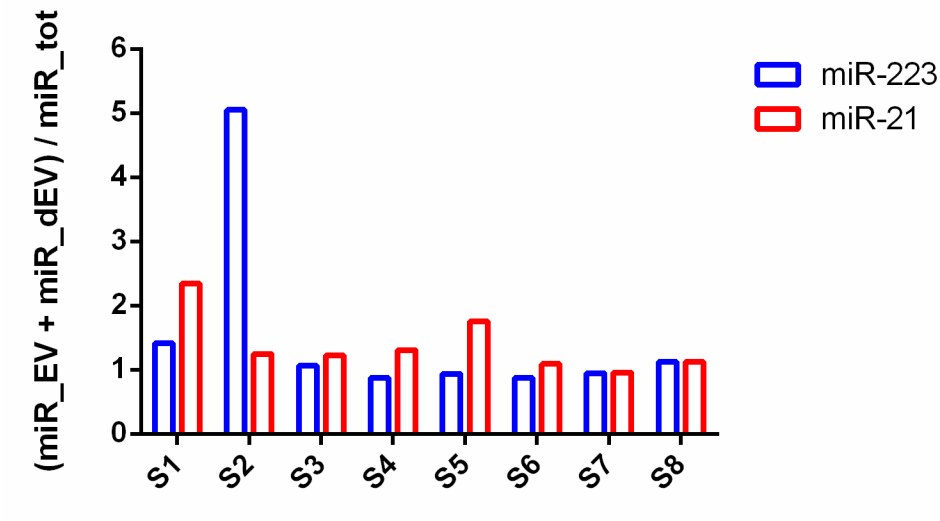

Figure 28. Ratio of miR_{EV} plus miR_{dEV} over miR_{tot} for miR-223-3p and miR-21-5p in all samples.

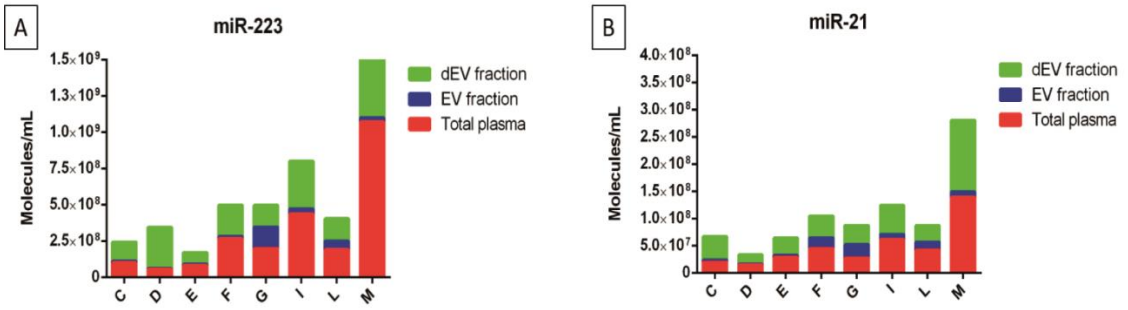

Figure 29. Box plot of miR distribution in the different plasma fractions for miR-223-3p (A) and miR-21-5p (B)

Correlating the number of vesicles and the miR molecules in the EV fraction we extrapolated an approximative number of miR per EV (Figure 30). The average miR-molecule number per EV is below 1, meaning that these miRNAs are not enriched in EVs of healthy volunteers. This has been previously reported (Andreu et al., 2016) and may be used as an advantage in discriminating pathological conditions where EVs number and miR-molecules per EV is evidently increased.

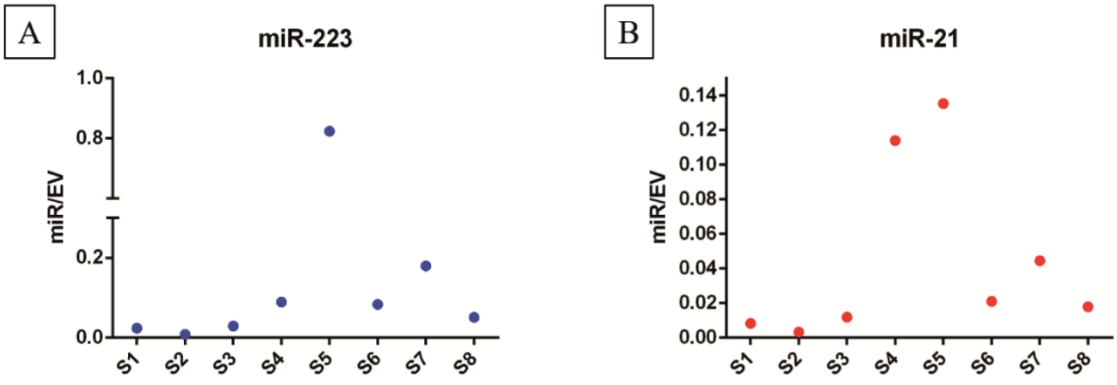

Figure 30. Number of miR-molecules per single vesicle for miR-223-3p (A) and miR-21-5p (B).

DISCUSSION

In clinical settings, biomarker evaluation is fundamental for an efficient patient's care. Molecular tools with diagnostic, prognostic and predictive capacity are of critical relevance in the era of precision medicine where for each subclass of patients a specific treatment is needed. In this context, it is important not only to diagnose a disease, but also to be able to understand its molecular features and to redirect the clinicians towards the best treatment available. This decision-making point in the clinical course is critical for the health of the subject involved and of the healthcare system. In fact, the sustainability of the medical apparatus is based on the efficiency of the care provided and on the costs held. In the last decade the term "financial toxicity" has been brought to the general attention because of its burden for nationals health systems and for the people with the disease and their families. Financial toxicity (or financial distress) is generally used to describe how out-of-pocket costs (not covered by insurance or national health systems) can cause financial problems to the patient (PDQ Adult Treatment Editorial Board, 2002a). These costs may be for outpatient services, medical appointments and drug prescriptions. Cancer is one of the major burdens regarding financial toxicity and in fact, cancer survivors usually show higher out-of-pocket costs compared to patients with no cancer history (PDQ Adult Treatment Editorial Board, 2002b). Financial distress has several effects on patients and family members (and/or friends): a) patients may not take medicines as directed to save money, b) lower quality of life, c) debt and bankruptcy and d) informal caregivers may share financial toxicity. Thus, besides the treatment of the disease *per se*, financial toxicity in cancer treatment is a burden for personal life, physically and mentally. Regarding national costs, in the US 165 billions of dollars are roughly estimated for cancer cost of care in 2020 (National Costs for Cancer Sites | Cancer

Prevalence and Cost of Care Projections): prostate cancer accounts for about 10% of the total amount. Cancer biomarkers would improve patient's health outcomes and potentially save costs, even if not this is not always the case (Seo and Cairns, 2018). For instance, as pointed out in an English report in 2014, early diagnosis for colorectal and ovarian cancer would bring about 50 millions of pounds saved per year in England; even in the case of NSCLC where the costs for early diagnosis would be actually higher, the use of biomarkers would still be highly cost-effective gaining about four thousands of years of life with a cost of about one thousand pounds per year of life. (https://www.cancerresearchuk.org/sites/default/files/saving_lives_averting_costs.pdf).

In our study, apart from AR-V7 (Antonarakis et al., 2014) and CTCs enumeration (Heller et al., 2018), very little has been achieved in predicting AA efficacy especially in liquid biopsies settings. The changes in the therapeutic landscape of mCRPC which occurred in the last decade represent a challenge for the clinicians, who have the possibility of choosing among different therapies. However, since all patients show a primary or acquired resistance to the active drugs, it is becoming crucial the availability of efficient biomarkers able to identify the patients who have a higher probability to achieve a benefit from a specific treatment. In this view, in several fields of oncologic diseases, miRNAs have drawn attention because of their potential. In particular, c-miRNAs found in biofluids such as plasma, serum or urine may be a fundamental tool for the clinicians in terms of diagnosis, prognosis and prediction of treatment efficacy. However, the role of miRNAs expression as predictive biomarkers of treatment efficacy has been rarely evaluated in mCRPC (Lin et al., 2014) (Lin et al., 2017). Moreover, to our knowledge, no study evaluated miRNAs' changes over time during the treatment. In our study, we demonstrate that two miRNAs are able to predict the response to AA and to signal the progression occurrence during the treatment. In the respondent patients, the difference

between the miRS of the preTRT samples and the miRS of the 3 months samples has a negative correlation with PFS, thus, greater is the change in miRS after AA administration, higher is the likelihood of a treatment failure. This is of great importance for a clinician who needs to understand whether the drug has to be suspended or not. In fact, PSA, the gold standard serological factor for detecting recurrences of prostate tumors, together with instrumental data, fail not only to predict AA efficacy – our primary aim – but also in helping the clinicians to take critical decisions after drug administration. Interestingly, the unsupervised clustering analysis confirmed our hypothesis and retrospectively re-classified in the R group 5 NR patients presenting a PFS higher than the average of the NR group. Moreover, 3 of the re-classified patients confirmed the negative trend with PFS after 3 months, highlighting how, even if indicated as initially responsive by the clinician, a patient with a low delta score may stop the administration of AA, because of a high likelihood of soon becoming not responsive anymore. Bioinformatic analysis support the two miRNAs as players of the resistance to AA treatment. PTEN is a validated target of miR-103a-3p and it has been demonstrated that PTEN loss has a negative impact on prognosis after AA treatment (Ferraldeschi et al., 2015). We may speculate that high levels of miR-103a-3p could impact on PTEN expression, increasing the aggressiveness of cancer. SP1, a validated target of miR-378a-5p, has been shown to positively regulate the expression of CYP17A1, the target of AA (Lin et al., 2001). Therefore, we may hypothesize that lower levels of miR-378a-5p – trend shown in NR patients – may increase consequently the levels of SP1, contributing to an unbalanced presence of CYP17A1. The usual AA administration could be then insufficient to dampen efficiently the action of its target. In this context, we analyzed with GeneXplain software, the enriched transcription factor binding sites on the promoter sequences of the two miRNAs. We found enriched consensus binding sites for

developmental genes, such as HOX and SOX family genes (HOXB13 and SOX10), and for well-known cancer-related genes, like BRCA. Interestingly, HOXB13 is highly expressed in circulating tumor cells predicting early death after treatment with AA (Miyamoto et al., 2018). MiR-103a-3p putative promoter is highly covered by consensus sequences for HOXB13 and we found it increased in plasma of the NR patients' group. HOXB13 high levels may push the expression of miR-103a-3p which subsequently dampens PTEN levels. To strengthen miRS significance, we also provide evidence that AA resistance is increased in LnCaP cell line upon over-expression of miR-103a-3p and inhibition of miR-378a-5p, the condition which reflects the level of expression of the two miRNAs in the plasma of NR patients. Clearly the present study is limited by the low number of patients involved in the analysis. However, this is the first study on c-miRNAs as predictive biomarkers for AA treatment in plasma of mCRPC patients. After a full surf into the miRNome expression, we suggest that miR-103a-3p and miR-378a-5p are able not only to predict the response to the treatment but also to dynamically reflect the disease course under the drug activity. Furthermore, our study shows some concordance with recent works on the prediction of AA efficacy from liquid biopsies, and provides cell line evidences of a probable direct involvement of miR-103a-3p in the mechanism of drug resistance. In conclusion, this study indicates a completely new molecular marker to further efficiently predict and follow the response to AA.

In this work we experienced several technical problems in analyzing the samples, from RNA extraction to PCR amplification and data analysis. RNA extraction, even though standard, is a multistep and complex procedure which may introduce variability. Our laboratory showed that RNA extraction from plasma samples is not efficient and not reproducible, conditions that are not acceptable in clinical settings where the biopsies are extremely precious and generally scarce. Additionally, the multi-enzimatic steps of RT-

qPCR increase the variability intra- and inter-samples, requiring the use of internal normalizers. Our laboratory, in a study on atrial fibrillation FFPE samples, showed that the selection of reference genes is critical for appropriate data analysis. Moreover, reporting U6 as the worst reference genes chosen, the work pointed out the well-known problem of the reproducibility of the results and the difficulty of comparing those of different studies (Masè et al., 2017). In fact, U6 is one of the most used reference genes for miRNAs analysis. If we add to these problems, the complexity of the biology of miRNAs, it comes to logic how c-miRNAs have not reached the clinics yet, even though considered potentially good biomarkers. Inspired by the relevant problems in preparing and analyzing clinically valuable miRNA biomarkers, in this work we successfully merge two innovative technologies, creating the ODG platform for the direct detection of miRNAs in patient plasma samples. The platform and simplified sample preparation deliver a specific, sensitive and rapid detection method, free of errors/variability. Being a direct detection method enabling read-outs of the absolute number of miRNAs, requiring neither pre-amplification nor pre-labeling of the target, ODG platform is a significant improvement over many current methods. The assay is faster (~3h) compared to standard methods (full-day) of miRNA analysis and combines this rapidity with ease of use. Its single-base specificity delivers accurate single mismatch discrimination. Moreover, the aPP design can be modified, enabling future biomarker panels of diagnostic and prognostic clinical importance. On the other side, the SiPM-based reader brings the advantages of being low cost, compact and with a high degree of miniaturization. In the future, the technology could be integrated into an automated system, to provide clinicians with a rapid assay from blood sampling to diagnostic information in few hours. Moreover, the ODG platform may be tailored for profiling miRNAs in different sources like urine, CSF and saliva. Indeed, the choice of the type of biopsy must be accurate and it may

change depending on the type of the disease. The use of CSF may be important in neurological diseases while saliva might represent better the changes occurring in the oral cavity; urine may be used for urogenital diseases and sperm specifically for prostate pathologies. Nevertheless, considering what is best from an analytical and biological point of view, it is critical to take into account also the patients' compliance. For instance, CSF sampling is not an easy and without-risk procedure. Blood, urine and saliva are, in this sense, the best liquid biopsies being minimally invasive. Therefore, studies using these samples even for diseases which may not have a logical direct connection to them may be fundamental. Another source may be the EVs coming from these biofluids. The ODG platform may be tailored for the measurements of analytes into carrier vessels, such as exosomes, whose interest in the diagnostic field is expanding (Zhang et al., 2015a). The use of the NBI technology for isolating EVs from liquid biopsies such as plasma, serum and urine represents a double opportunity for the ODG platform: 1) address biological information specific of the tissue of origin and 2) concentrate the analyte from a big volume. NBI technology cannot select for specific EVs, however, given the rapidity and simplicity of the protocol, and the wide spectrum of EVs collected, it can be coupled with other technologies, such as FACS, able to isolate sub-populations according to specific tissue markers. EVs subgroups divided for origin is another way to dissect the complexity of biological responses to pathological conditions and retrieve specific information (Pulliam et al., 2019) (Collino et al., 2017). MiRNAs might be enriched or selectively depleted in a specific sub-population of EVs (Guescini et al., 2015) (Haller et al., 2019). Additionally, because of the NBI protocol, it is possible to concentrate, for instance, 50-100mL of urine into 100-200uL (about a 500 concentration factor). This is an enormous advantage for the ODG technology which may suffer of high LOD levels when working with c-miRNAs.

FUTURE PERSPECTIVES

We showed preliminary evidence that at least miR-103a-3p is directly involved in the mechanism of resistance to AA in prostate cancer. More studies are needed to confirm this hypothesis and to better dissect the possible mechanism. First, the direct connection of miR-103a-3p to HOXB13 must be established. Confirming the putative axis HOXB13-miR-103a-3p-PTEN and miR-378a-5p-SP1 would corroborate and give strength to the role of the miRNAs as biomarkers for the resistance of AA in mCRPC. Second, the cell cycle will be investigated with FACS analysis of prostate cancer cell lines after the up-regulation of miR-103a-3p and inhibition of miR-378a-5p. In fact, in our laboratory we showed that AA impacts the cell cycle activity of LnCaP cells. This may unravel the role of these two miRNAs in the halt in S-phase mediated by AA.

Interestingly, detection of miR-103a-3p and miR-378a-5p as valid biomarkers or the prediction of AA resistance in mCRPC patients, may be performed via ODG platform. However, even if the focus of this work is on c-miRNAs, it is intended that the ODG platform may be used for other circulating nucleic acids such as ctDNA, lncRNA and mRNA. Therefore, the clinical utility of the platform may be expanded and it could bring more biomarkers together in the same assay, even of different nature (e.g. miRNAs plus mRNAs detection). The use of the ODG platform in clinical settings comes with two important future implementations: 1) throughputness and 2) multiplexity. Integration of the ODG platform into an automatized system such as a robot will not only improve the assay reproducibility, but also increase the samples processed per run and decrease user's hands-on steps, which could introduce variability. The detection of more than one analyte in the same assay, is also very important when working with biomarkers. In fact, if it is true that a low number of biomarkers is desirable for costs and feasibility issues, it is also

generally accepted that the more the molecules are detected, the higher is the specificity of the information retrieved. The ODG, as it is now, cannot perform multiplexing assays, however two are the developments we are currently working on: 1) use of a very low amount of sample and 2) fluorescent SMART-NBs. The optimization of the protocol is currently a major goal in our pipeline. We achieved a proof-of-concept of the technology, nevertheless an optimal protocol, tailored for each tissue type and analyte (miRNAs, mRNAs, lncRNAs) has to be assessed. The first improvement is the reduction of the sample used: currently we are working on the use of 10uL. Such an amount of samples would allow running the same sample several times in the same plate for different analytes. However, the best scenario would be the multiplexing in the same well. For this reason, we are working on fluorescent SMART-NBs which would allow the detection of four analytes in the same assay, exploiting different fluorescent signals, one for each SMART-NB.

Another important future improvement will be the coupling of the ODG platform with the NBI technology. In fact, the analysis of EVs, not only would address some specificity issues of miRNAs as biomarkers, but also, concentrating a high volume sample into a very small amount, it would tackle the limit of LOD of the ODG platform. EVs fraction from plasma and urine samples from healthy individuals and prostate cancer patients will be analyzed via ODG platform.

In conclusion, miRNAs may be an important tool in clinical settings helping physicians in diagnosis, prognosis and prediction of treatments' efficacy. In our work, we discovered miR-103a-3p and miR-378a-5p as biomarkers for the prediction and follow-up of AA efficacy in mCRPC patients. However, the problems of the current technologies for the detection of miRNAs, such as RNA extraction and PCR amplification, pose several

limitations to the use of miRNAs in clinics. For these reasons, we developed the ODG platform, which is able to detect miRNAs without RNA extraction, PCR amplification and pre-labeling of the target. The ODG promises to provide a reliable, rapid, cost-effective and straightforward method for screening of miRNAs, not only those associated with cancer, but also with genetic and cardiac diseases, as well as drug safety / toxicology testing. The ODG may be used to detect miRNAs in other sources than plasma and to be coupled with other technologies, like NBI method for the isolation of EVs.

MATERIALS AND METHODS

1. Prostate cancer study

1.1 Patients

We evaluated a consecutive series of 34 mCRPC patients who were treated with AA after docetaxel failure as part of regular clinical practice at Santa Chiara Hospital (Trento, Italy) from 2013 to 2015. All subjects participating in the study were informed and written consent was obtained after approval by the Santa Chiara Hospital Ethical Committee and following the principles of the Declaration of Helsinki. Daily oral AA (1000 mg) plus prednisone 5 mg was administered twice a day. Clinical examination with regular assesment of liver, renal and bone marrow functions and PSA levels was performed monthly. Radiological assessment of tumour was regularly performed every three months or whenever clinically indicated. The treatment was stopped when clinical (performance status deterioration) or radiological progression [according to PCWG2 (Prostate Cancer Working Group 2) guidelines] (Scher et al., 2008) were indicating disease progression. The increase of PSA alone was not sufficient to stop AA administration. The patients were considered respondent to AA if they showed a) radiological response without PSA progression and performance status deterioration, or b) PSA reduction ≥ 50% compared to the baseline values. 12 patients were classified as respondent while the remaining 22 patients were considered non-respondent to AA. Patients' characteristics are showed in Table 6.

1.2 Plasma samples processing

5-mL blood sample was obtained from each patient at the baseline (before starting AA administration), and every three months until treatment discontinuation. Another blood sample was obtained at the time of treatment suspension. Blood collection was done in EDTA-treated tubes and immediately centrifuged for 15 minutes at 2500 rpm at 4°C. Plasma layer was collected and stored at -80°C in 250-500 µL aliquots at the Trentino Biobank (Santa Chiara Hospital, Trento, Italy).

1.3 RNA extraction and quantification

miRNeasy® Mini Kit (Qiagen) was used for total RNA extraction from 250 uL of plasma samples, according to the manufacturer's instructions. RNA was collected in 40 uL of DNase- and RNase-free water. In brief, the plasma was mixed with QIAzol Lysis Reagent and MS2 RNA (1 ug). After chloroform addition, the aqueous phase was loaded onto RNeasy Mini Spin Columns performing several washing steps. Qubit RNA HS Assay Kit (catalog #Q32852) was used with the Qubit Fluorometer, for the quantification of the 18 samples used for Exiqon miRNome RT-qPCR panels (Qiagen).

1.4 Exiqon miRNome RT-qPCR

Universal cDNA Synthesis kit (catalog #339340) was used for retro-transcribing 80 ng of extracted RNA together with 4 uL 5X Reaction buffer, 2 uL enzyme and DNase and RNase free water up to 20 uL of total reaction volume. The reaction was performed in a T100 Thermal Cycler (BioRad) as follows: 42°C for 60 minutes and 95°C for 5 minutes. miRNA profiling was performed via Exiqon microRNA Ready-to-Use PCR (miRCURY

LNA Universal RT microRNA PCR Human panel I+II, V4.M – #203600-21 Qiagen). First, cDNA template was diluted 1:50 in nuclease-free water, then mixed 1:1 with 2X SYBR Green Universal PCR Master Mix (Exiqon – Qiagen) for 10 uL of total reaction volume. The reaction was performed on a CFX384 Real-Time PCR Detection System (BioRad) as follows: 95°C for 10 minutes, 40 amplification cycles at 95°C for 10 seconds and 60°C for 1 minute.

1.5 TaqMan RT-qPCR validation

Validation of individual miRNA expression was performed via TaqMan RT-qPCR technology. A single reverse transcription step was performed with 2 uL of extracted RNA, 0.15 uL dNTPs mix, 1.5 uL of 10X reaction buffer, 0.19 uL RNase inhibitor, 1 uL enzyme – from TaqMan® microRNA Reverse Transcription Kit (Thermo Fisher) - 3 uL of TaqMan® microRNA assay hsa-miR-182-5p (#002334), hsa-miR-29b-3p (#000413), hsa-miRNA-331-5p (#002233), hsa-miR-144-3p (#197375), hsa-miR-378a-5p (#000567), hsa-miR-363-3p (#001271), hsa-miR-33a-5p (#002135), hsa-miR-103a-3p (#000439), hsa-miR-425-3p (#001516) and DNase and RNase free water up to 15 uL of total reaction volume. TaqMan qPCR step was performed in triplicate with 1,33 uL of cDNA product, 5 uL of Buffer - Faststart TaqMan® probe master (Sigma Aldrich) -1 uL of TaqMan® microRNA assay (listed above) and DNase and RNase free water up to 10 uL total reaction volume. RT-qPCR steps were performed with a Biorad CFX 384 system at the following conditions: reverse transcription at 16°C for 30 minutes, 42°C for 30 minutes, 85°C for 5 minutes; qPCR at 95°C for 10 minutes followed by 40 amplification cycles at 95°C for 15 seconds and 60°C for 1 minute.

1.6 RT-qPCR data analyses

GenEX software was used for the analysis of the data from Exiqon microRNA Ready-to-Use PCR panels. Cq values of Exiqon panels were normalised on miR-425-5p, chosen by NormFinder software feeding the algorithm with the panels data. The volcano plot was produced dividing the samples in two groups [9 non-respondent to AA (NR) + 9 respondent to AA (R)]. Fold change was then evaluated with respect to the average of Cq values of NR group [2 EXP- (ΔCq NR – ΔCq R)]. TaqMan RT-qPCR Cq values were normalised on miR-425-5p. Statistical analysis for differential expression on Exiqon RT-qPCR panel data and TaqMan RT-qPCR were performed via Student's t-test (with Bonferroni correction for Exiqon panels' data). Unsupervised clustering was performed via RStudio (V 1.0.143) with "rpart" package (V 4.1-11).

1.7 Bioinformatic analyses

miR-103a-3p and miR-378a-5p predicted targets were retrieved via TargetScan (Agarwal et al., 2015), Pita (Kertesz et al., 2007) and MiRanda softwares (Betel et al., 2010) and the results were filtered for binding energy of -18kcal/mol or lower. Further analysis was performed on the targets coming from all the predicting softwares. Validated targets where retrieved from miRTarBase database (V7.0) (Vlachos et al., 2015). Promoter analysis on the two miRNAs was performed via GeneXplain software: the promoters of miR-103a1-3p, miR-103a2-3p, miR-378a-5p, and PANK2 for transcription factor analysis, were calculated considering different ranges from -4900 / -3900 / -2900 / -1900 / -900 to +100, where 0 was the transcription starting site (TSS). The TSS was automatically retrieved by GeneXplain software from miRBase (V21) (Koschmann et al., 2015). The ENSEMBL annotations used for transcription factor analysis were 1)

ENSG00000199035 (hsa-miR-103a1) 2) ENSG00000199047 (hsa-miR-378a) 3) ENSG00000125779 (PANK2) 4) ENSG00000199024 (hsa-miR-103a2).

1.8 Cell line analyses

LnCaP cell line was grown in RPMI medium supplemented with 10% fetal bovine serum and 1% Penicillin and Streptavidin.

a) *EC50 assay:* 20X10E+03 cells were seeded in a 96-well plate. After 24 hours, different concentration of AA (Sigma Aldrich) were administered to the cells. After 72 hours, the cells were incubated 1 hour with 100 uL Thiazolyl Blue Tetrazolium Bromide salt (Sigma Aldrich) 0,5 mg/mL diluted in RPMI supplemented (10% fetal bovine serum and 1% Penicillin and Streptavidin) medium. After incubation, Thiazolyl Blue Tetrazolium Bromide salt was discarded and 100 uL of DMSO was added to the cells for absorbance measurement (514 nm) via EL800 microplate reader (Biotek).

b) *FACS analysis*: 26X10E+04 cells were seeded in a 12-well plate. After 24 hours, 18uM of AA were administered to the cells and 5uM of paclitaxel were administered to the cells for apoptotic control. After 48 hours:

    a. *cell cycle analysis*: cells were detached and washed with PBS. Ethanol 70% was added and the cells were incubated for 20 minutes at -20°C. The cells were then washed via PBS + BSA 2%. 200 uL of RNAse 100ug/mL + 0-1% Triton-X was added and the cells transferred in FACS tubes. Propidium iodide was used as marker.

b. *cell death analysis*: 5uM paclitaxel has been used as apoptotic control and flash-frozen (liquid nitrogen) as necrotic control. The cells were detached and washed with PBS. 200 uL of ligation buffer was added and the cells were transferred in FACS tubes. Annexin and propidium iodide were used as markers.

c) *AA resistance analysis:* 12X10E+03 cells were seeded in a 96-well plate. After 24 hours, 50nM or 100 nM of miR-103a-3p mimic (Qiagen – YM00470828) and of miR-378a-5p inhibitor (Qiagen – YI04101420) were transfected via Lipofectamine 3000 (Thermo Fisher) and incubated for 48 hours. Subsequently, 18uM of AA (Sigma Aldrich) solved in DMSO was added to the cells. DMSO (Sigma Aldrich) was used as control. After 72 hours, the cells were incubated 1 hour with 100 uL Thiazolyl Blue Tetrazolium Bromide salt (Sigma Aldrich) 0,5 mg/mL diluted in RPMI supplemented (10% fetal bovine serum and 1% Penicillin and Streptavidin) medium. After incubation, Thiazolyl Blue Tetrazolium Bromide salt was discarded and 100 uL of DMSO was added to the cells for absorbance measurement (514 nm) via EL800 microplate reader (Biotek).

2. ODG

2.1 Materials and instrumentation

RNA oligomer mimic miRNAs were purchased HPLC-purified from Exiqon. Unless specified differently, all chemicals and solvents were obtained from Sigma Aldrich and used as received. Dynabeads® M-270 2.8-μm diameter superparamagnetic beads presenting carboxylic acid groups (30 mg/mL: 2X10E+09 beads catalog# 14305D),

Pierce™ High Sensitivity Streptavidin-HRP (catalog#21132), and SuperSignal™ ELISA Femto Substrate (catalog# 37075) were obtained from Thermo Fisher Scientific. HRP enzyme was diluted in HRP-StabilPLUS from Kementec (catalog# 4530L). Reaction buffer was prepared from 2X Saline Sodium Citrate (SSC) and 0.1% Sodium Dodecyl Sulphate (SDS) with the pH adjusted to 6.0 using HCl. Concentrations of RNA oligomers and abasic PNA probes solutions were determined using a Thermo Fisher NanoDrop 1000 spectrophotometer. Chem-NAT was conducted in a Techne Thermal cycler (TC-5000). A TECAN multi-mode microplate reader was used as final readout together with SiPM-based reader provided by OPTOELETTRONICA ITALIA S.R.L (Italy). RT-qPCR reaction was detected with CFX96™ Real-Time PCR Detection System (BIO-RAD).

2.2 DestiNA Genomics abasic PNA probes synthesis

Four abasic PNA probes terminated with an amino-PEG linker were synthesized (Table 8) by DestiNA Genomica S.L (Spain), using standard solid phase chemistry on a MultiPep Synthesiser (Intavis AG GmbH, Germany). All the sequences were designed to allow anti-parallel hybridization with hsa-miR-21-5p. Aldehyde-modified cytosine and adenine, tagged with biotin via a 12 ethylene glycol units spacer, were prepared using a synthetic route described elsewhere (Bowler et al., 2010).

2.3 Coupling of magnetic beads with abasic PNA probes

The abasic PNA probes were coupled to 2.8 μm in diameter carboxylated beads. Briefly, 100 uL of beads (containing 2 x 10E+06 beads) were washed by adding 100 μL 0.01 mol/L NaOH and mixing. The beads were pelleted, supernatant removed, washed once in

100 μL 0.01 mol/L NaOH, and three times in 100 μL distilled water. The beads were re-suspended in 150 μL of freshly-prepared 50 mg/mL 1-ethyl-3-(3-dimethylaminopropyl) carbodiimide (EDC) in water and incubated with slow tilt rotation at 23°C for 30 min. After activation, the beads were washed once with 100 μL cold water and once with 100 μL cold MES buffer (50 mmol/L, pH 5.0). 100 μL of a solution containing 2100 pmol abasic PNA probe in MES buffer 50 mmol/L (pH 5) was added to the activated beads. The mixture of probes and beads was incubated at 4°C for 4 h with slow tilt rotation, followed by washing with 50 mmol/L MES buffer (pH 5). The remaining activated carboxyl groups were quenched by incubating the beads with 100 μL of 50 mmol/L ethanolamine in PBS (pH 8) for 1 h, followed by three washes with 100 μL of 10% PEG10K and 0.1% Tween-20 in PBS. The capture beads were stored at 4°C in 100 μL 0.1% Tween-20 in PBS.

2.4 Patients

Plasma samples from eight different NSCLC patients were retrieved from the archives of the Trentino Biobank, at the Unit of Surgical Pathology of the S. Chiara Hospital, Trento, Italy. All cases were fully anonymized, and the use of the samples had been approved by the Ethical Committee of the Santa Chiara Hospital, Trento. After the informed consent was signed, 8 mL of blood was collected in EDTA tubes, and plasma was obtained by centrifugation at 1200g for 15 minutes then 3000g for 10 minutes. Each plasma sample was stored at -80°C until testing.

2.5 Generation of calibration curves with ODG platform and RT-qPCR

Synthetic RNA oligos (cel-miR-39: 5’ AGC UGA UUU CGU CUU GGU AAU A 3’; hsa-miR-21-5p: 5’ UAG CUU AUC AGA CUG AUG UUG A 3’) were stored at -80°C. All experiments were run in triplicates and negative controls were included in each assay.

a) *Calibration curve with ODG platform.* The calibration curve was performed with RNA oligos dilutions: 0.029, 0.059, 0.117, 0.469 nmol/L (final concentration) in DNase and RNase free water. Briefly, a Master Mix (Vf = 50 uL) was first added to perform Chem-NAT reaction for 1 hour at 41°C and 1200 r.p.m: 2X SSC + 0.1% SDS buffer, SMART-A-Biotin (2 umol/L), sodium cyanoborohydride (reducing agent - 4,5 mmol/L), 2.5 x 10E+05 of functionalized-beads with abasic PNA probe aPP4 and synthetic RNA mimic hsa-miR-21-5p. Negative control signal (NCS) was performed adding DNase and RNase free water to generate the assay background signal. Subsequently, the beads were washed three times with PBS + 0.1% Tween20 (200 uL) and once with HRP-StabilPLUS using a magnet to separate the beads from the supernatant. 100 uL HRP-streptavidin (1:8000) was added and incubated for 5 min at room temperature. Three washings with PBS + 0.1% Tween20 (200 uL) were performed. Detection was entrusted by a chemiluminescent reaction using 100 uL of SuperSignal™ ELISA Femto Substrate according to the manufacturer's

instructions. Output signal was measured using a multi-mode microplate reader and the SiPM-based reader. Linear fit was generated considering five points: the four positive signals and the NCS. The limit of detection (LOD) was calculated interpolating the background signal (NCS + 3*SD_{NCS}) into the linear fit.

b) *Calibration curves with RT-qPCR:* The calibration curves were generated using RNA oligos spiked into both a) 15 uL of aqueous solutions used for the reverse transcription and b) into 200 uL of plasma samples undergoing RNA extraction before being reverse transcripted. For (a), 2 uL of RNA oligos (6.4E-13; 3.20E-13; 8.00E-14; 1.00E-14; 1.25E-15; 1.56E-16; 1.95E-17; 2.44E-18; 3.05E-19 moles/uL) diluted in DNase and RNase free water were spiked in TaqMan® reverse transcription step together with 0.15 uL dNTPs mix, 1.5 uL of 10X reaction buffer, 0.19 uL RNase inhibitor, 1 uL enzyme – from TaqMan® microRNA Reverse Transcription Kit (catalog# 4366596 - Thermo Fisher), 3 uL of either TaqMan® microRNA assay cel-miR-39 (catalog# 464312_mat) or TaqMan® microRNA assay hsa-miR-21-5p (catalog# 4427975) and DNase and RNase free water up to 15 uL total reaction volume. TaqMan® qPCR step was performed with 1,33 uL of cDNA product, 5 uL of Buffer - Faststart TaqMan® probe master (catalog# 4673409001 – Sigma Aldrich) - and 1 uL of TaqMan® microRNA assay cel-miR-39 or TaqMan®

microRNA assay hsa-miR-21-5p and DNase and RNase free water up to 10 uL total reaction volume. For (b), 750uL of Qiazol plus 1,25 uL of 800 ng/uL MS2 were added to 200 uL of plasma; subsequently 40 uL of RNA oligos (6.4E-13; 3.20E-13; 8.00E-14; 1.00E-14; 1.25E-15; 1.56E-16; 1.95E-17; 2.44E-18; 3.05E-19 moles/uL) diluted in DNase and RNase free water were spiked in plasma-QIAzol mix. RNA was recovered in 40 uL of DNase and RNase free water. 2 uL of extracted RNA was used for TaqMan® reverse transcription step as previously described. TaqMan® qPCR step was performed as previously described. RT-qPCR steps were performed with a Biorad CFX 96 system with the following conditions: reverse transcription at 16°C for 30 minutes, 42°C for 30 minutes, 85°C for 5 minutes; qPCR at 95°C for 10 minutes followed by 40 cycles of 95°C for 15 seconds and 60°C for 1 minute.

2.6 RNA extraction and RT-qPCR for lung cancer patients

RNA from the plasma samples (200 uL) was extracted using miRNeasy Mini Kit (Qiagen) according to the manufacturer's instructions and collected in 40 uL of DNase- and RNase-free water. In brief, the plasma was lysed with a mix of QIAzol Lysis Reagent and MS2 RNA (1ug). After chloroform addition, the aqueous phase was loaded onto RNeasy Mini Spin Columns where several washing steps were performed according to the manufacturer’s protocol. RNA was eventually eluted in 40 uL of DNase and RNase free

water. TaqMan® RT-qPCR for hsa-miR-21-5p was performed using 2 uL of extracted RNA as explained above.

2.7 Chem-NAT reaction for plasma samples analysis

In order to detect hsa-miR-21-5p from plasma samples of NSCLC patients, 100 uL of plasma was analyzed in technical triplicates. DestiNA's proprietary lysis buffer was added to the plasma aliquots in a 2:1 ratio. 2.5 x 10E+05 functionalized-beads with abasic PNA probe 4 were added to the crude lysate. The solutions were incubated by rotating on a mixer for 1 h at room temperature. The vials were placed on a magnet and washing steps were performed as follows: a) removing the supernatant b) washing the beads three times using the magnet to separate the beads from the supernatant (lysate debris) with Buffer 2X SSC + 0.1% SDS (200 uL). The Master Mix was added and Chem-NAT reaction was performed as explained above. Negative control was generated adding a wrong SMART-base [SMART-C-Biotin (5 umol/L) instead of SMART-A-Biotin (2 umol/L)] which cannot be incorporated by the abasic PNA probe, but which would still generate a signal in case of inappropriate binding.

3. Extracellular vesicles and microRNAs

3.1 Isolation of extracellular vesicles

9 mL of blood were sampled from 8 volunteers in EDTA-tubes. Whole blood was centrifuged at 1700g for 15 minutes. Plasma was collected and further centrifuged at 3000g for ten minutes to remove platelets. 1.5 mL of plasma was used for the isolation of

extracellular vesicles NBI technology as explained elsewhere (Notarangelo et al., 2019). Briefly, the plasma was diluted in PBS and NBI-beads were added. The mixture was incubated at room temperature for 30 minutes in slow tilt rotation and then centrifuged at 500g for 3 minutes to pellet the beads. The supernatant (plasma EV-depleted – dEV) was collected. The beads were resuspended in 1.5 mL of elution buffer, incubated at 28°C for 10 minutes at 600rpm and then centrifuged at 500g for 3 minutes to pellet the beads . The supernatant containing EVs was collected and kept at 4°C for experiments run within 24 hours or at -80°C for long storage.

3.2 EVs characterization

Size and concentration of EVs isolated by NBI were analyzed by TRPS using qNano (IZON). The measurements were done using two nanopores: NP200 (size range: 85 - 500 nm) and NP400 (size range: 185 – 1100 nm) and the instrument was calibrated with CPC200 and CPC400 calibration particles (IZON). 10 uL of isolated EVs were used for size and number characterization via TRPS.

3.3 RNA extraction and RT-qPCR

RNA from isolated EVs, plasma depleted from EVs and total plasma, for each individual (100 uL) was extracted using miRNeasy Mini Kit (Qiagen) according to the manufacturer's instructions and collected in 40 uL of DNase- and RNase-free water. In brief, the plasma was lysed with a mix of QIAzol Lysis Reagent and MS2 RNA (1ug). After chloroform addition, the aqueous phase was loaded onto RNeasy Mini Spin Columns where several washing steps were performed according to manufacturer’s protocol. RNA was eventually eluted in 40 uL of DNase and RNase free water. TaqMan® RT-qPCR for hsa-miR-21-5p (catalog #4427975) and hsa-miR-223-3p (catalog

#4427975) was performed using 2 uL of extracted RNA for reverse transcription and 1,33 uL of cDNA for qPCR as explained in Materials and Methods, paragraph 1.5 "*TaqMan RT-qPCR validation*".

REFERENCES

Admyre, C., Johansson, S. M., Qazi, K. R., Filén, J.-J., Lahesmaa, R., Norman, M., et al. (2007). Exosomes with Immune Modulatory Features Are Present in Human Breast Milk. *J. Immunol.* 179, 1969–1978. doi:10.4049/jimmunol.179.3.1969.

Agalliu, I., Karlins, E., Kwon, E. M., Iwasaki, L. M., Diamond, A., Ostrander, E. A., et al. (2007). Rare germline mutations in the BRCA2 gene are associated with early-onset prostate cancer. *Br. J. Cancer* 97, 826–31. doi:10.1038/sj.bjc.6603929.

Agarwal, V., Bell, G. W., Nam, J.-W., and Bartel, D. P. (2015). Predicting effective microRNA target sites in mammalian mRNAs. *Elife* 4. doi:10.7554/eLife.05005.

Aghdam, S. G., Ebrazeh, M., Hemmatzadeh, M., Seyfizadeh, N., Shabgah, A. G., Azizi, G., et al. (2019). The role of microRNAs in prostate cancer migration, invasion, and metastasis. *J. Cell. Physiol.* 234, 9927–9942. doi:10.1002/jcp.27948.

Ahmad, I., and Sansom, O. J. (2018). Role of Wnt signalling in advanced prostate cancer. *J. Pathol.* 245, 3–5. doi:10.1002/path.5029.

Akers, J. C., Hua, W., Li, H., Ramakrishnan, V., Yang, Z., Quan, K., et al. (2017). A cerebrospinal fluid microRNA signature as biomarker for glioblastoma. *Oncotarget* 8. doi:10.18632/oncotarget.18332.

Al-Nedawi, K., Meehan, B., Micallef, J., Lhotak, V., May, L., Guha, A., et al. (2008). Intercellular transfer of the oncogenic receptor EGFRvIII by microvesicles derived from tumour cells. *Nat. Cell Biol.* 10, 619–624. doi:10.1038/ncb1725.

Almog, N., Briggs, C., Beheshti, A., Ma, L., Wilkie, K. P., Rietman, E., et al. (2013). Transcriptional changes induced by the tumor dormancy-associated microRNA-190. *Transcription* 4. doi:10.4161/trns.25558.

Almog, N., Ma, L., Schwager, C., Brinkmann, B. G., Beheshti, A., Vajkoczy, P., et al. (2012). Consensus Micro RNAs Governing the Switch of Dormant Tumors to the

Fast-Growing Angiogenic Phenotype. *PLoS One* 7. doi:10.1371/journal.pone.0044001.

Andersen, C. L., Jensen, J. L., and Ørntoft, T. F. (2004). Normalization of real-time quantitative reverse transcription-PCR data: a model-based variance estimation approach to identify genes suited for normalization, applied to bladder and colon cancer data sets. *Cancer Res.* 64, 5245–50. doi:10.1158/0008-5472.CAN-04-0496.

Andreu, Z., Rivas, E., Sanguino-Pascual, A., Lamana, A., Marazuela, M., González-Alvaro, I., et al. (2016). Comparative analysis of EV isolation procedures for miRNAs detection in serum samples. *J. Extracell. Vesicles* 5. doi:10.3402/jev.v5.31655.

Angélica Luque-González, M., Tabraue-Chávez, M., López-Longarela, B., María Sánchez-Martín, R., Ortiz-González, M., Soriano-Rodríguez, M., et al. (2018). Identification of Trypanosomatids by detecting Single Nucleotide Fingerprints using DNA analysis by dynamic chemistry with MALDI-ToF. *Talanta* 176, 299–307. doi:10.1016/j.talanta.2017.07.059.

Antonarakis, E. S., Lu, C., Wang, H., Luber, B., Nakazawa, M., Roeser, J. C., et al. (2014). AR-V7 and resistance to enzalutamide and abiraterone in prostate cancer. *N. Engl. J. Med.* 371, 1028–1038. doi:10.1056/NEJMoa1315815.

Arroyo, J. D., Chevillet, J. R., Kroh, E. M., Ruf, I. K., Pritchard, C. C., Gibson, D. F., et al. (2011). Argonaute2 complexes carry a population of circulating microRNAs independent of vesicles in human plasma. *Proc. Natl. Acad. Sci. U. S. A.* 108, 5003–8. doi:10.1073/pnas.1019055108.

Asaga, S., Kuo, C., Nguyen, T., Terpenning, M., Giuliano, A. E., and Hoon, D. S. B. (2011). Direct serum assay for microRNA-21 concentrations in early and advanced breast cancer. *Clin. Chem.* 57, 84–91. doi:10.1373/clinchem.2010.151845.

Au Yeung, C. L., Co, N. N., Tsuruga, T., Yeung, T. L., Kwan, S. Y., Leung, C. S., et al. (2016). Exosomal transfer of stroma-derived miR21 confers paclitaxel resistance in ovarian cancer cells through targeting APAF1. *Nat. Commun.* 7. doi:10.1038/ncomms11150.

Auyeung, V. C., Ulitsky, I., McGeary, S. E., and Bartel, D. P. (2013). Beyond secondary structure: Primary-sequence determinants license Pri-miRNA hairpins for processing. *Cell* 152, 844–858. doi:10.1016/j.cell.2013.01.031.

Avgeris, M., Stravodimos, K., and Scorilas, A. (2014). Loss of miR-378 in prostate cancer, a common regulator of KLK2 and KLK4, correlates with aggressive disease phenotype and predicts the short-term relapse of the patients. *Biol. Chem.* 395, 1095–104. doi:10.1515/hsz-2014-0150.

Baggish, A. L., Hale, A., Weiner, R. B., Lewis, G. D., Systrom, D., Wang, F., et al. (2011). Dynamic regulation of circulating microRNA during acute exhaustive exercise and sustained aerobic exercise training. *J. Physiol.* 589, 3983–3994. doi:10.1113/jphysiol.2011.213363.

Balaj, L., Lessard, R., Dai, L., Cho, Y. J., Pomeroy, S. L., Breakefield, X. O., et al. (2011). Tumour microvesicles contain retrotransposon elements and amplified oncogene sequences. *Nat. Commun.* 2. doi:10.1038/ncomms1180.

Bartel, D. P. (2009). MicroRNAs: Target Recognition and Regulatory Functions. *Cell* 136, 215–233. doi:10.1016/j.cell.2009.01.002.

Ben-Dov, I. Z., Whalen, V. M., Goilav, B., Max, K. E. A., and Tuschl, T. (2016). Cell and Microvesicle Urine microRNA Deep Sequencing Profiles from Healthy Individuals: Observations with Potential Impact on Biomarker Studies. *PLoS One* 11. doi:10.1371/journal.pone.0147249.

Bergers, G., and Benjamin, L. E. (2003). Tumorigenesis and the angiogenic switch. *Nat.*

Rev. Cancer 3, 401–410. doi:10.1038/nrc1093.

Betel, D., Koppal, A., Agius, P., Sander, C., and Leslie, C. (2010). Comprehensive modeling of microRNA targets predicts functional non-conserved and non-canonical sites. *Genome Biol.* 11, R90. doi:10.1186/gb-2010-11-8-r90.

Bian, X.-J., Zhang, G.-M., Gu, C.-Y., Cai, Y., Wang, C.-F., Shen, Y.-J., et al. (2014). Down-regulation of Dicer and Ago2 is associated with cell proliferation and apoptosis in prostate cancer. *Tumor Biol.* 35, 11571–11578. doi:10.1007/s13277-014-2462-3.

Bian, X., Shen, Y., Zhang, G., Gu, C., Cai, Y., Wang, C., et al. (2015). Expression of Dicer and Its Related MiRNAs in the Progression of Prostate Cancer. *PLoS One* 10, e0120159. doi:10.1371/journal.pone.0120159.

Blenkiron, C., Goldstein, L. D., Thorne, N. P., Spiteri, I., Chin, S.-F., Dunning, M. J., et al. (2007). MicroRNA expression profiling of human breast cancer identifies new markers of tumor subtype. *Genome Biol.* 8, R214. doi:10.1186/gb-2007-8-10-r214.

Boeckel, J.-N., Thomé, C. E., Leistner, D., Zeiher, A. M., Fichtlscherer, S., and Dimmeler, S. (2013). Heparin Selectively Affects the Quantification of MicroRNAs in Human Blood Samples. *Clin. Chem.* 59, 1125–1127. doi:10.1373/clinchem.2012.199505.

Bolstad, B. M., Irizarry, R. A., Åstrand, M., and Speed, T. P. (2003). A comparison of normalization methods for high density oligonucleotide array data based on variance and bias. *Bioinformatics* 19, 185–193. doi:10.1093/bioinformatics/19.2.185.

Bottani, M., Banfi, G., and Lombardi, G. (2019). Circulating miRNAs as Diagnostic and Prognostic Biomarkers in Common Solid Tumors: Focus on Lung, Breast, Prostate Cancers, and Osteosarcoma. *J. Clin. Med.* 8, 1661. doi:10.3390/jcm8101661.

Bowler, F. R., Diaz-Mochon, J. J., Swift, M. D., and Bradley, M. (2010a). DNA Analysis

by Dynamic Chemistry. *Angew. Chemie Int. Ed.* 49, 1809–1812. doi:10.1002/anie.200905699.

Bowler, F. R., Diaz-Mochon, J. J., Swift, M. D., and Bradley, M. (2010b). DNA Analysis by Dynamic Chemistry. *Angew. Chemie Int. Ed.* 49, 1809–1812. doi:10.1002/anie.200905699.

Brandt, O., and Hoheisel, J. D. (2004). Peptide nucleic acids on microarrays and other biosensors. *Trends Biotechnol.* 22, 617–622. doi:10.1016/j.tibtech.2004.10.003.

Briones, C., and Moreno, M. (2012). Applications of peptide nucleic acids (PNAs) and locked nucleic acids (LNAs) in biosensor development. *Anal. Bioanal. Chem.* 402, 3071–89. doi:10.1007/s00216-012-5742-z.

Broughton, J. P., Lovci, M. T., Huang, J. L., Yeo, G. W., and Pasquinelli, A. E. (2016). Pairing beyond the Seed Supports MicroRNA Targeting Specificity. *Mol. Cell* 64, 320–333. doi:10.1016/j.molcel.2016.09.004.

Brown, S., Thomson, S., Veal, J., and Davis, D. (1994). NMR solution structure of a peptide nucleic acid complexed with RNA. *Science (80-.).* 265, 777–780. doi:10.1126/science.7519361.

Caby, M.-P., Lankar, D., Vincendeau-Scherrer, C., Raposo, G., and Bonnerot, C. (2005). Exosomal-like vesicles are present in human blood plasma. *Int. Immunol.* 17, 879–887. doi:10.1093/intimm/dxh267.

Caffo, O., Veccia, A., Kinspergher, S., and Maines, F. (2018). Abiraterone acetate and its use in the treatment of metastatic prostate cancer: A review. *Futur. Oncol.* 14, 431–442. doi:10.2217/fon-2017-0430.

Calatayud, D., Dehlendorff, C., Boisen, M. K., Hasselby, J. P., Schultz, N. A., Werner, J., et al. (2017). Tissue MicroRNA profiles as diagnostic and prognostic biomarkers in patients with resectable pancreatic ductal adenocarcinoma and periampullary

cancers. *Biomark. Res.* 5, 8. doi:10.1186/s40364-017-0087-6.

Calin, G. A., Cimmino, A., Fabbri, M., Ferracin, M., Wojcik, S. E., Shimizu, M., et al. (2008). MiR-15a and miR-16-1 cluster functions in human leukemia. *Proc. Natl. Acad. Sci. U. S. A.* 105, 5166–5171. doi:10.1073/pnas.0800121105.

Calin, G. A., and Croce, C. M. (2006). MicroRNA-cancer connection: The beginning of a new tale. *Cancer Res.* 66, 7390–7394. doi:10.1158/0008-5472.CAN-06-0800.

Cao, Y., Zhao, D., Li, P., Wang, L., Qiao, B., Qin, X., et al. (2017). MicroRNA-181a-5p Impedes IL-17-Induced Nonsmall Cell Lung Cancer Proliferation and Migration through Targeting VCAM-1. *Cell. Physiol. Biochem.* 42, 346–356. doi:10.1159/000477389.

Cappuzzo, F., Sacconi, A., Landi, L., Ludovini, V., Biagioni, F., D'Incecco, A., et al. (2014). MicroRNA Signature in Metastatic Colorectal Cancer Patients Treated With Anti-EGFR Monoclonal Antibodies. *Clin. Colorectal Cancer* 13, 37-45.e4. doi:10.1016/j.clcc.2013.11.006.

Cha, D. J., Franklin, J. L., Dou, Y., Liu, Q., Higginbotham, J. N., Demory Beckler, M., et al. (2015). KRAS-dependent sorting of miRNA to exosomes. *Elife* 4, e07197. doi:10.7554/eLife.07197.

Chang, B. L., Zheng, S. L., Isaacs, S. D., Turner, A. R., Bleecker, E. R., Walsh, P. C., et al. (2003). Evaluation of SRD5A2 sequence variants in susceptibility to hereditary and sporadic prostate cancer. *Prostate* 56, 37–44. doi:10.1002/pros.10225.

Chang, B., Zheng, S. L., Hawkins, G. A., Isaacs, S. D., Wiley, K. E., Turner, A., et al. (2002). Joint Effect of HSD3B1 and HSD3B2 Genes Is Associated with Hereditary and Sporadic Prostate Cancer Susceptibility. *Cancer Res.* 62, 1784–1789.

Chen, B., Liu, Y., Jin, X., Lu, W., Liu, J., Xia, Z., et al. (2014). MicroRNA-26a regulates glucose metabolism by direct targeting PDHX in colorectal cancer cells. *BMC*

Cancer 14. doi:10.1186/1471-2407-14-443.

Chen, L., Guan, H., Gu, C., Cao, Y., Shao, J., and Wang, F. (2016a). miR-383 inhibits hepatocellular carcinoma cell proliferation via targeting APRIL. *Tumor Biol.* 37, 2497–2507. doi:10.1007/s13277-015-4071-1.

Chen, Q., Zhao, X., Zhang, H., Yuan, H., Zhu, M., Sun, Q., et al. (2015). MiR-130b suppresses prostate cancer metastasis through down-regulation of MMP2. *Mol. Carcinog.* 54, 1292–1300. doi:10.1002/mc.22204.

Chen, Q., Zhou, W., Han, T., Du, S., Li, Z., Zhang, Z., et al. (2016b). MiR-378 suppresses prostate cancer cell growth through downregulation of MAPK1 in vitro and in vivo. *Tumor Biol.* 37, 2095–2103. doi:10.1007/s13277-015-3996-8.

Chen, X., Ba, Y., Ma, L., Cai, X., Yin, Y., Wang, K., et al. (2008). Characterization of microRNAs in serum: a novel class of biomarkers for diagnosis of cancer and other diseases. *Cell Res.* 18, 997–1006. doi:10.1038/cr.2008.282.

CHEN, Y., LU, X., WU, B., SU, Y., LI, J., and WANG, H. (2015). MicroRNA 363 mediated positive regulation of c-myc translation affect prostate cancer development and progress. *Neoplasma* 62, 191–198. doi:10.4149/neo_2015_024.

Chen, Z., Yu, T., Cabay, R. J., Jin, Y., Mahjabeen, I., Luan, X., et al. (2017). miR-486-3p, miR-139-5p, and miR-21 as Biomarkers for the Detection of Oral Tongue Squamous Cell Carcinoma. *Biomark. Cancer* 9, 1–8. doi:10.4137/BIC.S40981.

Cheng, H. H., Yi, H. S., Kim, Y., Kroh, E. M., Chien, J. W., Eaton, K. D., et al. (2013). Plasma processing conditions substantially influence circulating microRNA biomarker levels. *PLoS One* 8, e64795. doi:10.1371/journal.pone.0064795.

Cheng, X., Xi, Q. Y., Wei, S., Wu, D., Ye, R. S., Chen, T., et al. (2016). Critical role of miR-125b in lipogenesis by targeting stearoyl-CoA desaturase-1 (SCD-1). *J. Anim. Sci.* 94, 65–76. doi:10.2527/jas.2015-9456.

Cheng, Y. Q., Ren, J. P., Zhao, J., Wang, J. M., Zhou, Y., Li, G. Y., et al. (2015). MicroRNA-155 regulates interferon- γ production in natural killer cells via Tim-3 signalling in chronic hepatitis C virus infection. *Immunology* 145, 485–497. doi:10.1111/imm.12463.

Cheng, Z., Liu, F., Zhang, H., Li, X., Li, Y., Li, J., et al. (2017). miR-135a inhibits tumor metastasis and angiogenesis by targeting FAK pathway. *Oncotarget* 8, 31153–31168. doi:10.18632/oncotarget.16098.

Chevillet, J. R., Kang, Q., Ruf, I. K., Briggs, H. A., Vojtech, L. N., Hughes, S. M., et al. (2014). Quantitative and stoichiometric analysis of the microRNA content of exosomes. *Proc. Natl. Acad. Sci. U. S. A.* 111, 14888–93. doi:10.1073/pnas.1408301111.

Chhabra, R., Dubey, R., and Saini, N. (2011). Gene expression profiling indicate role of ER stress in miR-23a∼27a∼24-2 cluster induced apoptosis in HEK293T cells. *RNA Biol.* 8. doi:10.4161/rna.8.4.15583.

Chistiakov, D. A., Myasoedova, V. A., Grechko, A. V., Melnichenko, A. A., and Orekhov, A. N. (2018). New biomarkers for diagnosis and prognosis of localized prostate cancer. *Semin. Cancer Biol.* 52, 9–16. doi:10.1016/j.semcancer.2018.01.012.

Chivet, M., Javalet, C., Laulagnier, K., Blot, B., Hemming, F. J., and Sadoul, R. (2014). Exosomes secreted by cortical neurons upon glutamatergic synapse activation specifically interact with neurons. *J. Extracell. Vesicles* 3. doi:10.3402/jev.v3.24722.

Chugh, P., and Dittmer, D. P. (2012). Potential pitfalls in microRNA profiling. *Wiley Interdiscip. Rev. RNA* 3, 601–616. doi:10.1002/wrna.1120.

Chung, A. S., Lee, J., and Ferrara, N. (2010). Targeting the tumour vasculature: Insights

from physiological angiogenesis. *Nat. Rev. Cancer* 10, 505–514. doi:10.1038/nrc2868.

Cimmino, A., Calin, G. A., Fabbri, M., Iorio, M. V., Ferracin, M., Shimizu, M., et al. (2005). miR-15 and miR-16 induce apoptosis by targeting BCL2. *Proc. Natl. Acad. Sci.* 102, 13944–13949. doi:10.1073/pnas.0506654102.

Collino, F., Deregibus, M. C., Bruno, S., Sterpone, L., Aghemo, G., Viltono, L., et al. (2010). Microvesicles Derived from Adult Human Bone Marrow and Tissue Specific Mesenchymal Stem Cells Shuttle Selected Pattern of miRNAs. *PLoS One* 5, e11803. doi:10.1371/journal.pone.0011803.

Collino, F., Pomatto, M., Bruno, S., Lindoso, R. S., Tapparo, M., Sicheng, W., et al. (2017). Exosome and Microvesicle-Enriched Fractions Isolated from Mesenchymal Stem Cells by Gradient Separation Showed Different Molecular Signatures and Functions on Renal Tubular Epithelial Cells. *Stem Cell Rev. Reports* 13, 226–243. doi:10.1007/s12015-016-9713-1.

Conde-Vancells, J., Rodriguez-Suarez, E., Embade, N., Gil, D., Matthiesen, R., Valle, M., et al. (2008). Characterization and Comprehensive Proteome Profiling of Exosomes Secreted by Hepatocytes. *J. Proteome Res.* 7, 5157–5166. doi:10.1021/pr8004887.

Connor, D. E., Exner, T., Ma, D. D. F., and Joseph, J. E. (2010). The majority of circulating platelet-derived microparticles fail to bind annexin V, lack phospholipid-dependent procoagulant activity and demonstrate greater expression of glycoprotein Ib. *Thromb. Haemost.* 103, 1044–1052. doi:10.1160/TH09-09-0644.

Costa Verdera, H., Gitz-Francois, J. J., Schiffelers, R. M., and Vader, P. (2017). Cellular uptake of extracellular vesicles is mediated by clathrin-independent endocytosis and macropinocytosis. *J. Control. Release* 266, 100–108.

doi:10.1016/j.jconrel.2017.09.019.

Cui, M., Liu, W., Zhang, L., Guo, F., Liu, Y., Chen, F., et al. (2017). Over-Expression of miR-21 and Lower PTEN Levels in Wilms' Tumor with Aggressive Behavior. *Tohoku J. Exp. Med.* 242, 43–52. doi:10.1620/tjem.242.43.

da Silva Oliveira, K. C., Thomaz Araújo, T. M., Albuquerque, C. I., Barata, G. A., Gigek, C. O., Leal, M. F., et al. (2016). Role of miRNAs and their potential to be useful as diagnostic and prognostic biomarkers in gastric cancer. *World J. Gastroenterol.* 22, 7951–62. doi:10.3748/wjg.v22.i35.7951.

Daugaard, I., Ven?, M. T., Yan, Y., Kjeldsen, T. E., Lamy, P., Hager, H., et al. (2017). Small RNA sequencing reveals metastasis-related microRNAs in lung adenocarcinoma. *Oncotarget* 8, 27047–27061. doi:10.18632/oncotarget.15968.

Davalos, V., Moutinho, C., Villanueva, A., Boque, R., Silva, P., Carneiro, F., et al. (2012). Dynamic epigenetic regulation of the microRNA-200 family mediates epithelial and mesenchymal transitions in human tumorigenesis. *Oncogene* 31, 2062–2074. doi:10.1038/onc.2011.383.

De Luca, L., Trino, S., Laurenzana, I., Tagliaferri, D., Falco, G., Grieco, V., et al. (2017). Knockdown of miR-128a induces Lin28a expression and reverts myeloid differentiation blockage in acute myeloid leukemia. *Cell Death Dis.* 8. doi:10.1038/cddis.2017.253.

De Marzo, A. M., Platz, E. A., Sutcliffe, S., Xu, J., Grönberg, H., Drake, C. G., et al. (2007). Inflammation in prostate carcinogenesis. *Nat. Rev. Cancer* 7, 256–269. doi:10.1038/nrc2090.

De Mattos-Arruda, L., Bottai, G., Nuciforo, P. G., Di Tommaso, L., Giovannetti, E., Peg, V., et al. (2015). MicroRNA-21 links epithelial-to-mesenchymal transition and inflammatory signals to confer resistance to neoadjuvant trastuzumab and

chemotherapy in HER2-positive breast cancer patients. *Oncotarget* 6, 37269–80. doi:10.18632/oncotarget.5495.

De, S. N. (1959). Enterotoxicity of bacteria-free culture-filtrate of vibrio cholerae. *Nature* 183, 1533–1534. doi:10.1038/1831533a0.

De Spiegelaere, W., Dern-Wieloch, J., Weigel, R., Schumacher, V., Schorle, H., Nettersheim, D., et al. (2015). Reference gene validation for RT-qPCR, a note on different available software packages. *PLoS One* 10. doi:10.1371/journal.pone.0122515.

Dear, J. W. (2018). New biomarkers for drug-induced liver injury. *Hepatology* 67, 2480–2481. doi:10.1002/hep.29865.

Del Vescovo, V., Cantaloni, C., Cucino, A., Girlando, S., Silvestri, M., Bragantini, E., et al. (2011). miR-205 Expression Levels in Nonsmall Cell Lung CancerDo Not Always Distinguish Adenocarcinomas From Squamous Cell Carcinomas. *Am. J. Surg. Pathol.* 35, 268–275. doi:10.1097/PAS.0b013e3182068171.

Delgado-Gonzalez, A., Robles-Remacho, A., Marin-Romero, A., Detassis, S., Lopez-Longarela, B., Lopez-Delgado, F. J., et al. (2019). PCR-free and chemistry-based technology for miR-21 rapid detection directly from tumour cells. *Talanta* 200, 51–56. doi:10.1016/j.talanta.2019.03.039.

Detassis, S., Grasso, M., Del Vescovo, V., and Denti, M. A. (2017). microRNAs Make the Call in Cancer Personalized Medicine. *Front. cell Dev. Biol.* 5, 86. doi:10.3389/fcell.2017.00086.

Detassis, S., Grasso, M., Tabraue-Chávez, M., Marín-Romero, A., López-Longarela, B., Ilyine, H., et al. (2019). New Platform for the Direct Profiling of microRNAs in Biofluids. *Anal. Chem.* 91, 5874–5880. doi:10.1021/acs.analchem.9b00213.

Di Meo, A., Brown, M. D., Finelli, A., Jewett, M. A. S., Diamandis, E. P., and Yousef,

G. M. (2020). Prognostic urinary miRNAs for the assessment of small renal masses. *Clin. Biochem.* 75, 15–22. doi:10.1016/j.clinbiochem.2019.10.002.

Dinu, N., Battiston, R., Boscardin, M., Collazuol, G., Corsi, F., Dalla Betta, G. F., et al. (2007). Development of the first prototypes of Silicon PhotoMultiplier (SiPM) at ITC-irst. *Nucl. Instruments Methods Phys. Res. Sect. A Accel. Spectrometers, Detect. Assoc. Equip.* 572, 422–426. doi:10.1016/j.nima.2006.10.305.

Diosdado, B., Van De Wiel, M. A., Terhaar Sive Droste, J. S., Mongera, S., Postma, C., Meijerink, W. J. H. J., et al. (2009). MiR-17-92 cluster is associated with 13q gain and c-myc expression during colorectal adenoma to adenocarcinoma progression. *Br. J. Cancer* 101, 707–714. doi:10.1038/sj.bjc.6605037.

Donatelli, S. S., Zhou, J. M., Gilvary, D. L., Eksioglu, E. A., Chen, X., Cress, W. D., et al. (2014). TGF-β-inducible microRNA-183 silences tumor-associated natural killer cells. *Proc. Natl. Acad. Sci. U. S. A.* 111, 4203–4208. doi:10.1073/pnas.1319269111.

Duttagupta, R., Jiang, R., Gollub, J., Getts, R. C., and Jones, K. W. (2011). Impact of Cellular miRNAs on Circulating miRNA Biomarker Signatures. *PLoS One* 6, e20769. doi:10.1371/journal.pone.0020769.

Epis, M. R., Giles, K. M., Barker, A., Kendrick, T. S., and Leedman, P. J. (2009). miR-331-3p Regulates ERBB-2 Expression and Androgen Receptor Signaling in Prostate Cancer. *J. Biol. Chem.* 284, 24696–24704. doi:10.1074/jbc.M109.030098.

Fabbri, M., Paone, A., Calore, F., Galli, R., Gaudio, E., Santhanam, R., et al. (2012). MicroRNAs bind to Toll-like receptors to induce prometastatic inflammatory response. *Proc. Natl. Acad. Sci. U. S. A.* 109, E2110. doi:10.1073/pnas.1209414109.

Fang, C., Chen, Y.-X., Wu, N.-Y., Yin, J.-Y., Li, X.-P., Huang, H.-S., et al. (2017). MiR-488 inhibits proliferation and cisplatin sensibility in non-small-cell lung cancer (NSCLC) cells by activating the eIF3a-mediated NER signaling pathway. *Sci. Rep.*

7, 40384. doi:10.1038/srep40384.

Fang, C., Li, X.-P., Gong, W.-J., Wu, N.-Y., Tang, J., Yin, J.-Y., et al. (2016). Age-related common miRNA polymorphism associated with severe toxicity in lung cancer patients treated with platinum-based chemotherapy. *Clin. Exp. Pharmacol. Physiol.* doi:10.1111/1440-1681.12704.

Fang, W., and Bartel, D. P. (2015). The Menu of Features that Define Primary MicroRNAs and Enable De Novo Design of MicroRNA Genes. *Mol. Cell* 60, 131–145. doi:10.1016/j.molcel.2015.08.015.

Fassan, M., Saraggi, D., Balsamo, L., Realdon, S., Scarpa, M., Castoro, C., et al. (2017). Early miR-223 Upregulation in Gastroesophageal Carcinogenesis. *Am. J. Clin. Pathol.* 147, 301–308. doi:10.1093/ajcp/aqx004.

Fazi, F., Rosa, A., Fatica, A., Gelmetti, V., De Marchis, M. L., Nervi, C., et al. (2005). A minicircuitry comprised of microRNA-223 and transcription factors NFI-A and C/EBPα regulates human granulopoiesis. *Cell* 123, 819–831. doi:10.1016/j.cell.2005.09.023.

Felli, N., Fontana, L., Pelosi, E., Botta, R., Bonci, D., Facchiano, F., et al. (2005). MicroRNAs 221 and 222 inhibit normal erythropoiesis and erythroleukemic cell growth via kit receptor down-modulation. *Proc. Natl. Acad. Sci. U. S. A.* 102, 18081–18086. doi:10.1073/pnas.0506216102.

Feng, Z., Zhang, C., Wu, R., and Hu, W. (2011). Tumor suppressor p53 meets microRNAs. *J. Mol. Cell Biol.* 3, 44–50. doi:10.1093/jmcb/mjq040.

Ferraldeschi, R., Nava Rodrigues, D., Riisnaes, R., Miranda, S., Figueiredo, I., Rescigno, P., et al. (2015). PTEN Protein Loss and Clinical Outcome from Castration-resistant Prostate Cancer Treated with Abiraterone Acetate. *Eur. Urol.* 67, 795–802. doi:10.1016/J.EURURO.2014.10.027.

Fimognari, C. (2015). Role of oxidative RNA damage in chronic-degenerative diseases. *Oxid. Med. Cell. Longev.* 2015. doi:10.1155/2015/358713.

Fitzner, D., Schnaars, M., Van Rossum, D., Krishnamoorthy, G., Dibaj, P., Bakhti, M., et al. (2011). Selective transfer of exosomes from oligodendrocytes to microglia by macropinocytosis. *J. Cell Sci.* 124, 447–458. doi:10.1242/jcs.074088.

Fredsøe, J., Rasmussen, A. K. I., Mouritzen, P., Bjerre, M. T., Østergren, P., Fode, M., et al. (2020). Profiling of Circulating microRNAs in Prostate Cancer Reveals Diagnostic Biomarker Potential. *Diagnostics* 10, 188. doi:10.3390/diagnostics10040188.

Fredsøe, J., Rasmussen, A. K. I., Mouritzen, P., Borre, M., Ørntoft, T., and Sørensen, K. D. (2019). A five-microRNA model (*pCaP*) for predicting prostate cancer aggressiveness using cell-free urine. *Int. J. Cancer* 145, 2558–2567. doi:10.1002/ijc.32296.

Fu, X., Zhang, W., Su, Y., Lu, L., Wang, D., and Wang, H. (2016). MicroRNA-103 suppresses tumor cell proliferation by targeting PDCD10 in prostate cancer. *Prostate* 76, 543–551. doi:10.1002/pros.23143.

Fujii, T., Shimada, K., Tatsumi, Y., Tanaka, N., Fujimoto, K., and Konishi, N. (2016). Syndecan-1 up-regulates microRNA-331-3p and mediates epithelial-to-mesenchymal transition in prostate cancer. *Mol. Carcinog.* 55, 1378–1386. doi:10.1002/mc.22381.

Fusco, A., Piccaluga, P. P., Fabbri, M., and Neviani, P. (2015). MINI REVIEWS IN MEDICINE Exosomic microRNAs in the tumor microenvironment. doi:10.3389/fmed.2015.00047.

Galardi, S., Mercatelli, N., Giorda, E., Massalini, S., Frajese, G. V., Ciafrè, S. A., et al. (2007). miR-221 and miR-222 expression affects the proliferation potential of

human prostate carcinoma cell lines by targeting p27Kip1. *J. Biol. Chem.* 282, 23716–23724. doi:10.1074/jbc.M701805200.

Gao, H., Chakraborty, G., Lee-Lim, A. P., Mavrakis, K. J., Wendel, H. G., and Giancotti, F. G. (2014). Forward genetic screens in mice uncover mediators and suppressors of metastatic reactivation. *Proc. Natl. Acad. Sci. U. S. A.* 111, 16532–16537. doi:10.1073/pnas.1403234111.

Gao, W., Lu, X., Liu, L., Xu, Ji., Feng, D., and Shu, Y. (2012). MiRNA-21. *Cancer Biol. Ther.* 13, 330–340. doi:10.4161/cbt.19073.

Gao, Z., and Peng, Y. (2011). A highly sensitive and specific biosensor for ligation- and PCR-free detection of MicroRNAs. *Biosens. Bioelectron.* 26, 3768–3773. doi:10.1016/j.bios.2011.02.029.

Garcìa-Donas, J., Beuselinck, B., Inglada-P?rez, L., Gra?a, O., Sch?ffski, P., Wozniak, A., et al. (2016). Deep sequencing reveals microRNAs predictive of antiangiogenic drug response. *JCI Insight* 1, e86051. doi:10.1172/jci.insight.86051.

Ghizoni, J. S., Nichele, R., de Oliveira, M. T., Pamato, S., and Pereira, J. R. (2019). The utilization of saliva as an early diagnostic tool for oral cancer: microRNA as a biomarker. *Clin. Transl. Oncol.* doi:10.1007/s12094-019-02210-y.

Giannopoulou, L., Zavridou, M., Kasimir-Bauer, S., and Lianidou, E. S. (2019). Liquid biopsy in ovarian cancer: the potential of circulating miRNAs and exosomes. *Transl. Res.* 205, 77–91. doi:10.1016/j.trsl.2018.10.003.

Go, H., Jang, J.-Y., Kim, P.-J., Kim, Y.-G., Nam, S. J., Paik, J. H., et al. (2015). MicroRNA-21 plays an oncogenic role by targeting FOXO1 and activating the PI3K/AKT pathway in diffuse large B-cell lymphoma. *Oncotarget* 6, 15035–15049. doi:10.18632/oncotarget.3729.

Godnic, I., Zorc, M., Jevsinek Skok, D., Calin, G. A., Horvat, S., Dovc, P., et al. (2013).

Genome-Wide and Species-Wide In Silico Screening for Intragenic MicroRNAs in Human, Mouse and Chicken. *PLoS One* 8, e65165. doi:10.1371/journal.pone.0065165.

Gonzales, P. A., Zhou, H., Pisitkun, T., Wang, N. S., Star, R. A., Knepper, M. A., et al. (2010). Isolation and purification of exosomes in urine. *Methods Mol. Biol.* 641, 89–99. doi:10.1007/978-1-60761-711-2_6.

Grundhoff, A., and Sullivan, C. S. (2011). Virus-encoded microRNAs. *Virology* 411, 325–343. doi:10.1016/j.virol.2011.01.002.

Gu, D., Jiang, M., Mei, Z., Dai, J., Dai, C., Fang, C., et al. (2017). microRNA-7 impairs autophagy-derived pools of glucose to suppress pancreatic cancer progression. *Cancer Lett.* 400, 69–78. doi:10.1016/j.canlet.2017.04.020.

Guay, C., and Regazzi, R. (2013). Circulating microRNAs as novel biomarkers for diabetes mellitus. *Nat. Rev. Endocrinol.* 9, 513–521. doi:10.1038/nrendo.2013.86.

Guescini, M., Canonico, B., Lucertini, F., Maggio, S., Annibalini, G., Barbieri, E., et al. (2015). Muscle releases alpha-sarcoglycan positive extracellular vesicles carrying miRNAs in the bloodstream. *PLoS One* 10. doi:10.1371/journal.pone.0125094.

Guo, C., Song, W. Q., Sun, P., Jin, L., and Dai, H. Y. (2015). LncRNA-GAS5 induces PTEN expression through inhibiting MIR-103 in endometrial cancer cells. *J. Biomed. Sci.* 22. doi:10.1186/s12929-015-0213-4.

Guo, J. F., Zhang, Y., Zheng, Q. X., Zhang, Y., Zhou, H. H., and Cui, L. M. (2018). Association between elevated plasma microRNA-223 content and severity of coronary heart disease. *Scand. J. Clin. Lab. Invest.* 78, 373–378. doi:10.1080/00365513.2018.1480059.

Guo, K., Liang, Z., Li, F., and Wang, H. (2017). Comparison of miRNA and gene expression profiles between metastatic and primary prostate cancer. *Oncol. Lett.* 14,

6085–6090. doi:10.3892/ol.2017.6969.

Guo, Q., Zheng, M., Xu, Y., Wang, N., and Zhao, W. (2019). MiR-384 induces apoptosis and autophagy of non-small cell lung cancer cells through the negative regulation of Collagen α-1(X) chain gene. *Biosci. Rep.* 39. doi:10.1042/BSR20181523.

Guzman, N., Agarwal, K., Asthagiri, D., Yu, L., Saji, M., Ringel, M. D., et al. (2015). Breast Cancer–Specific miR Signature Unique to Extracellular Vesicles Includes "microRNA-like" tRNA Fragments. *Mol. Cancer Res.* 13.

György, B., Szabó, T. G., Pásztói, M., Pál, Z., Misják, P., Aradi, B., et al. (2011). Membrane vesicles, current state-of-the-art: Emerging role of extracellular vesicles. *Cell. Mol. Life Sci.* 68, 2667–2688. doi:10.1007/s00018-011-0689-3.

Hafner, M., Landthaler, M., Burger, L., Khorshid, M., Hausser, J., Berninger, P., et al. (2010). Transcriptome-wide Identification of RNA-Binding Protein and MicroRNA Target Sites by PAR-CLIP. *Cell* 141, 129–141. doi:10.1016/j.cell.2010.03.009.

Haller, P. M., Stojkovic, S., Piackova, E., Andric, T., Wisgrill, L., Spittler, A., et al. (2019). The association of P2Y12 inhibitors with pro-coagulatory extracellular vesicles and microRNAs in stable coronary artery disease. *Platelets*. doi:10.1080/09537104.2019.1648780.

Hanahan, D., and Weinberg, R. (2011). Hallmarks of Cancer: The Next Generation. *Cell* 144, 646–674. doi:10.1016/j.cell.2011.02.013.

Hannafon, B. N., Trigoso, Y. D., Calloway, C. L., Zhao, Y. D., Lum, D. H., Welm, A. L., et al. (2016). Plasma exosome microRNAs are indicative of breast cancer. *Breast Cancer Res.* 18. doi:10.1186/s13058-016-0753-x.

Hao, J., Zhao, S., Zhang, Y., Zhao, Z., Ye, R., Wen, J., et al. (2014). Emerging role of MicroRNAs in cancer and cancer stem cells. *J. Cell. Biochem.* 115, 605–610. doi:10.1002/jcb.24702.

Haraldsdottir, S., Hampel, H., Wei, L., Wu, C., Frankel, W., Bekaii-Saab, T., et al. (2014). Prostate cancer incidence in males with Lynch syndrome. *Genet. Med.* 16, 553–7. doi:10.1038/gim.2013.193.

He, J., Xu, Q., Jing, Y., Agani, F., Qian, X., Carpenter, R., et al. (2012). Reactive oxygen species regulate ERBB2 and ERBB3 expression via miR-199a/125b and DNA methylation. *EMBO Rep.* 13, 1116–1122. doi:10.1038/embor.2012.162.

He, Q., Cai, L., Shuai, L., Li, D., Wang, C., Liu, Y., et al. (2013a). Ars2 is overexpressed in human cholangiocarcinomas and its depletion increases PTEN and PDCD4 by decreasing microRNA-21. *Mol. Carcinog.* 52, 286–296. doi:10.1002/mc.21859.

He, Z., Cen, D., Luo, X., Li, D., Li, P., Liang, L., et al. (2013b). Downregulation of miR-383 promotes glioma cell invasion by targeting insulin-like growth factor 1 receptor. *Med. Oncol.* 30, 557. doi:10.1007/s12032-013-0557-0.

Hejazi, M. S., Pournaghi-Azar, M. H., and Ahour, F. (2010). Electrochemical detection of short sequences of hepatitis C 3a virus using a peptide nucleic acid-assembled gold electrode. *Anal. Biochem.* 399, 118–124. doi:10.1016/j.ab.2009.11.019.

Heller, G., McCormack, R., Kheoh, T., Molina, A., Smith, M. R., Dreicer, R., et al. (2018). Circulating tumor cell number as a response measure of prolonged survival for metastatic castration-resistant prostate cancer: A comparison with prostate-specific antigen across five randomized phase III clinical trials. in *Journal of Clinical Oncology* (American Society of Clinical Oncology), 572–580. doi:10.1200/JCO.2017.75.2998.

Henne, W. M., Stenmark, H., and Emr, S. D. (2013). Molecular mechanisms of the membrane sculpting ESCRT pathway. *Cold Spring Harb. Perspect. Biol.* 5. doi:10.1101/cshperspect.a016766.

Hennessey, P. T., Sanford, T., Choudhary, A., Mydlarz, W. W., Brown, D., Adai, A. T.,

et al. (2012). Serum microrna biomarkers for detection of non-small cell lung cancer. *PLoS One* 7. doi:10.1371/journal.pone.0032307.

Hermeking, H. (2012). MicroRNAs in the p53 network: Micromanagement of tumour suppression. *Nat. Rev. Cancer* 12, 613–626. doi:10.1038/nrc3318.

Hezova, R., Kovarikova, A., Srovnal, J., Zemanova, M., Harustiak, T., Ehrmann, J., et al. (2015). Diagnostic and prognostic potential of miR-21, miR-29c, miR-148 and miR-203 in adenocarcinoma and squamous cell carcinoma of esophagus. *Diagn. Pathol.* 10, 42. doi:10.1186/s13000-015-0280-6.

Hjelmborg, J. B., Scheike, T., Holst, K., Skytthe, A., Penney, K. L., Graff, R. E., et al. (2014). The heritability of prostate cancer in the Nordic twin study of cancer. *Cancer Epidemiol. Biomarkers Prev.* 23, 2303–2310. doi:10.1158/1055-9965.EPI-13-0568.

Hsu, Y.-L., Hung, J.-Y., Chang, W.-A., Lin, Y.-S., Pan, Y.-C., Tsai, P.-H., et al. (2017). Hypoxic lung cancer-secreted exosomal miR-23a increased angiogenesis and vascular permeability by targeting prolyl hydroxylase and tight junction protein ZO-1. *Oncogene*. doi:10.1038/onc.2017.105.

Huang, H., Tian, H., Duan, Z., Cao, Y., Zhang, X.-S., and Sun, F. (2014). microRNA-383 impairs phosphorylation of H2AX by targeting PNUTS and inducing cell cycle arrest in testicular embryonal carcinoma cells. *Cell. Signal.* 26, 903–11. doi:10.1016/j.cellsig.2014.01.016.

Huang, X., and Lu, S. (2017). MicroR-545 mediates colorectal cancer cells proliferation through up-regulating epidermal growth factor receptor expression in HOTAIR long non-coding RNA dependent. *Mol. Cell. Biochem.* 431, 45–54. doi:10.1007/s11010-017-2974-4.

Huang, Z., Huang, D., Ni, S., Peng, Z., Sheng, W., and Du, X. (2010). Plasma microRNAs are promising novel biomarkers for early detection of colorectal cancer. *Int. J.*

cancer 127, 118–26. doi:10.1002/ijc.25007.

Hurteau, G. J., Carlson, J. A., Spivack, S. D., and Brock, G. J. (2007). Overexpression of the MicroRNA hsa-miR-200c leads to reduced expression of transcription factor 8 and increased expression of E-cadherin. *Cancer Res.* 67, 7972–7976. doi:10.1158/0008-5472.CAN-07-1058.

Hwang, J.-H., Voortman, J., Giovannetti, E., Steinberg, S. M., Leon, L. G., Kim, Y.-T., et al. (2010). Identification of MicroRNA-21 as a Biomarker for Chemoresistance and Clinical Outcome Following Adjuvant Therapy in Resectable Pancreatic Cancer. *PLoS One* 5, e10630. doi:10.1371/journal.pone.0010630.

Igarashi, H., Kurihara, H., Mitsuhashi, K., Ito, M., Okuda, H., Kanno, S., et al. (2015). Association of MicroRNA-31-5p with Clinical Efficacy of Anti-EGFR Therapy in Patients with Metastatic Colorectal Cancer. *Ann. Surg. Oncol.* 22, 2640–2648. doi:10.1245/s10434-014-4264-7.

Ingenito, F., Roscigno, G., Affinito, A., Nuzzo, S., Scognamiglio, I., Quintavalle, C., et al. (2019). The Role of Exo-miRNAs in Cancer: A Focus on Therapeutic and Diagnostic Applications. *Int. J. Mol. Sci.* 20, 4687. doi:10.3390/ijms20194687.

Iorio, M. V., Ferracin, M., Liu, C.-G., Veronese, A., Spizzo, R., Sabbioni, S., et al. (2005). MicroRNA Gene Expression Deregulation in Human Breast Cancer. *Cancer Res.* 65. Available at: http://cancerres.aacrjournals.org/content/65/16/7065.long [Accessed June 29, 2017].

Iorio, M. V., Visone, R., Di Leva, G., Donati, V., Petrocca, F., Casalini, P., et al. (2007). MicroRNA Signatures in Human Ovarian Cancer. *Cancer Res.* 67, 8699–8707. doi:10.1158/0008-5472.CAN-07-1936.

Ipsaro, J. J., and Joshua-Tor, L. (2015). From guide to target: molecular insights into eukaryotic RNA-interference machinery. *Nat. Struct. Mol. Biol.* 22, 20–8.

doi:10.1038/nsmb.2931.

Iwasaki, S., Kobayashi, M., Yoda, M., Sakaguchi, Y., Katsuma, S., Suzuki, T., et al. (2010). Hsc70/Hsp90 chaperone machinery mediates ATP-dependent RISC loading of small RNA duplexes. *Mol. Cell* 39, 292–299. doi:10.1016/j.molcel.2010.05.015.

Izadpanah, M., Seddigh, A., Ebrahimi Barough, S., Fazeli, S. A. S., and Ai, J. (2018). Potential of Extracellular Vesicles in Neurodegenerative Diseases: Diagnostic and Therapeutic Indications. *J. Mol. Neurosci.* 66, 172–179. doi:10.1007/s12031-018-1135-x.

Janas, T., Janas, M. M., Sapoń, K., and Janas, T. (2015). Mechanisms of RNA loading into exosomes. *FEBS Lett.* 589, 1391–1398. doi:10.1016/j.febslet.2015.04.036.

Jenkins, R. B., Qian, J., Lieber, M. M., and Bostwick, D. G. (1997). Detection of c-myc oncogene amplification and chromosomal anomalies in metastatic prostatic carcinoma by fluorescence in Situ hybridization. *Cancer Res.* 57, 524–531.

Jensen, W. A. (1965). The composition and ultrastructure of the nucellus in cotton. *J. Ultrasructure Res.* 13, 112–128. doi:10.1016/S0022-5320(65)80092-2.

Ji, F., Zhang, H., Wang, Y., Li, M., Xu, W., Kang, Y., et al. (2013). MicroRNA-133a, downregulated in osteosarcoma, suppresses proliferation and promotes apoptosis by targeting Bcl-xL and Mcl-1. *Bone* 56, 220–226. doi:10.1016/j.bone.2013.05.020.

Jin, X., Chen, Y., Chen, H., Fei, S., Chen, D., Cai, X., et al. (2017). Evaluation of tumor-derived exosomal miRNA as potential diagnostic biomarkers for early-stage non-small cell lung cancer using next-generation sequencing. *Clin. Cancer Res.* 23, 5311–5319. doi:10.1158/1078-0432.CCR-17-0577.

Jones-Rhoades, M. W., Bartel, D. P., and Bartel, B. (2006). MicroRNAS and their regulatory roles in plants. *Annu. Rev. Plant Biol.* 57, 19–53. doi:10.1146/annurev.arplant.57.032905.105218.

Kakimoto, Y., Tanaka, M., Kamiguchi, H., Ochiai, E., and Osawa, M. (2016). MicroRNA stability in FFPE tissue samples: Dependence on gc content. *PLoS One* 11. doi:10.1371/journal.pone.0163125.

Kanada, M., Bachmann, M. H., Hardy, J. W., Frimannson, D. O., Bronsart, L., Wang, A., et al. (2015). Differential fates of biomolecules delivered to target cells via extracellular vesicles. *Proc. Natl. Acad. Sci. U. S. A.* 112, E1433–E1442. doi:10.1073/pnas.1418401112.

Kanwal, R., Plaga, A. R., Liu, X., Shukla, G. C., and Gupta, S. (2017). MicroRNAs in prostate cancer: Functional role as biomarkers. *Cancer Lett.* 407, 9–20. doi:10.1016/j.canlet.2017.08.011.

Kapodistrias, N., Mavridis, K., Batistatou, A., Gogou, P., Karavasilis, V., Sainis, I., et al. (2016). Assessing the clinical value of microRNAs in formalin-fixed paraffin-embedded liposarcoma tissues: Overexpressed miR-155 is an indicator of poor prognosis. *Oncotarget* 8, 6896–6913. doi:10.18632/oncotarget.14320.

Karatas, O. F., Wang, J., Shao, L., Ozen, M., Zhang, Y., Creighton, C. J., et al. (2017). miR-33a is a tumor suppressor microRNA that is decreased in prostate cancer. *Oncotarget* 8, 60243–60256. doi:10.18632/oncotarget.19521.

Kerman, K., Vestergaard, M., Nagatani, N., Takamura, Y., and Tamiya, E. (2006). Electrochemical Genosensor Based on Peptide Nucleic Acid-Mediated PCR and Asymmetric PCR Techniques: Electrostatic Interactions with a Metal Cation. *Anal. Chem.* 78, 2182–2189. doi:10.1021/ac051526a.

Kertesz, M., Iovino, N., Unnerstall, U., Gaul, U., and Segal, E. (2007). The role of site accessibility in microRNA target recognition. *Nat. Genet.* 39, 1278–84. doi:10.1038/ng2135.

Khalighfard, S., Alizadeh, A. M., Irani, S., and Omranipour, R. (2018). Plasma miR-21,

miR-155, miR-10b, and Let-7a as the potential biomarkers for the monitoring of breast cancer patients. *Sci. Rep.* 8. doi:10.1038/s41598-018-36321-3.

Khan, Ahmed, Elareer, Junejo, Steinhoff, and Uddin (2019a). Role of miRNA-Regulated Cancer Stem Cells in the Pathogenesis of Human Malignancies. *Cells* 8, 840. doi:10.3390/cells8080840.

Khan, S., Ayub, H., Khan, T., and Wahid, F. (2019b). MicroRNA biogenesis, gene silencing mechanisms and role in breast, ovarian and prostate cancer. *Biochimie* 167, 12–24. doi:10.1016/j.biochi.2019.09.001.

Khorrami, S., Zavaran Hosseini, A., Mowla, S. J., Soleimani, M., Rakhshani, N., and Malekzadeh, R. (2017). MicroRNA-146a induces immune suppression and drug-resistant colorectal cancer cells. *Tumor Biol.* 39, 101042831769836. doi:10.1177/1010428317698365.

Kijima, T., Hazama, S., Tsunedomi, R., Tanaka, H., Takenouchi, H., Kanekiyo, S., et al. (2016). MicroRNA-6826 and -6875 in plasma are valuable non?invasive biomarkers that predict the efficacy of vaccine treatment against metastatic colorectal cancer. *Oncol. Rep.* 37, 23–30. doi:10.3892/or.2016.5267.

Kim, Y. K., Yeo, J., Kim, B., Ha, M., and Kim, V. N. (2012). Short Structured RNAs with Low GC Content Are Selectively Lost during Extraction from a Small Number of Cells. *Mol. Cell* 46, 893–895. doi:10.1016/j.molcel.2012.05.036.

Knudsen, B. S., and Vasioukhin, V. (2010). "Mechanisms of Prostate Cancer Initiation and Progression," in *Advances in Cancer Research* (Academic Press Inc.), 1–50. doi:10.1016/B978-0-12-380890-5.00001-6.

Kobayashi, H., and Tomari, Y. (2016). RISC assembly: Coordination between small RNAs and Argonaute proteins. *Biochim. Biophys. Acta - Gene Regul. Mech.* 1859, 71–81. doi:10.1016/j.bbagrm.2015.08.007.

Kopkova, A., Sana, J., Fadrus, P., and Slaby, O. (2018). Cerebrospinal fluid microRNAs as diagnostic biomarkers in brain tumors. *Clin. Chem. Lab. Med.* 56, 869–879. doi:10.1515/cclm-2017-0958.

Koppers-Lalic, D., Hackenberg, M., Bijnsdorp, I. V, van Eijndhoven, M. A. J., Sadek, P., Sie, D., et al. (2014). Nontemplated nucleotide additions distinguish the small RNA composition in cells from exosomes. *Cell Rep.* 8, 1649–58. doi:10.1016/j.celrep.2014.08.027.

Kosaka, N., Iguchi, H., Yoshioka, Y., Takeshita, F., Matsuki, Y., and Ochiya, T. (2010). Secretory mechanisms and intercellular transfer of microRNAs in living cells. *J. Biol. Chem.* 285, 17442–52. doi:10.1074/jbc.M110.107821.

Koschmann, J., Bhar, A., Stegmaier, P., Kel, A., Wingender, E., Koschmann, J., et al. (2015). "Upstream Analysis": An Integrated Promoter-Pathway Analysis Approach to Causal Interpretation of Microarray Data. *Microarrays* 4, 270–286. doi:10.3390/microarrays4020270.

Kowal, J., Tkach, M., and Théry, C. (2014). Biogenesis and secretion of exosomes. *Curr. Opin. Cell Biol.* 29, 116–125. doi:10.1016/j.ceb.2014.05.004.

Kuhn, H., Demidov, V. V., Coull, J. M., Fiandaca, M. J., Gildea, B. D., and Frank-Kamenetskii, M. D. (2002). Hybridization of DNA and PNA molecular beacons to single-stranded and double-stranded DNA targets. *J. Am. Chem. Soc.* 124, 1097–1103. doi:10.1021/ja0041324.

Kumarswamy, R., Mudduluru, G., Ceppi, P., Muppala, S., Kozlowski, M., Niklinski, J., et al. (2012). MicroRNA-30a inhibits epithelial-to-mesenchymal transition by targeting Snai1 and is downregulated in non-small cell lung cancer. *Int. J. Cancer* 130, 2044–2053. doi:10.1002/ijc.26218.

Le Floch, F., Ho, H. A., and Leclerc, M. (2006). Label-free electrochemical detection of

protein based on a ferrocene-bearing cationic polythiophene and aptamer. *Anal. Chem.* 78, 4727–4731. doi:10.1021/ac0521955.

Lebanony, D., Benjamin, H., Gilad, S., Ezagouri, M., Dov, A., Ashkenazi, K., et al. (2009). Diagnostic assay based on hsa-miR-205 expression distinguishes squamous from nonsquamous non-small-cell lung carcinoma. *J. Clin. Oncol.* 27, 2030–7. doi:10.1200/JCO.2008.19.4134.

Lee, R. C., Feinbaum, R. L., Ambros, V., Arasu, P., Ruvkun, G., Staden, R., et al. (1993). The C. elegans heterochronic gene lin-4 encodes small RNAs with antisense complementarity to lin-14. *Cell* 75, 843–54. doi:10.1016/0092-8674(93)90529-Y.

Lee, W. H., Morton, R. A., Epstein, J. I., Brooks, J. D., Campbell, P. A., Bova, G. S., et al. (1994). Cytidine methylation of regulatory sequences near the π-class glutathione S-transferase gene accompanies human prostatic carcinogenesis. *Proc. Natl. Acad. Sci. U. S. A.* 91, 11733–11737. doi:10.1073/pnas.91.24.11733.

Lee, Y., Ahn, C., Han, J., Choi, H., Kim, J., Yim, J., et al. (2003). The nuclear RNase III Drosha initiates microRNA processing. *Nature* 425, 415–419. doi:10.1038/nature01957.

Leinonen, K. A., Tolonen, T. T., Bracken, H., Stenman, U. H., Tammela, T. L. J., Saramäki, O. R., et al. (2010). Association of SPINK1 expression and TMPRSS2:ERG fusion with prognosis in endocrine-treated prostate cancer. *Clin. Cancer Res.* 16, 2845–2851. doi:10.1158/1078-0432.CCR-09-2505.

Lewis, H., Lance, R., Troyer, D., Beydoun, H., Hadley, M., Orians, J., et al. (2014). MiR-888 is an expressed prostatic secretionsderived microRNA that promotes prostate cell growth and migration. *Cell Cycle* 13, 227–239. doi:10.4161/cc.26984.

Li, B., Ge, L., Li, M., Wang, L., and Li, Z. (2016). miR-448 suppresses proliferation and invasion by regulating IGF1R in colorectal cancer cells. *Am. J. Transl. Res.* 8, 3013–

22. Available at: http://www.ncbi.nlm.nih.gov/pubmed/27508021 [Accessed June 29, 2017].

Li, H., Jiang, T., Li, M. Q., Zheng, X. L., and Zhao, G. J. (2018). Transcriptional regulation of macrophages polarization by microRNAs. *Front. Immunol.* 9. doi:10.3389/fimmu.2018.01175.

Li, J., Li, X., Ren, S., Chen, X., Zhang, Y., Zhou, F., et al. (2014a). miR-200c overexpression is associated with better efficacy of EGFR-TKIs in non-small cell lung cancer patients with EGFR wild-type. *Oncotarget* 5, 7902–7916. doi:10.18632/oncotarget.2302.

Li, K. K.-W., Pang, J. C.-S., Lau, K.-M., Zhou, L., Mao, Y., Wang, Y., et al. (2013). MiR-383 is Downregulated in Medulloblastoma and Targets Peroxiredoxin 3 (PRDX3). *Brain Pathol.* 23, 413–425. doi:10.1111/bpa.12014.

Li, L., and Luo, Z. (2017). Dysregulated miR-27a-3p promotes nasopharyngeal carcinoma cell proliferation and migration by targeting Mapk10. *Oncol. Rep.* 37, 2679–2687. doi:10.3892/or.2017.5544.

Li, Q.-Q., Chen, Z.-Q., Cao, X.-X., Xu, J.-D., Xu, J.-W., Chen, Y.-Y., et al. (2011). Involvement of NF-?B/miR-448 regulatory feedback loop in chemotherapy-induced epithelial?mesenchymal transition of breast cancer cells. *Cell Death Differ.* 18, 16–25. doi:10.1038/cdd.2010.103.

Li, Q., Lu, S., Li, X., Hou, G., Yan, L., Zhang, W., et al. (2017). Biological function and mechanism of miR-33a in prostate cancer survival and metastasis: via downregulating Engrailed-2. *Clin. Transl. Oncol.* 19, 562–570. doi:10.1007/s12094-016-1564-3.

Li, S. Z., Hu, Y. Y., Zhao, J., Zhao, Y. B., Sun, J. D., Yang, Y. F., et al. (2014b). MicroRNA-34a induces apoptosis in the human glioma cell line, A172, through

enhanced ROS production and NOX2 expression. *Biochem. Biophys. Res. Commun.* 444, 6–12. doi:10.1016/j.bbrc.2013.12.136.

Lian, J., Tian, H., Liu, L., Zhang, X.-S., Li, W.-Q., Deng, Y.-M., et al. (2010). Downregulation of microRNA-383 is associated with male infertility and promotes testicular embryonal carcinoma cell proliferation by targeting IRF1. *Cell Death Dis.* 1, e94. doi:10.1038/cddis.2010.70.

Lianidou, E., and Pantel, K. (2019). Liquid biopsies. *Genes Chromosom. Cancer* 58, 219–232. doi:10.1002/gcc.22695.

Lin, C. J., Martens, J. W. M., and Miller, W. L. (2001). NF-1C, Sp1, and Sp3 Are Essential for Transcription of the Human Gene for P450c17 (Steroid 17α-hydroxylase/17,20 lyase) in Human Adrenal NCI-H295A Cells. *Mol. Endocrinol.* 15, 1277–1293. doi:10.1210/mend.15.8.0679.

Lin, H.-M., Castillo, L., Mahon, K. L., Chiam, K., Lee, B. Y., Nguyen, Q., et al. (2014). Circulating microRNAs are associated with docetaxel chemotherapy outcome in castration-resistant prostate cancer. *Br. J. Cancer* 110, 2462–71. doi:10.1038/bjc.2014.181.

Lin, H.-M., Mahon, K. L., Spielman, C., Gurney, H., Mallesara, G., Stockler, M. R., et al. (2017). Phase 2 study of circulating microRNA biomarkers in castration-resistant prostate cancer. *Br. J. Cancer* 116, 1002–1011. doi:10.1038/bjc.2017.50.

Ling, M., Li, Y., Xu, Y., Pang, Y., Shen, L., Jiang, R., et al. (2012). Regulation of miRNA-21 by reactive oxygen species-activated ERK/NF-κB in arsenite-induced cell transformation. *Free Radic. Biol. Med.* 52, 1508–1518. doi:10.1016/j.freeradbiomed.2012.02.020.

Litwin, M. S., and Tan, H. J. (2017). The diagnosis and treatment of prostate cancer: A review. *JAMA - J. Am. Med. Assoc.* 317, 2532–2542. doi:10.1001/jama.2017.7248.

Liu, Y., Liu, R., Yang, F., Cheng, R., Chen, X., Cui, S., et al. (2017). miR-19a promotes colorectal cancer proliferation and migration by targeting TIA1. *Mol. Cancer* 16, 53. doi:10.1186/s12943-017-0625-8.

López-Longarela, B., Morrison, E. E., Tranter, J. D., Chahman-Vos, L., Léonard, J.-F., Gautier, J.-C., et al. (2020). Direct Detection of miR-122 in Hepatotoxicity Using Dynamic Chemical Labeling Overcomes Stability and isomiR Challenges. *Anal. Chem.*, acs.analchem.9b05449. doi:10.1021/acs.analchem.9b05449.

Lorente, D., Mateo, J., Perez-Lopez, R., de Bono, J. S., and Attard, G. (2015). Sequencing of agents in castration-resistant prostate cancer. *Lancet Oncol.* 16, e279–e292. doi:10.1016/S1470-2045(15)70033-1.

Lu, J., Getz, G., Miska, E. A., Alvarez-Saavedra, E., Lamb, J., Peck, D., et al. (2005). MicroRNA expression profiles classify human cancers. *Nature* 435, 834–838. doi:10.1038/nature03702.

Lu, L., McCurdy, S., Huang, S., Zhu, X., Peplowska, K., Tiirikainen, M., et al. (2016). Time Series miRNA-mRNA integrated analysis reveals critical miRNAs and targets in macrophage polarization. *Sci. Rep.* 6. doi:10.1038/srep37446.

Lu, M., Kong, X., Wang, H., Huang, G., Ye, C., and He, Z. (2017). A novel microRNAs expression signature for hepatocellular carcinoma diagnosis and prognosis. *Oncotarget* 8, 8775–8784. doi:10.18632/oncotarget.14452.

Lv, Y., Lei, Y., Hu, Y., Ding, W., Zhang, C., and Fang, C. (2015). miR-448 negatively regulates ovarian cancer cell growth and metastasis by targeting CXCL12. *Clin. Transl. Oncol.* 17, 903–9. doi:10.1007/s12094-015-1325-8.

Lyu, J., Zhao, L., Wang, F., Ji, J., Cao, Z., Xu, H., et al. (2019). Discovery and Validation of Serum MicroRNAs as Early Diagnostic Biomarkers for Prostate Cancer in Chinese Population. doi:10.1155/2019/9306803.

Machtinger, R., Laurent, L. C., and Baccarelli, A. A. (2016). Extracellular vesicles: Roles in gamete maturation, fertilization and embryo implantation. *Hum. Reprod. Update* 22, 182–193. doi:10.1093/humupd/dmv055.

Mack, M., Kleinschmidt, A., Brühl, H., Klier, C., Nelson, P. J., Cihak, J., et al. (2000). Transfer of the chemokine receptor CCR5 between cells by membrane- derived microparticles: A mechanism for cellular human immunodeficiency virus 1 infection. *Nat. Med.* 6, 769–775. doi:10.1038/77498.

MacRae, I. J., Zhou, K., Li, F., Repic, A., Brooks, A. N., Cande, W. Z., et al. (2006). Structural basis for double-stranded RNA processing by Dicer. *Science (80-.).* 311, 195–198. doi:10.1126/science.1121638.

Makarova, J. A., Shkurnikov, M. U., Wicklein, D., Lange, T., Samatov, T. R., Turchinovich, A. A., et al. (2016). Intracellular and extracellular microRNA: An update on localization and biological role. *Prog. Histochem. Cytochem.* doi:10.1016/j.proghi.2016.06.001.

Marín-Romero, A., Robles-Remacho, A., Tabraue-Chávez, M., López-Longarela, B., Sánchez-Martín, R. M., Guardia-Monteagudo, J. J., et al. (2018). A PCR-free technology to detect and quantify microRNAs directly from human plasma. *Analyst* 143, 5676–5682. doi:10.1039/c8an01397g.

Markou, A., Tsaroucha, E. G., Kaklamanis, L., Fotinou, M., Georgoulias, V., and Lianidou, E. S. (2008). Prognostic Value of Mature MicroRNA-21 and MicroRNA-205 Overexpression in Non-Small Cell Lung Cancer by Quantitative Real-Time RT-PCR. *Clin. Chem.* 54, 1696–1704. doi:10.1373/clinchem.2007.101741.

Masè, M., Grasso, M., Avogaro, L., D'Amato, E., Tessarolo, F., Graffigna, A., et al. (2017). Selection of reference genes is critical for miRNA expression analysis in human cardiac tissue. A focus on atrial fibrillation. *Sci. Rep.* 7, 41127.

doi:10.1038/srep41127.

Mathieu, M., Martin-Jaular, L., Lavieu, G., and Théry, C. (2019). Specificities of secretion and uptake of exosomes and other extracellular vesicles for cell-to-cell communication. *Nat. Cell Biol.* 21, 9–17. doi:10.1038/s41556-018-0250-9.

Max, K. E. A., Bertram, K., Akat, K. M., Bogardus, K. A., Li, J., Morozov, P., et al. (2018). Human plasma and serum extracellular small RNA reference profiles and their clinical utility. *Proc. Natl. Acad. Sci. U. S. A.* 115, E5334–E5343. doi:10.1073/pnas.1714397115.

Maxim, L. D., Niebo, R., and Utell, M. J. (2014). Screening tests: A review with examples. *Inhal. Toxicol.* 26, 811–828. doi:10.3109/08958378.2014.955932.

McMahon, H. T., and Boucrot, E. (2015). Membrane curvature at a glance. *J. Cell Sci.* 128, 1065–1070. doi:10.1242/jcs.114454.

Mello-Grand, M., Gregnanin, I., Sacchetto, L., Ostano, P., Zitella, A., Bottoni, G., et al. (2019). Circulating microRNAs combined with PSA for accurate and non-invasive prostate cancer detection. *Carcinogenesis* 40, 246–253. doi:10.1093/carcin/bgy167.

Menchise, V., De Simone, G., Tedeschi, T., Corradini, R., Sforza, S., Marchelli, R., et al. (2003). Insights into peptide nucleic acid (PNA) structural features: The crystal structure of a D-lysine-based chiral PNA-DNA duplex. *Proc. Natl. Acad. Sci. U. S. A.* 100, 12021–12026. doi:10.1073/pnas.2034746100.

Meng, F., Henson, R., Wehbe-Janek, H., Ghoshal, K., Jacob, S. T., and Patel, T. (2007). MicroRNA-21 regulates expression of the PTEN tumor suppressor gene in human hepatocellular cancer. *Gastroenterology* 133, 647–58. doi:10.1053/j.gastro.2007.05.022.

Meng, W., McElroy, J. P., Volinia, S., Palatini, J., Warner, S., Ayers, L. W., et al. (2013). Comparison of MicroRNA Deep Sequencing of Matched Formalin-Fixed Paraffin-

Embedded and Fresh Frozen Cancer Tissues. *PLoS One* 8. doi:10.1371/journal.pone.0064393.

Mi, Y., Zhang, D., Jiang, W., Weng, J., Zhou, C., Huang, K., et al. (2017). miR-181a-5p promotes the progression of gastric cancer via RASSF6-mediated MAPK signalling activation. *Cancer Lett.* 389, 11–22. doi:10.1016/j.canlet.2016.12.033.

Mihelich, B. L., Dambal, S., Lin, S., and Nonn, L. (2016). miR-182, of the miR-183 cluster family, is packaged in exosomes and is detected in human exosomes from serum, breast cells and prostate cells. *Oncol. Lett.* 12, 1197–1203. doi:10.3892/ol.2016.4710.

Mitchell, P. S., Parkin, R. K., Kroh, E. M., Fritz, B. R., Wyman, S. K., Pogosova-Agadjanyan, E. L., et al. (2008). Circulating microRNAs as stable blood-based markers for cancer detection. *Proc. Natl. Acad. Sci. U. S. A.* 105, 10513–8. doi:10.1073/pnas.0804549105.

Miyamoto, D. T., Lee, R. J., Kalinich, M., LiCausi, J. A., Zheng, Y., Chen, T., et al. (2018). An RNA-Based Digital Circulating Tumor Cell Signature Is Predictive of Drug Response and Early Dissemination in Prostate Cancer. *Cancer Discov.* 8, 288–303. doi:10.1158/2159-8290.CD-16-1406.

Miyoshi, T., Takeuchi, A., Siomi, H., and Siomi, M. C. (2010). A direct role for Hsp90 in pre-RISC formation in Drosophila. *Nat. Struct. Mol. Biol.* 17, 1024–1026. doi:10.1038/nsmb.1875.

Mlcochova, J., Faltejskova-Vychytilova, P., Ferracin, M., Zagatti, B., Radova, L., Svoboda, M., et al. (2015). MicroRNA expression profiling identifies miR-31-5p/3p as associated with time to progression in wild-type RAS metastatic colorectal cancer treated with cetuximab. *Oncotarget* 6, 38695–704. doi:10.18632/oncotarget.5735.

Mohammadi, A., Mansoori, B., and Baradaran, B. (2016). The role of microRNAs in

colorectal cancer. *Biomed. Pharmacother.* 84, 705–713. doi:10.1016/j.biopha.2016.09.099.

Molasy, M., Walczak, A., Szaflik, J., Szaflik, J. P., and Majsterek, I. (2016). MicroRNAs in glaucoma and neurodegenerative diseases. *J. Hum. Genet.* doi:10.1038/jhg.2016.91.

Momen-Heravi, F., Bala, S., Bukong, T., and Szabo, G. (2014). Exosome-mediated delivery of functionally active miRNA-155 inhibitor to macrophages. *Nanomedicine Nanotechnology, Biol. Med.* 10, 1517–1527. doi:10.1016/j.nano.2014.03.014.

Monleau, M., Bonnel, S., Gostan, T., Blanchard, D., Courgnaud, V., Lecellier, C.-H., et al. (2014). Comparison of different extraction techniques to profile microRNAs from human sera and peripheral blood mononuclear cells. *BMC Genomics* 15, 395. doi:10.1186/1471-2164-15-395.

Mosakhani, N., Lahti, L., Borze, I., Karjalainen-Lindsberg, M.-L., Sundström, J., Ristamäki, R., et al. (2012). MicroRNA profiling predicts survival in anti-EGFR treated chemorefractory metastatic colorectal cancer patients with wild-type KRAS and BRAF. *Cancer Genet.* 205, 545–51. doi:10.1016/j.cancergen.2012.08.003.

Mott, J. L., Kobayashi, S., Bronk, S. F., and Gores, G. J. (2007). mir-29 regulates Mcl-1 protein expression and apoptosis. *Oncogene* 26, 6133–6140. doi:10.1038/sj.onc.1210436.

Mousavi, S., Moallem, R., Hassanian, S. M., Sadeghzade, M., Mardani, R., Ferns, G. A., et al. (2019). Tumor-derived exosomes: Potential biomarkers and therapeutic target in the treatment of colorectal cancer. *J. Cell. Physiol.* 234, 12422–12432. doi:10.1002/jcp.28080.

Mulcahy, L. A., Pink, R. C., and Carter, D. R. F. (2014). Routes and mechanisms of extracellular vesicle uptake. *J. Extracell. Vesicles* 3. doi:10.3402/jev.v3.24641.

Nakka, M., Allen-Rhoades, W., Li, Y., Kelly, A. J., Shen, J., Taylor, A. M., et al. (2017a). Biomarker significance of plasma and tumor miR-21, miR-221, and miR-106a in osteosarcoma. *Oncotarget*. doi:10.18632/oncotarget.18236.

Nakka, M., Allen-Rhoades, W., Li, Y., Kelly, A. J., Shen, J., Taylor, A. M., et al. (2017b). Biomarker significance of plasma and tumor miR-21, miR-221, and miR-106a in osteosarcoma. *Oncotarget* 8, 96738–96752. doi:10.18632/oncotarget.18236.

Namkung, J., Kwon, W., Choi, Y., Yi, S. G., Han, S., Kang, M. J., et al. (2016). Molecular subtypes of pancreatic cancer based on miRNA expression profiles have independent prognostic value. *J. Gastroenterol. Hepatol.* 31, 1160–1167. doi:10.1111/jgh.13253.

National Costs for Cancer Sites | Cancer Prevalence and Cost of Care Projections Available at: https://costprojections.cancer.gov/expenditures.html [Accessed February 1, 2020].

Neal, C. S., Michael, M. Z., Pimlott, L. K., Yong, T. Y., Li, J. Y. Z., and Gleadle, J. M. (2011). Circulating microRNA expression is reduced in chronic kidney disease. *Nephrol. Dial. Transplant.* 26, 3794–3802. doi:10.1093/ndt/gfr485.

Neault, M., Mallette, F. A., and Richard, S. (2016). miR-137 Modulates a Tumor Suppressor Network-Inducing Senescence in Pancreatic Cancer Cells. *Cell Rep.* 14, 1966–1978. doi:10.1016/j.celrep.2016.01.068.

Ng, E. K. O., Chong, W. W. S., Jin, H., Lam, E. K. Y., Shin, V. Y., Yu, J., et al. (2009). Differential expression of microRNAs in plasma of patients with colorectal cancer: a potential marker for colorectal cancer screening. *Gut* 58, 1375–81. doi:10.1136/gut.2008.167817.

Nguyen, T. A., Jo, M. H., Choi, Y. G., Park, J., Kwon, S. C., Hohng, S., et al. (2015). Functional anatomy of the human microprocessor. *Cell* 161, 1374–1387.

doi:10.1016/j.cell.2015.05.010.

Nishida, N., Arizumi, T., Hagiwara, S., Ida, H., Sakurai, T., and Kudo, M. (2017). MicroRNAs for the Prediction of Early Response to Sorafenib Treatment in Human Hepatocellular Carcinoma. *Liver Cancer* 6, 113–125. doi:10.1159/000449475.

Notarangelo, M., Zucal, C., Modelska, A., Pesce, I., Scarduelli, G., Potrich, C., et al. (2019). Ultrasensitive detection of cancer biomarkers by nickel-based isolation of polydisperse extracellular vesicles from blood. *EBioMedicine* 43, 114–126. doi:10.1016/j.ebiom.2019.04.039.

O'Donnell, K. A., Wentzel, E. A., Zeller, K. I., Dang, C. V., and Mendell, J. T. (2005). c-Myc-regulated microRNAs modulate E2F1 expression. *Nature* 435, 839–843. doi:10.1038/nature03677.

Ochoa, A. E., Choi, W., Su, X., Siefker-Radtke, A., Czerniak, B., Dinney, C., et al. (2016). Specific micro-RNA expression patterns distinguish the basal and luminal subtypes of muscle-invasive bladder cancer. *Oncotarget*. doi:10.18632/oncotarget.13284.

Ohno, S. I., Takanashi, M., Sudo, K., Ueda, S., Ishikawa, A., Matsuyama, N., et al. (2013). Systemically injected exosomes targeted to EGFR deliver antitumor microrna to breast cancer cells. *Mol. Ther.* 21, 185–191. doi:10.1038/mt.2012.180.

Oksuz, Z., Serin, M. S., Kaplan, E., Dogen, A., Tezcan, S., Aslan, G., et al. (2015). Serum microRNAs; miR-30c-5p, miR-223-3p, miR-302c-3p and miR-17-5p could be used as novel non-invasive biomarkers for HCV-positive cirrhosis and hepatocellular carcinoma. *Mol. Biol. Rep.* 42, 713–720. doi:10.1007/s11033-014-3819-9.

Palanisamy, V., Sharma, S., Deshpande, A., Zhou, H., Gimzewski, J., and Wong, D. T. (2010). Nanostructural and Transcriptomic Analyses of Human Saliva Derived Exosomes. *PLoS One* 5, e8577. doi:10.1371/journal.pone.0008577.

Parafioriti, A., Bason, C., Armiraglio, E., Calciano, L., Daolio, P. A., Berardocco, M., et al. (2016). Ewing's Sarcoma: An Analysis of miRNA Expression Profiles and Target Genes in Paraffin-Embedded Primary Tumor Tissue. *Int. J. Mol. Sci.* 17. doi:10.3390/ijms17050656.

Parolini, I., Federici, C., Raggi, C., Lugini, L., Palleschi, S., De Milito, A., et al. (2009). Microenvironmental pH is a key factor for exosome traffic in tumor cells. *J. Biol. Chem.* 284, 34211–34222. doi:10.1074/jbc.M109.041152.

Patnaik, S., Mallick, R., Kannisto, E., Sharma, R., Bshara, W., Yendamuri, S., et al. (2015). MiR-205 and MiR-375 microRNA assays to distinguish squamous cell carcinoma from adenocarcinoma in lung cancer biopsies. *J. Thorac. Oncol.* 10, 446–53. doi:10.1097/JTO.0000000000000423.

Paydas, S., Acikalin, A., Ergin, M., Celik, H., Yavuz, B., and Tanriverdi, K. (2016). Micro-RNA (miRNA) profile in Hodgkin lymphoma: association between clinical and pathological variables. *Med. Oncol.* 33, 34. doi:10.1007/s12032-016-0749-5.

PDQ Adult Treatment Editorial Board (2002a). *Financial Toxicity (Financial Distress) and Cancer Treatment (PDQ®): Patient Version*. Available at: http://www.ncbi.nlm.nih.gov/pubmed/28682576 [Accessed February 1, 2020].

PDQ Adult Treatment Editorial Board (2002b). *Financial Toxicity and Cancer Treatment (PDQ®): Health Professional Version*. Available at: http://www.ncbi.nlm.nih.gov/pubmed/27583328 [Accessed February 1, 2020].

PDQ Cancer Genetics Editorial Board (2002). *Genetics of Prostate Cancer (PDQ®): Health Professional Version*. Available at: http://www.ncbi.nlm.nih.gov/pubmed/26389227 [Accessed February 3, 2020].

Peng, J., Liu, H.-Z., Zhong, J., Deng, Z.-F., Tie, C.-R., Rao, Q., et al. (2016). MicroRNA-187 is an independent prognostic factor in lung cancer and promotes

lung cancer cell invasion via targeting of PTRF. *Oncol. Rep.* 36, 2609–2618. doi:10.3892/or.2016.5083.

Pezaro, C., Woo, H. H., and Davis, I. D. (2014). Prostate cancer: measuring PSA. *Intern. Med. J.* 44, 433–440. doi:10.1111/imj.12407.

Pigati, L., Yaddanapudi, S. C. S., Iyengar, R., Kim, D. J., Hearn, S. A., Danforth, D., et al. (2010). Selective release of MicroRNA species from normal and malignant mammary epithelial cells. *PLoS One* 5. doi:10.1371/journal.pone.0013515.

Piva, R., Spandidos, D. A., and Gambari, R. (2013). From microRNA functions to microRNA therapeutics: Novel targets and novel drugs in breast cancer research and treatment (Review). *Int. J. Oncol.* 43, 985–994. doi:10.3892/ijo.2013.2059.

Preis, M., Gardner, T. B., Gordon, S. R., Pipas, J. M., Mackenzie, T. A., Klein, E. E., et al. (2011). MicroRNA-10b Expression Correlates with Response to Neoadjuvant Therapy and Survival in Pancreatic Ductal Adenocarcinoma. *Clin. Cancer Res.* 17. Available at: http://clincancerres.aacrjournals.org/content/17/17/5812.short [Accessed June 29, 2017].

Pritchard, C. C., Kroh, E., Wood, B., Arroyo, J. D., Dougherty, K. J., Miyaji, M. M., et al. (2012). Blood cell origin of circulating microRNAs: a cautionary note for cancer biomarker studies. *Cancer Prev. Res. (Phila).* 5, 492–7. doi:10.1158/1940-6207.CAPR-11-0370.

Pulliam, L., Sun, B., Mustapic, M., Chawla, S., and Kapogiannis, D. (2019). Plasma neuronal exosomes serve as biomarkers of cognitive impairment in HIV infection and Alzheimer's disease. *J. Neurovirol.* 25, 702–709. doi:10.1007/s13365-018-0695-4.

Qu, W., Ding, S. mei, Cao, G., Wang, S. jiao, Zheng, X. hong, and Li, G. hui (2016). miR-132 mediates a metabolic shift in prostate cancer cells by targeting Glut1. *FEBS*

Open Bio 6, 735–741. doi:10.1002/2211-5463.12086.

Qureshi, R., and Sacan, A. (2013). A novel method for the normalization of microRNA RT-PCR data. in *BMC Medical Genomics* doi:10.1186/1755-8794-6-S1-S14.

Ramalho-Carvalho, J., Gra?a, I., Gomez, A., Oliveira, J., Henrique, R., Esteller, M., et al. (2017). Downregulation of miR-130b~301b cluster is mediated by aberrant promoter methylation and impairs cellular senescence in prostate cancer. *J. Hematol. Oncol.* 10, 43. doi:10.1186/s13045-017-0415-1.

Rao, Y., Lee, Y., Jarjoura, D., Ruppert, A. S., Liu, C. G., Hsu, J. C., et al. (2008). A comparison of normalization techniques for microRNA microarray data. *Stat. Appl. Genet. Mol. Biol.* 7. doi:10.2202/1544-6115.1287.

Raoof, J. B., Ojani, R., Golabi, S. M., Hamidi-Asl, E., and Hejazi, M. S. (2011). Preparation of an electrochemical PNA biosensor for detection of target DNA sequence and single nucleotide mutation on p53 tumor suppressor gene corresponding oligonucleotide. *Sensors Actuators, B Chem.* 157, 195–201. doi:10.1016/j.snb.2011.03.049.

Rapa, I., Votta, A., Felice, B., Righi, L., Giorcelli, J., Scarpa, A., et al. (2015). Identification of MicroRNAs Differentially Expressed in Lung Carcinoid Subtypes and Progression. *Neuroendocrinology* 101, 246–55. doi:10.1159/000381454.

Rapado-González, Ó., Majem, B., Muinelo-Romay, L., álvarez-Castro, A., Santamaría, A., Gil-Moreno, A., et al. (2018). Human salivary microRNAs in Cancer. *J. Cancer* 9, 638–649. doi:10.7150/jca.21180.

Raponi, M., Dossey, L., Jatkoe, T., Wu, X., Chen, G., Fan, H., et al. (2009). MicroRNA Classifiers for Predicting Prognosis of Squamous Cell Lung Cancer. *Cancer Res.* 69. Available at: http://cancerres.aacrjournals.org/content/69/14/5776 [Accessed June 29, 2017].

Raposo, G., Nijman, H. W., Stoorvogel, W., Leijendekker, R., Harding, C. V., Melief, C. J. M., et al. (1996). B lymphocytes secrete antigen-presenting vesicles. *J. Exp. Med.* 183, 1161–1172. doi:10.1084/jem.183.3.1161.

Ratilainen, T., Holmén, A., Tuite, E., Nielsen, P. E., and Nordén, B. (2000). Thermodynamics of Sequence-Specific Binding of PNA to DNA †. *Biochemistry* 39, 7781–7791. doi:10.1021/bi000039g.

Reddy, P. H., Tonk, S., Kumar, S., Vijayan, M., Kandimalla, R., Kuruva, C. S., et al. (2016). A critical evaluation of neuroprotective and neurodegenerative MicroRNAs in Alzheimer's disease. *Biochem. Biophys. Res. Commun.* doi:10.1016/j.bbrc.2016.08.067.

Rissin, D. M., López-Longarela, B., Pernagallo, S., Ilyine, H., Vliegenthart, A. D. B., Dear, J. W., et al. (2017). Polymerase-free measurement of microRNA-122 with single base specificity using single molecule arrays: Detection of drug-induced liver injury. *PLoS One* 12, e0179669. doi:10.1371/journal.pone.0179669.

Rivoli, L., Vliegenthart, A. D. B., de Potter, C. M. J., van Bragt, J. J. M. H., Tzoumas, N., Gallacher, P., et al. (2017). The effect of renal dysfunction and haemodialysis on circulating liver specific miR-122. *Br. J. Clin. Pharmacol.* 83, 584–592. doi:10.1111/bcp.13136.

Rosenfeld, N., Aharonov, R., Meiri, E., Rosenwald, S., Spector, Y., Zepeniuk, M., et al. (2008). MicroRNAs accurately identify cancer tissue origin. *Nat. Biotechnol.* 26, 462–469. doi:10.1038/nbt1392.

Rusca, N., and Monticelli, S. (2011). MiR-146a in Immunity and Disease. *Mol. Biol. Int.* 2011, 437301. doi:10.4061/2011/437301.

Sacconi, A., Biagioni, F., Canu, V., Mori, F., Di Benedetto, A., Lorenzon, L., et al. (2012). MiR-204 targets Bcl-2 expression and enhances responsiveness of gastric cancer.

Cell Death Dis. 3. doi:10.1038/cddis.2012.160.

SAGER, R., and PALADE, G. E. (1957). Structure and development of the chloroplast in Chlamydomonas. I. The normal green cell. *J. Biophys. Biochem. Cytol.* 3, 463–488. doi:10.1083/jcb.3.3.463.

Sarma, A. V., Dunn, R. L., Lange, L. A., Ray, A., Wang, Y., Lange, E. M., et al. (2008). Genetic polymorphisms in CYP17, CYP3A4, CYP19A1, SRD5A2, IGF-1, and IGFBP-3 and prostate cancer risk in African-American men: The flint men's health study. *Prostate* 68, 296–305. doi:10.1002/pros.20696.

Scher, H. I., Halabi, S., Tannock, I., Morris, M., Sternberg, C. N., Carducci, M. A., et al. (2008). Design and end points of clinical trials for patients with progressive prostate cancer and castrate levels of testosterone: Recommendations of the Prostate Cancer Clinical Trials Working Group. *J. Clin. Oncol.* 26, 1148–1159. doi:10.1200/JCO.2007.12.4487.

Schetter, A. J., Leung, S. Y., Sohn, J. J., Zanetti, K. A., Bowman, E. D., Yanaihara, N., et al. (2008). MicroRNA Expression Profiles Associated With Prognosis and Therapeutic Outcome in Colon Adenocarcinoma. *JAMA* 299, 425–36. doi:10.1001/jama.299.4.425.

Schetter, A. J., Nguyen, G. H., Bowman, E. D., Mathé, E. A., Yuen, S. T., Hawkes, J. E., et al. (2009). Association of Inflammation-Related and microRNA Gene Expression with Cancer-Specific Mortality of Colon Adenocarcinoma. *Clin. Cancer Res.* 15. Available at: http://clincancerres.aacrjournals.org/content/15/18/5878 [Accessed June 29, 2017].

Segura, M. F., Hanniford, D., Menendez, S., Reavie, L., Zou, X., Alvarez-Diaz, S., et al. (2009). Aberrant miR-182 expression promotes melanoma metastasis by repressing FOXO3 and microphthalmia-associated transcription factor. *Proc. Natl. Acad. Sci.*

U. S. A. 106, 1814–1819. doi:10.1073/pnas.0808263106.

Selth, L. A., Roberts, M. J., Chow, C. W. K., Marshall, V. R., Doi, S. A. R., Vincent, A. D., et al. (2014). Human seminal fluid as a source of prostate cancer-specific microRNA biomarkers. *Endocr. Relat. Cancer* 21. doi:10.1530/ERC-14-0234.

Seo, M. K., and Cairns, J. (2018). Do cancer biomarkers make targeted therapies cost-effective? A systematic review in metastatic colorectal cancer. *PLoS One* 13, e0204496. doi:10.1371/journal.pone.0204496.

Shan, C., Fei, F., Li, F., Zhuang, B., Zheng, Y., Wan, Y., et al. (2017). miR-448 is a novel prognostic factor of lung squamous cell carcinoma and regulates cells growth and metastasis by targeting DCLK1. *Biomed. Pharmacother.* 89, 1227–1234. doi:10.1016/j.biopha.2017.02.017.

Shang, Y., Zang, A., Li, J., Jia, Y., Li, X., Zhang, L., et al. (2016). MicroRNA-383 is a tumor suppressor and potential prognostic biomarker in human non-small cell lung caner. *Biomed. Pharmacother.* 83, 1175–1181. doi:10.1016/j.biopha.2016.08.006.

Sharma, N., and Baruah, M. M. (2019). The microRNA signatures: aberrantly expressed miRNAs in prostate cancer. *Clin. Transl. Oncol.* 21, 126–144. doi:10.1007/s12094-018-1910-8.

Shen, J., Liu, Z., Todd, N. W., Zhang, H., Liao, J., Yu, L., et al. (2011). Diagnosis of lung cancer in individuals with solitary pulmonary nodules by plasma microRNA biomarkers. *BMC Cancer* 11, 374. doi:10.1186/1471-2407-11-374.

Shen, M. M., and Abate-Shen, C. (2007). Pten inactivation and the emergence of androgen-independent prostate cancer. *Cancer Res.* 67, 6535–6538. doi:10.1158/0008-5472.CAN-07-1271.

Shende, V. R., Goldrick, M. M., Ramani, S., and Earnest, D. J. (2011). Expression and rhythmic modulation of circulating micrornas targeting the clock gene Bmal1 in

mice. *PLoS One* 6. doi:10.1371/journal.pone.0022586.

Shi, L., Cheng, Z., Zhang, J., Li, R., Zhao, P., Fu, Z., et al. (2008). hsa-mir-181a and hsa-mir-181b function as tumor suppressors in human glioma cells. *Brain Res.* 1236, 185–193. doi:10.1016/j.brainres.2008.07.085.

Shi, R., Wang, P. Y., Li, X. Y., Chen, J. X., Li, Y., Zhang, X. Z., et al. (2015). Exosomal levels of miRNA-21 from cerebrospinal fluids associated with poor prognosis and tumor recurrence of glioma patients. *Oncotarget* 6, 26971–26981. doi:10.18632/oncotarget.4699.

Si, M.-L., Zhu, S., Wu, H., Lu, Z., Wu, F., and Mo, Y.-Y. (2007). miR-21-mediated tumor growth. *Oncogene* 26, 2799–2803. doi:10.1038/sj.onc.1210083.

Sindeeva, Verkhovskii, Sarimollaoglu, Afanaseva, Fedonnikov, Osintsev, et al. (2019). New Frontiers in Diagnosis and Therapy of Circulating Tumor Markers in Cerebrospinal Fluid In Vitro and In Vivo. *Cells* 8, 1195. doi:10.3390/cells8101195.

Singh, P. K., Preus, L., Hu, Q., Yan, L., Long, M. D., Morrison, C. D., et al. (2014). Serum microRNA expression patterns that predict early treatment failure in prostate cancer patients. *Oncotarget* 5, 824–40. doi:10.18632/oncotarget.1776.

Singh, R., and Saini, N. (2012). Downregulation of BCL2 by miRNAs augments druginduced apoptosis - A combined computational and experimental approach. *J. Cell Sci.* 125, 1568–1578. doi:10.1242/jcs.095976.

Siu-Chi Lam, C., Ng, L., Ka-Man Chow, A., Ming-Hun Wan, T., Yau, S., Shiu-Man Cheng, N., et al. (2017). Identification of microRNA 885-5p as a novel regulator of tumor metastasis by targeting CPEB2 in colorectal cancer. *Oncotarget* 8, 26858–26870. doi:10.18632/oncotarget.15844.

Skog, J., Würdinger, T., van Rijn, S., Meijer, D. H., Gainche, L., Curry, W. T., et al. (2008). Glioblastoma microvesicles transport RNA and proteins that promote

tumour growth and provide diagnostic biomarkers. *Nat. Cell Biol.* 10, 1470–1476. doi:10.1038/ncb1800.

Song, C.-J., Chen, H., Chen, L.-Z., Ru, G.-M., Guo, J.-J., and Ding, Q.-N. (2018). The potential of microRNAs as human prostate cancer biomarkers: A meta-analysis of related studies. *J. Cell. Biochem.* 119, 2763–2786. doi:10.1002/jcb.26445.

Song, Z., Wu, Y., Yang, J., Yang, D., and Fang, X. (2017). Progress in the treatment of advanced gastric cancer. *Tumor Biol.* 39. doi:10.1177/1010428317714626.

Songia, P., Chiesa, M., Valerio, V., Moschetta, D., Myasoedova, V. A., D'Alessandra, Y., et al. (2018). Direct screening of plasma circulating microRNAs. *RNA Biol.* 15, 1268–1272. doi:10.1080/15476286.2018.1526538.

Soravia, C., van der Klift, H., Bründler, M.-A., Blouin, J.-L., Wijnen, J., Hutter, P., et al. (2003). Prostate cancer is part of the hereditary non-polyposis colorectal cancer (HNPCC) tumor spectrum. *Am. J. Med. Genet. A* 121A, 159–62. doi:10.1002/ajmg.a.20106.

SOTELO, J. R., and PORTER, K. R. (1959). An electron microscope study of the rat ovum. *J. Biophys. Biochem. Cytol.* 5, 327–342. doi:10.1083/jcb.5.2.327.

Sourvinou, I. S., Markou, A., and Lianidou, E. S. (2013). Quantification of circulating miRNAs in plasma: Effect of preanalytical and analytical parameters on their isolation and stability. *J. Mol. Diagnostics* 15, 827–834. doi:10.1016/j.jmoldx.2013.07.005.

Squadrito, M. L., Baer, C., Burdet, F., Maderna, C., Gilfillan, G. D., Lyle, R., et al. (2014). Endogenous RNAs modulate microRNA sorting to exosomes and transfer to acceptor cells. *Cell Rep.* 8, 1432–46. doi:10.1016/j.celrep.2014.07.035.

Ståhlberg, A., Kubista, M., and Pfaffl, M. (2004). Comparison of Reverse Transcriptases in Gene Expression Analysis. *Clin. Chem.* 50, 1678–1680.

doi:10.1373/clinchem.2004.035469.

Strimbu, K., and Tavel, J. A. (2010). What are biomarkers? *Curr. Opin. HIV AIDS* 5, 463–6. doi:10.1097/COH.0b013e32833ed177.

Stuffers, S., Sem Wegner, C., Stenmark, H., and Brech, A. (2009). Multivesicular Endosome Biogenesis in the Absence of ESCRTs. *Traffic* 10, 925–937. doi:10.1111/j.1600-0854.2009.00920.x.

Su, Y., Li, X., Ji, W., Sun, B., Xu, C., Li, Z., et al. (2014). Small molecule with big role: MicroRNAs in cancer metastatic microenvironments. *Cancer Lett.* 344, 147–156. doi:10.1016/j.canlet.2013.10.024.

Subra, C., Grand, D., Laulagnier, K., Stella, A., Lambeau, G., Paillasse, M., et al. (2010). Exosomes account for vesicle-mediated transcellular transport of activatable phospholipases and prostaglandins. *J. Lipid Res.* 51, 2105–2120. doi:10.1194/jlr.M003657.

Subramaniam, S., Jeet, V., Clements, J. A., Gunter, J. H., and Batra, J. (2019). Emergence of MicroRNAs as Key Players in Cancer Cell Metabolism. *Clin. Chem.* 65, 1090–1101. doi:10.1373/clinchem.2018.299651.

Sullivan, R. P., Fogel, L. A., Leong, J. W., Schneider, S. E., Wong, R., Romee, R., et al. (2013). MicroRNA-155 Tunes Both the Threshold and Extent of NK Cell Activation via Targeting of Multiple Signaling Pathways. *J. Immunol.* 191, 5904–5913. doi:10.4049/jimmunol.1301950.

Sundarbose, K., Kartha, R., and Subramanian, S. (2013). MicroRNAs as Biomarkers in Cancer. *Diagnostics* 3, 84–104. doi:10.3390/diagnostics3010084.

Sung, M. T., Jiang, Z., Montironi, R., MacLennan, G. T., Mazzucchelli, R., and Cheng, L. (2007). α-methylacyl-CoA racemase (P504S)/34βE12/p63 triple cocktail stain in prostatic adenocarcinoma after hormonal therapy. *Hum. Pathol.* 38, 332–341.

doi:10.1016/j.humpath.2006.08.016.

Svensson, K. J., Christianson, H. C., Wittrup, A., Bourseau-Guilmain, E., Lindqvist, E., Svensson, L. M., et al. (2013). Exosome uptake depends on ERK1/2-heat shock protein 27 signaling and lipid raft-mediated endocytosis negatively regulated by caveolin-1. *J. Biol. Chem.* 288, 17713–17724. doi:10.1074/jbc.M112.445403.

Swalwell, J. I., Vocke, C. D., Yang, Y., Walker, J. R., Grouse, L., Myers, S. H., et al. (2002). Determination of a minimal deletion interval on chromosome band 8p21 in sporadic prostate cancer. *Genes Chromosom. Cancer* 33, 201–205. doi:10.1002/gcc.10015.

Szafranska, A. E., Davison, T. S., Shingara, J., Doleshal, M., Riggenbach, J. A., Morrison, C. D., et al. (2008). Accurate molecular characterization of formalin-fixed, paraffin-embedded tissues by microRNA expression profiling. *J. Mol. Diagnostics* 10, 415–423. doi:10.2353/jmoldx.2008.080018.

Takahashi, K., Yokota, S. ichi, Tatsumi, N., Fukami, T., Yokoi, T., and Nakajima, M. (2013). Cigarette smoking substantially alters plasma microRNA profiles in healthy subjects. *Toxicol. Appl. Pharmacol.* 272, 154–160. doi:10.1016/j.taap.2013.05.018.

Takahashi, M., Cuatrecasas, M., Balaguer, F., Hur, K., Toiyama, Y., Castells, A., et al. (2012). The clinical significance of MiR-148a as a predictive biomarker in patients with advanced colorectal cancer. *PLoS One* 7, e46684. doi:10.1371/journal.pone.0046684.

Takamizawa, J., Konishi, H., Yanagisawa, K., Tomida, S., Osada, H., Endoh, H., et al. (2004). Reduced Expression of the let-7 MicroRNAs in Human Lung Cancers in Association with Shortened Postoperative Survival. *Cancer Res.* 64. Available at: http://cancerres.aacrjournals.org/content/64/11/3753 [Accessed June 29, 2017].

Tanaka, Y., Kamohara, H., Kinoshita, K., Kurashige, J., Ishimoto, T., Iwatsuki, M., et al.

(2013). Clinical impact of serum exosomal microRNA-21 as a clinical biomarker in human esophageal squamous cell carcinoma. *Cancer* 119, 1159–1167. doi:10.1002/cncr.27895.

Taniai, M., Grambihler, A., Higuchi, H., Werneburg, N., Bronk, S. F., Farrugia, D. J., et al. (2004). Mcl-1 mediates tumor necrosis factor-related apoptosis-inducing ligand resistance in human cholangiocarcinoma cells. *Cancer Res.* 64, 3517–3524. doi:10.1158/0008-5472.CAN-03-2770.

Thakral, S., and Ghoshal, K. (2015). miR-122 is a Unique Molecule with Great Potential in Diagnosis, Prognosis of Liver Disease, and Therapy Both as miRNA Mimic and Antimir. *Curr. Gene Ther.* 15, 142–150. doi:10.2174/1566523214666141224095610.

Thomou, T., Mori, M. A., Dreyfuss, J. M., Konishi, M., Sakaguchi, M., Wolfrum, C., et al. (2017). Adipose-derived circulating miRNAs regulate gene expression in other tissues. *Nature* 542, 450–455. doi:10.1038/nature21365.

Tkach, M., Kowal, J., Zucchetti, A. E., Enserink, L., Jouve, M., Lankar, D., et al. (2017). Qualitative differences in T-cell activation by dendritic cell-derived extracellular vesicle subtypes. *EMBO J.* 36, 3012–3028. doi:10.15252/embj.201696003.

Tomlins, S. A., Rhodes, D. R., Perner, S., Dhanasekaran, S. M., Mehra, R., Sun, X. W., et al. (2005). Recurrent fusion of TMPRSS2 and ETS transcription factor genes in prostate cancer. *Science (80-.).* 310, 644–648. doi:10.1126/science.1117679.

Tosar, J. P., Gámbaro, F., Sanguinetti, J., Bonilla, B., Witwer, K. W., and Cayota, A. (2015). Assessment of small RNA sorting into different extracellular fractions revealed by high-throughput sequencing of breast cell lines. *Nucleic Acids Res.* 43, 5601–16. doi:10.1093/nar/gkv432.

Trajkovic, K., Hsu, C., Chiantia, S., Rajendran, L., Wenzel, D., Wieland, F., et al. (2008).

Ceramide triggers budding of exosome vesicles into multivesicular endosomes. *Science (80-.).* 319, 1244–1247. doi:10.1126/science.1153124.

Turchinovich, A., Weiz, L., Langheinz, A., and Burwinkel, B. (2011). Characterization of extracellular circulating microRNA. *Nucleic Acids Res.* 39, 7223–33. doi:10.1093/nar/gkr254.

USCS Data Visualizations - CDC Available at: https://gis.cdc.gov/cancer/USCS/DataViz.html [Accessed February 3, 2020].

Valadi, H., Ekström, K., Bossios, A., Sjöstrand, M., Lee, J. J., and Lötvall, J. O. (2007). Exosome-mediated transfer of mRNAs and microRNAs is a novel mechanism of genetic exchange between cells. *Nat. Cell Biol.* 9, 654–659. doi:10.1038/ncb1596.

Van Houten, B., Santa-Gonzalez, G. A., and Camargo, M. (2018). DNA repair after oxidative stress: Current challenges. *Curr. Opin. Toxicol.* 7, 9–16. doi:10.1016/j.cotox.2017.10.009.

Van Niel, G., D'Angelo, G., and Raposo, G. (2018). Shedding light on the cell biology of extracellular vesicles. *Nat. Rev. Mol. Cell Biol.* 19, 213–228. doi:10.1038/nrm.2017.125.

Vella, L., Sharples, R., Lawson, V., Masters, C., Cappai, R., and Hill, A. (2007). Packaging of prions into exosomes is associated with a novel pathway of PrP processing. *J. Pathol.* 211, 582–590. doi:10.1002/path.2145.

Venkateswaran, S., Luque-González, M. A., Tabraue-Chávez, M., Fara, M. A., López-Longarela, B., Cano-Cortes, V., et al. (2016). Novel bead-based platform for direct detection of unlabelled nucleic acids through Single Nucleobase Labelling. *Talanta* 161, 489–496. doi:10.1016/j.talanta.2016.08.072.

Villarroya-Beltri, C., Gutiérrez-Vázquez, C., Sánchez-Cabo, F., Pérez-Hernández, D., Vázquez, J., Martin-Cofreces, N., et al. (2013). Sumoylated hnRNPA2B1 controls

the sorting of miRNAs into exosomes through binding to specific motifs. *Nat. Commun.* 4, 2980. doi:10.1038/ncomms3980.

Vivier, E., Raulet, D. H., Moretta, A., Caligiuri, M. A., Zitvogel, L., Lanier, L. L., et al. (2011). Innate or adaptive immunity? The example of natural killer cells. *Science (80-.).* 331, 44–49. doi:10.1126/science.1198687.

Vlachos, I. S., Paraskevopoulou, M. D., Karagkouni, D., Georgakilas, G., Vergoulis, T., Kanellos, I., et al. (2015). DIANA-TarBase v7.0: Indexing more than half a million experimentally supported miRNA:mRNA interactions. *Nucleic Acids Res.* 43, D153–D159. doi:10.1093/nar/gku1215.

Volinia, S., Calin, G. A., Liu, C.-G., Ambs, S., Cimmino, A., Petrocca, F., et al. (2006). A microRNA expression signature of human solid tumors defines cancer gene targets. *Proc. Natl. Acad. Sci. U. S. A.* 103, 2257–61. doi:10.1073/pnas.0510565103.

Wang, D., Lu, G., Shao, Y., and Xu, D. (2018). MiR-182 promotes prostate cancer progression through activating Wnt/β-catenin signal pathway. *Biomed. Pharmacother.* 99, 334–339. doi:10.1016/j.biopha.2018.01.082.

Wang, J., Palecek, E., Nielsen, P. E., Rivas, G., Cai, X., Shiraishi, H., et al. (1996). Peptide Nucleic Acid Probes for Sequence-Specific DNA Biosensors. *J. Am. Chem. Soc.* 118, 7667–7670. doi:10.1021/ja9608050.

Wang, L.-J., He, C.-C., Sui, X., Cai, M.-J., Zhou, C.-Y., Ma, J.-L., et al. (2015). MiR-21 promotes intrahepatic cholangiocarcinoma proliferation and growth in vitro and in vivo by targeting PTPN14 and PTEN. *Oncotarget* 6, 5932–5946. doi:10.18632/oncotarget.3465.

Wang, Q., Zhong, M., Liu, W., Li, J., Huang, J., and Zheng, L. (2011). Alterations of microRNAs in Cisplatin-resistant Human Non-small Cell Lung Cancer Cells (A549/DDP). *Exp. Lung Res.* 37, 427–434. doi:10.3109/01902148.2011.584263.

Wang, Y., Wang, D., Xie, G., Yin, Y., Zhao, E., Tao, K., et al. (2017). MicroRNA-152 regulates immune response via targeting B7-H1 in gastric carcinoma. *Oncotarget* 8, 28125–28134. doi:10.18632/oncotarget.15924.

Wei, J., Lv, L., Wan, Y., Cao, Y., Li, G., Lin, H., et al. (2015). Vps4A functions as a tumor suppressor by regulating the secretion and uptake of exosomal microRNAs in human hepatoma cells. *Hepatology* 61, 1284–94. doi:10.1002/hep.27660.

Williams, M., Kirschner, M. B., Cheng, Y. Y., Hanh, J., Weiss, J., Mugridge, N., et al. (2015). miR-193a-3p is a potential tumor suppressor in malignant pleural mesothelioma. *Oncotarget* 6, 23480–23495. doi:10.18632/oncotarget.4346.

Wilson, R. C., Tambe, A., Kidwell, M. A., Noland, C. L., Schneider, C. P., Doudna, J. A., et al. (2015). Dicer-TRBP complex formation ensures accurate mammalian microRNA biogenesis. *Mol. Cell* 57, 397–407. doi:10.1016/j.molcel.2014.11.030.

Witwer, K. W. (2012). XenomiRs and miRNA homeostasis in health and disease: Evidence that diet and dietary miRNAs directly and indirectly influence circulating miRNA profiles. *RNA Biol.* 9, 1147–1154. doi:10.4161/rna.21619.

Woith, E., Fuhrmann, G., and Melzig, M. F. (2019). Extracellular Vesicles—Connecting Kingdoms. *Int. J. Mol. Sci.* 20, 5695. doi:10.3390/ijms20225695.

Xiao, C., Srinivasan, L., Calado, D. P., Patterson, H. C., Zhang, B., Wang, J., et al. (2008). Lymphoproliferative disease and autoimmunity in mice with increased miR-17-92 expression in lymphocytes. *Nat. Immunol.* 9, 405–414. doi:10.1038/ni1575.

Xiong, D.-D., Lv, J., Wei, K.-L., Feng, Z.-B., Chen, J.-T., Liu, K.-C., et al. (2017). A nine-miRNA signature as a potential diagnostic marker for breast carcinoma: An integrated study of 1,110 cases. *Oncol. Rep.* doi:10.3892/or.2017.5600.

Xu, W., Zhang, Z., Zou, K., Cheng, Y., Yang, M., Chen, H., et al. (2017). MiR-1 suppresses tumor cell proliferation in colorectal cancer by inhibition of Smad3-

mediated tumor glycolysis. *Cell Death Dis.* 8, e2761. doi:10.1038/cddis.2017.60.

Xu, Z., Zeng, X., Tian, D., Xu, H., Cai, Q., Wang, J., et al. (2014). MicroRNA-383 inhibits anchorage-independent growth and induces cell cycle arrest of glioma cells by targeting CCND1. *Biochem. Biophys. Res. Commun.* 453, 833–838. doi:10.1016/j.bbrc.2014.10.047.

Xue, D., Zhou, C., Lu, H., Xu, R., Xu, X., and He, X. (2016). LncRNA GAS5 inhibits proliferation and progression of prostate cancer by targeting miR-103 through AKT/mTOR signaling pathway. *Tumor Biol.* 37, 16187–16197. doi:10.1007/s13277-016-5429-8.

Yagi, Y., Ohkubo, T., Kawaji, H., Machida, A., Miyata, H., Goda, S., et al. (2017). Next-generation sequencing-based small RNA profiling of cerebrospinal fluid exosomes. *Neurosci. Lett.* 636, 48–57. doi:10.1016/j.neulet.2016.10.042.

Yanaihara, N., Caplen, N., Bowman, E., Seike, M., Kumamoto, K., Yi, M., et al. (2006a). Unique microRNA molecular profiles in lung cancer diagnosis and prognosis. *Cancer Cell* 9, 189–98. doi:10.1016/j.ccr.2006.01.025.

Yanaihara, N., Caplen, N., Bowman, E., Seike, M., Kumamoto, K., Yi, M., et al. (2006b). Unique microRNA molecular profiles in lung cancer diagnosis and prognosis. *Cancer Cell* 9, 189–198. doi:10.1016/j.ccr.2006.01.025.

Yang, J.-R., Yan, B., Guo, Q., Nan, X., Wang, Z., Yin, Z., et al. (2015). Micro-ribonucleic acid 29b inhibits cell proliferation and invasion and enhances cell apoptosis and chemotherapy effects of cisplatin via targeting of DNMT3b and AKT3 in prostate cancer. *Onco. Targets. Ther.* 8, 557. doi:10.2147/OTT.S76484.

Yekta, S., Shih, I., and Bartel, D. P. (2004). MicroRNA-Directed Cleavage of HOXB8 mRNA. *Science (80-.).* 304.

Yu, Q. F., Liu, P., Li, Z. Y., Zhang, C. F., Chen, S. Q., Li, Z. H., et al. (2018). MiR-

103/107 induces tumorigenicity in bladder cancer cell by suppressing PTEN. *Eur. Rev. Med. Pharmacol. Sci.* 22, 8616–8623. doi:10.26355/eurrev_201812_16625.

Yu, S.-L., Chen, H.-Y., Chang, G.-C., Chen, C.-Y., Chen, H.-W., Singh, S., et al. (2008). MicroRNA Signature Predicts Survival and Relapse in Lung Cancer. *Cancer Cell* 13, 48–57. doi:10.1016/j.ccr.2007.12.008.

Zahran, F., Ghalwash, D., Shaker, O., Al-Johani, K., and Scully, C. (2015). Salivary microRNAs in oral cancer. *Oral Dis.* 21, 739–747. doi:10.1111/odi.12340.

Zhang, G. J. (2011). Silicon nanowire biosensor for ultrasensitive and label-free direct detection of miRNAs. *Methods Mol. Biol.* 676, 111–121. doi:10.1007/978-1-60761-863-8_9.

Zhang, H., Mao, F., Shen, T., Luo, Q., Ding, Z., Qian, L., et al. (2017). Plasma miR-145, miR-20a, miR-21 and miR-223 as novel biomarkers for screening early-stage non-small cell lung cancer. *Oncol. Lett.* 13, 669–676. doi:10.3892/ol.2016.5462.

Zhang, J., Li, S., Li, L., Li, M., Guo, C., Yao, J., et al. (2015a). Exosome and exosomal microRNA: Trafficking, sorting, and function. *Genomics, Proteomics Bioinforma.* 13, 17–24. doi:10.1016/j.gpb.2015.02.001.

Zhang, Q., Di, W., Dong, Y., Lu, G., Yu, J., Li, J., et al. (2015b). High serum miR-183 level is associated with poor responsiveness of renal cancer to natural killer cells. *Tumor Biol.* 36, 9245–9249. doi:10.1007/s13277-015-3604-y.

Zhang, X., Ng, W. L., Wang, P., Tian, L. L., Werner, E., Wang, H., et al. (2012). MicroRNA-21 modulates the levels of reactive oxygen species by targeting SOD3 and TNFα. *Cancer Res.* 72, 4707–4713. doi:10.1158/0008-5472.CAN-12-0639.

Zhang, Y., Shi, J., Rassoulzadegan, M., Tuorto, F., and Chen, Q. (2019). Sperm RNA code programmes the metabolic health of offspring. *Nat. Rev. Endocrinol.* 15, 489–498. doi:10.1038/s41574-019-0226-2.

Zhao, F., Vesprini, D., Liu, R. S. C., Olkhov-Mitsel, E., Klotz, L. H., Loblaw, A., et al. (2019). Combining urinary DNA methylation and cell-free microRNA biomarkers for improved monitoring of prostate cancer patients on active surveillance. *Urol. Oncol. Semin. Orig. Investig.* 37, 297.e9-297.e17. doi:10.1016/j.urolonc.2019.01.031.

Zheng, H., Guo, Z., Zheng, X., Cheng, W., and Huang, X. (2018). MicroRNA-144-3p inhibits cell proliferation and induces cell apoptosis in prostate cancer by targeting CEP55. *Am. J. Transl. Res.* 10, 2457–2468. Available at: http://www.ncbi.nlm.nih.gov/pubmed/30210684 [Accessed December 10, 2018].

Zhou, B., Xu, H., Xia, M., Sun, C., Li, N., Guo, E., et al. (2017). Overexpressed miR-9 promotes tumor metastasis via targeting E-cadherin in serous ovarian cancer. *Front. Med.* 11, 214–222. doi:10.1007/s11684-017-0518-7.

Zhou, W., Fong, M. Y., Min, Y., Somlo, G., Liu, L., Palomares, M. R., et al. (2014). Cancer-Secreted miR-105 destroys vascular endothelial barriers to promote metastasis. *Cancer Cell* 25, 501–515. doi:10.1016/j.ccr.2014.03.007.

Zhu, C., Hou, X., Zhu, J., Jiang, C., and Wei, W. (2018). Expression of miR-30c and miR-29b in prostate cancer and its diagnostic significance. *Oncol. Lett.* 16, 3140–3144. doi:10.3892/ol.2018.9007.

Zhu, H.-T., Dong, Q.-Z., Wang, G., Zhou, H.-J., Ren, N., Jia, H.-L., et al. (2012). Identification of suitable reference genes for qRT-PCR analysis of circulating microRNAs in hepatitis B virus-infected patients. *Mol. Biotechnol.* 50, 49–56. doi:10.1007/s12033-011-9414-6.

Zhu, H., Zhou, X., Ma, C., Chang, H., Li, H., Liu, F., et al. (2015). Low Expression of miR-448 Induces EMT and Promotes Invasion by Regulating ROCK2 in Hepatocellular Carcinoma. *Cell. Physiol. Biochem.* 36, 487–98.

doi:10.1159/000430114.

Zhu, S., Si, M.-L., Wu, H., and Mo, Y.-Y. (2007). MicroRNA-21 targets the tumor suppressor gene tropomyosin 1 (TPM1). *J. Biol. Chem.* 282, 14328–36. doi:10.1074/jbc.M611393200.